Attachment I

Attachment I

Serial No.	09/826,118	02/14/2006
Filing date	01/09/2001	
Name	Urbain A. von der Embse	
Unit	2124	
Examiner	Chat C. Do	

Response to Office Action 02/07/2006

I have corrected the amendment to the specification in the substitute specification by underlining the new paragraph in page 9 lines 12-35, to be compliant to the Office Action.

ENCLOSURES

- PTO/SB/21 Transmittal form
- A copy of the Notice of Non-Compliant Amendment (37 CFR1.121) Office Action mailed to me on 02/07/2006
- Marked up version of the substitute specification with the underlining of the new paragraph on page 9 lines 12-35 to be compliant with the "Notice of Non-Compliant Amendment"

Thanks for all of your help and guidance.

Sincerely,

Contact No. 310.641.0488
Address Urbain A. von der Embse
7323 W. 85th St.
Westchester, CA 90045-2444
Signature
Name Urbain A. von der Embse

Attachment II

Attachment II

Serial No.	09/826,118	06/29/2006
Filing date	01/09/2001	
Name	Urbain A. von der Embse	
Unit	2193	
Examiner	Chat C. Do	

Response to Office Action 04/10/2006

PTO-1449 information disclosure is submitted. The abstract is amended to respond to your guidelines and is limited to 144 words. Claims 1-6 are amended to respond to your objections and to follow your recommendations. The substitute specification is the original specification with editing corrections. Amended drawings are the original drawings with editing corrections that follow your guidelines.

ENCLOSURES

- PTO/SB/21 Transmittal form
- Copy of the "Office Action" mailed to me on 04/10/2006
- PTO/SB/08a (replaces PTO-1449) information disclosure
- PTO/SB/08b (replaces PTO-1449) information disclosure
- Marked up version of the amended abstract of the disclosure
- Clean version of how the abstract of the disclosure will read
- Complete list of claims with their status identifiers and current amendments with strikethrough and underline markups.
- Clean version of how the claims will read
- Marked up version of the substitute specification
- Clean version of how the specification will read
- Amended drawings with proper identification in the top margins

Attachment II

REMARKS

1. Office Action

The amendments being submitted are in reference to the amendment filed on 02/21/2006.

2. Office Action

Claims 1-6 are amended to address your objections and recommendations.

3. Information Disclosure Statement

References are listed on form PTO/SB/08a for patents and on form PTO/SB/08b for technical articles which forms are replacements for form PTO-1449.

4. Drawings

Figure 1-2 are designated as "Prior Art" in their legends. Corrected drawings are labeled as "Deleted Sheet" in their top margins and replacement sheets are labeled as "Replacement Sheet" in their top margins.

5. Drawings

Corrected original sheets are labeled as "Deleted Sheet" and corrected sheets are labeled as "Replacement Sheet" in the top margins. Drawings 1-8 are the originals. Shading is removed from drawings 1-5 and drawing 2 has a correction in element 8. Original drawings as part of the specification have their cross-out markings removed.

6. Drawings

New drawings 5B-5L have been deleted since they list the Matlab software used to calculate performance in the

Attachment II

specification and are objected to by the examiner as not being supported by the original specification.

Remaining drawings 1-8 are the original drawings with editing corrections and corrections recommended in your "Office Action" and are consecutively numbered from 1-8. No drawings have been deleted.

7. Specification

The abstract of the disclosure has been amended to follow your guidelines. As it now reads the abstract describes the enclosure sufficiently to assist the reader in deciding if there is a need to consult the full patent in that it identifies the combined requirements for a least squares LS solution for Wavelets and finite impulse response FIR filters that include requirements not currently available in FIR design algorithms, it points out that the harmonics of the Wavelets are the design coordinates being optimized and these are mapped into the FIR time response for implementation, and it points out that these harmonic design coordinates provide a single design to generate Wavelets at arbitrary parameters which capability is not currently available with any design algorithm.

8. Specification

The amended abstract has been limited to 144 words.

9. Claim Objections

The referenced "for" and "means for generating complex wavelet waveform and filters" have been removed in the amended claim 1 which lists the steps required to implement the iterative eigenvalue least squares LS algorithm derived in the specification.

Attachment II

10. Claim Objections

Objections to claims 3-4 are believed to have been corrected in the amended claims 1-6. Claim 1 lists the detailed steps in the method claimed for generating the digital mother Wavelet at baseband using an iterative eigenvalue least squares LS algorithm. Claims 3-4 list the steps and design for generating multi-resolution Wavelets from the mother Wavelets in claims 1-2.

11. Claim Rejections - 35 USC § 112

Requirements for one or more of the claims "particularly pointing out and distinctly claiming the subject matter which the appliant regards as his invention" are believed to be met by the amended claims 1-6. Claims 1-2 list the steps in the method for calculating the mother Wavelet time response $\psi(n)$ using the design harmonic coordinates $\psi_k(k)$ and claims 3-5 list the steps and designs for the mother Wavelet $\psi_k(k)$ to the generate multi-resolution Wavelet time response for scale and translation parameters. Claim 6 has been amended to list the properties of the Wavelets in claims 1-5.

12. Claim Rejections - 35 USC § 112

Objections to claim 1-6 are believed to have been corrected in the amended claims which particularly point out and distinctly claim the subject matter which is regarded as the invention.

"Scale" is defined in the clean version of the amended claim 3 in lines 9-10 in page 5. "Scale" parameters are the dilation p, symbol interval M, and symbol length L and wherein p can be either positive or negative. "Scale" parameter p in current Wavelets is restricted to positive values.

Attachment II

Translation parameters q,k are defined in claim 3 in lines 11-13 in page 5.

"Fourier harmonics $\psi_k(k)$" are defined in the clean version of the amended claim 1 in lines 4-15 in page 2 in the inverse discrete Fourier transform format which derives the time response $\psi(n)$ as a function of the frequency response harmonics $\psi_k(k)$. Designation of $\psi_k(k)$ as "design harmonics" is in the clean version of the amended claim 3 in line 17 in page 5.

13. Claim Rejections - 35 USC § 112

"Means" has been eliminated in the amended claims.

14. Claim Rejections - 35 USC § 112

Amended claims 1-6 have been rewritten to eliminate the objection that the claims are "narrative in form and replete with indefinite and functional or operational language".

Amended claims 1-2 clearly and positively define the steps comprising the method for designing the LS algorithms using design coordinates $\psi_k(k)$ to find the optimum $\psi(n)$ for implementation and using one sentence formats. Likewise claims 3-5 clearly and positively define the steps and design parameters to enable $\psi_k(k)$ in claim 1-2 to generate the multi-resolution Wavelet examples. Claim 6 clearly and positively summarizes the properties of the new Wavelets which are the subject matter of this invention.

Attachment II

15,16 Claim Rejections - 35 USC § 101

Amended claims 1-2 are believed to be in compliance under 35 USC § 101 since they define in clear detail the steps in the new method for designing the mother Wavelet time response $\psi(n)$ which is the format required for direct implementation in communications and radar applications.

Amended claims 3-5 are believed to be in compliance under 35 USC § 101 since they define in clear detail the steps and design parameters for generating the multi-resolution Wavelet time response for scales p,M,L and sampling rate 1/T from $\psi(n)$ using the design harmonics $\psi_k(k)$ for the mother Wavelet and which time response is the format required for direct implementation in communications and radar applications and which mplementations will add the translations q,k.

Amended claim 6 is in compliance under 35 USC § 101 since it lists the properties of the Wavelets for implementation in communications and radar transmitters and receivers.

Demonstrated performance for linear communications, BEM, SAR is summarized in the specification drawings in FIG. 4,7,8 respectively.

17,18 Claim Rejections - 35 USC § 102

Amended claims 1-6 are believed to be in compliance under 35 USC § 102 since the amended claims 1-6 clearly define the subject matter of this invention that was not patented or described in a printed publication prior to this invention application and was not anticipated by prior art summarized in pages 2-8 in the specification.

Attachment II

In claims 1-2 prior art Wavelet and FIR filter designs select time domain coordinates $\psi(n)$ to optimize performance for this baseband waveform whereas this invention replaces $\psi(n)$ with $\psi_k(k)$, combines Wavelet and FIR requirements, and finds the optimum $\psi_k(k)$ to generate the optimum $\psi(n)$ at baseband and for all scales p,M,L and all translations q,k.

Claims 3-5 demonstrate how $\psi_k(k)$ generates the optimal baseband time response $\psi(n_p)$ wherein n_p is the sample index for scale p, when scale p down-samples or equivalently dilates the digital sampling, when scale p dilate M,L at a constant sample rate, when scale p up-samples, and by obvious implication for any set of scales p,M,L and design parameter 1/T. Current Wavelets can only be dilated or dowm-sampled using scaling equations or equivalently the trellis construction in FIG. 2. Current FIR designs support up-sampling followed by a bandwidth limiting filter.

Application examples in FIG. 6,7,8 demonstrate improved performance offered by combining Wavelet and FIR requirements.

18. Claim Rejections - 35 USC § 102

Amended claims 1-6 are believed to clearly demonstrate they have not been anticipated by prior art in compliance with 35 USC § 102.

¶1 of the "Office Action" correctly observes that prior art on pages 2-8 provides methods for designing waveforms and filters and the Wavelet art in lines 15-35 in page 5 defines the multi-resoluion Wavelet as a function of the mother Wavelet at

Attachment II

baseband. This definition enables the mother Wavelet to generate multi-resolution waveforms at lower bandwidths to tile the time-frequency t-f space in Figure 1 using the procedure described in lines 6-16 in page 7. There is no mention of "using a subset of the Fourier harmonics as the desicn coordinates (harmonics) specifying the waveform design" and no mention of "design harmonics" in prior Wavelet art and in prior waveform and filter art. In line 15 in page 2 to line 4 in page 4 the waveform and filter design techniques in categories C1 to C7 including the Wavelet in category C5 are described. There is no prior art suggesting the concept of a "means for using the design harmonics and frequency translation property to generate wavelet waveforms at multiple scales and frequencies". "Frequency translation" is a common property of all waveform and filter design except possibly category C7.

¶2 of the "Office Action" correctly observes that prior art in pages 2-8 discloses in lines 15-37 in page 5 the Wavelet equation, properties, and its use for generating multi-resolution Wavelets at scale p with time translation q which can be used to tile the t-f space in Figure 1 as described in lines 6-16 page 7. Scale p is a dilation parameter which means the mother Wavelet at scale p=0 can generate multi-resolution replicas at scales p=1,2,…. corresponding to reductions in sample rate rate bandwidth by the factor 2^p and a stretching by the factor 2^p to tile the t-f space in Figue 1. Another method to tile the t-f space uses the iterated filter bank construcion in line 18 page 8 to line 10 page 9 to generate the multi-resolution Wavelets at scales "p=1,2…" with a reduced capability to design the multi-resolution Wavelets to be replicas of the mother Wavelet due to the multi-stage filtering impacts. Wavelets are real so the

Attachment II

multi-resolution Wavelets are real. There is no concept nor use of "Fourier harmonics" as design harmonics since all implementations are in the time domain as convolutions and sub-sampling operations. Frequency response is a performnce metric of this design.

Current Wavelet multi-resolution Wavelet generation is restricted to p=1,2,… with corresponding subsampling reducing the Nyquist bandwidth 1/T to 1/T2^p. The new Wavelets support the design of multi-resolution waveforms with this dilation as well as with dilation of bandwidth with constant 1/T, negative values for scale p corresponding to up-sampling, and complete flexibility in the control of the scale parameters p,M,L. and the design sampling rate 1/T. Design coordinates $\psi_k(k)$ for the mother Wavelet generate all of these multi-resolution waveforms as demonstrated in claims 3-5.

¶2 of the "Office Action" correctly observes that prior art in line 15 page 3 to line 4 page 4 includes designing waveforms and filters using analytical equations such as the square-root raised-cosine definition of a FIR waveform time response that allows it to generate multi-resolution waveforms, iterative design techniques such as the Remez Exchange and eigenvalue LS techniques for designing filters with passband and stopband requirements, and polyphase filters which have multi-resolution capabilities. There is no concept nor use of "Fourier harmonics" as design harmonics since all implementations are in the time domain. Frequency response is a performnce metric of these designs.

Attachment II

19. Response to Amendment

The Matlab code has been deleted from the drawings and its description has been deleted from the specification. Amended substitute specification is the original specification with some minor editing corrections. Amended drawings are the original drawings with some minor edition corrections including your requested insertion of "Prior Art" in the legend of drawings 1-2. Abstract has been amended to follow your guidelines and consists of 144 words. Claims 1-2 have been amended to clearly define the method for designing the mother Wavelets described in the specification. Claims 3-5 illustrate the derivation of multi-resolution Wavelets from the mother Wavelets in claims 1-2 using the equations defined in the specification. Claim 6 summarizes the claimed properties of the new Wavelets disclosed in claims 1-5.

Objection 1 is believed to be satisfied in that the claims only refer to matter in the specification.

Objection 2 referencing lines 13-35 page 9, Figure 5, and Matlab code pages 37-44 is believed to be satisfied in that the Matlab code 5.0 and all reference to it has been deleted both from the amended drawings and the substitute specification.

20. Response to Arguments

The amended claims 1-6 have been rewritten to address your objections. Your detailed objections and recommendations were most helpful.

UNITED STATES PATENT AND TRADEMARK OFFICE

OIPE
OCT 06 2006
PATENT & TRADEMARK OFFICE

UNITED STATES DEPARTMENT OF COMMERCE
United States Patent and Trademark Office
Address: COMMISSIONER FOR PATENTS
P.O. Box 1450
Alexandria, Virginia 22313-1450
www.uspto.gov

APPLICATION NO.	FILING DATE	FIRST NAMED INVENTOR	ATTORNEY DOCKET NO.	CONFIRMATION NO.
09/826,118	01/09/2001	Urbain Alfred Von der Embse		4398

7590 09/08/2006

URBAIN A. VON DER EMBER
7323 W. 85TH STREET
WESTCHESTER, CA 90045-2444

EXAMINER	
DO, CHAT C	

ART UNIT	PAPER NUMBER
2193	

DATE MAILED: 09/08/2006

Please find below and/or attached an Office communication concerning this application or proceeding.

Attachment II

21. Response to Arguments

I am extremely grateful for pointing out all of my mistakes and lack of understanding of the USPTO rules.

Thanks ever for all of your help and guidance.

Sincerely,

Name	Urbain A. von der Embse
Contact No.	310.641.0488
Address	Urbain A. von der Embse
	7323 W. 85th St.
	Westchester, CA 90045-2444

Notice of Non-Compliant Amendment (37 CFR 1.121)

Application No.	Applicant(s)	
09/826,118	VON DER EMBSE, URBAIN ALFRED	
Examiner	**Art Unit**	
Chat C. Do	2193	

-- The MAILING DATE of this communication appears on the cover sheet with the correspondence address --

The amendment document filed on *05 July 2006* is considered non-compliant because it has failed to meet the requirements of 37 CFR 1.121 or 1.4. In order for the amendment document to be compliant, correction of the following item(s) is required.

THE FOLLOWING MARKED (X) ITEM(S) CAUSE THE AMENDMENT DOCUMENT TO BE NON-COMPLIANT:

- ☒ 1. Amendments to the specification:
  - ☐ A. Amended paragraph(s) do not include markings.
  - ☐ B. New paragraph(s) should not be underlined.
  - ☒ C. Other *See Continuation Sheet*.
- ☒ 2. Abstract:
  - ☐ A. Not presented on a separate sheet. 37 CFR 1.72.
  - ☒ B. Other *See Continuation Sheet*.
- ☒ 3. Amendments to the drawings:
  - ☐ A. The drawings are not properly identified in the top margin as "Replacement Sheet," "New Sheet," or "Annotated Sheet" as required by 37 CFR 1.121(d).
  - ☐ B. The practice of submitting proposed drawing correction has been eliminated. Replacement drawings showing amended figures, without markings, in compliance with 37 CFR 1.84 are required.
  - ☒ C. Other *See Continuation Sheet*.
- ☒ 4. Amendments to the claims:
  - ☐ A. A complete listing of all of the claims is not present.
  - ☐ B. The listing of claims does not include the text of all pending claims (including withdrawn claims)
  - ☐ C. Each claim has not been provided with the proper status identifier, and as such, the individual status of each claim cannot be identified. Note: the status of every claim must be indicated after its claim number by using one of the following status identifiers: (Original), (Currently amended), (Canceled), (Previously presented), (New), (Not entered), (Withdrawn) and (Withdrawn-currently amended).
  - ☐ D. The claims of this amendment paper have not been presented in ascending numerical order.
  - ☒ E. Other: *See Continuation Sheet*.
- ☐ 5. Other (e.g., the amendment is unsigned or not signed in accordance with 37 CFR 1.4):

For further explanation of the amendment format required by 37 CFR 1.121, see MPEP § 714.

TIME PERIODS FOR FILING A REPLY TO THIS NOTICE:

1. Applicant is given **no new time period** if the non-compliant amendment is an after-final amendment or an amendment filed after allowance. If applicant wishes to resubmit the non-compliant after-final amendment with corrections, the **entire corrected amendment** must be resubmitted.
2. Applicant is given **one month**, or thirty (30) days, whichever is longer, from the mail date of this notice to supply the correction, if the non-compliant amendment is one of the following: a preliminary amendment, a non-final amendment (including a submission for a request for continued examination (RCE) under 37 CFR 1.114), a supplemental amendment filed within a suspension period under 37 CFR 1.103(a) or (c), and an amendment filed in response to a *Quayle* action. If any of above boxes 1. to 4. are checked, the correction required is only the **corrected section** of the non-compliant amendment in compliance with 37 CFR 1.121.

   Extensions of time are available under 37 CFR 1.136(a) only if the non-compliant amendment is a non-final amendment or an amendment filed in response to a *Quayle* action.

   Failure to timely respond to this notice will result in:
   Abandonment of the application if the non-compliant amendment is a non-final amendment or an amendment filed in response to a *Quayle* action; or
   Non-entry of the amendment if the non-compliant amendment is a preliminary amendment or supplemental amendment.

Legal Instruments Examiner (LIE), if applicable

Telephone No.

Continuation of 1(c) Other: specification should be amended based on the latest previous amendment version which is filed in 12/13/2005..

Continuation of 2(b) Other: abstract should be amended based on the latest previous amendment version which is filed in 12/13/2005..

Continuation of 3(c) Other: drawings should be amended based on the latest previous amendment version which is filed in 12/13/2005..

Continuation of 4(e) Other: Claims should be amended based on the latest previous amendment version which is filed in 12/13/2005.

KAKALI CHAKI
SUPERVISORY PATENT EXAMINER
TECHNOLOGY CENTER 2100

Notice of Non-Compliant Amendment (37 CFR 1.121)

Continuation Sheet (PTOL-324)

Continuation of 1(c) Other: specification should be amended based on the latest previous amendment version which is filed in 12/13/2005..

Continuation of 2(b) Other: abstract should be amended based on the latest previous amendment version which is filed in 12/13/2005..

Continuation of 3(c) Other: drawings should be amended based on the latest previous amendment version which is filed in 12/13/2005..

Continuation of 4(e) Other: Claims should be amended based on the latest previous amendment version which is filed in 12/13/2005.

KAKALI CHAKI
SUPERVISORY PATENT EXAMINER
TECHNOLOGY CENTER 2100

APPLICATION NO. 09/826,118

TITLE OF INVENTION: Wavelet Multi-Resolution Waveforms

INVENTOR: Urbain A. von der Embse

Marked up version of SUBSTITUTE SPECIFICATION

APPLICATION NO. 09/826,118

TITLE OF INVENTION: ~~New~~ Wavelet Multi-Resolution Waveforms

INVENTOR: Urbain ~~Alfred~~ A. von der Embse

BACKGROUND OF THE INVENTION

I. Field of the Invention

~~TECHNICAL FIELD~~

The present invention relates to CDMA (Code Division Multiple Access) cellular telephone and wireless data communications with data rates up to multiple T1 (1.544 Mbps) and higher (>100 Mbps), and to optical CDMA. Applications are mobile, point-to-point and satellite communication networks. More specifically the present invention relates to a new and novel ~~means for a new~~ approach to the design of waveforms and filters using mathematical formulations which generalize the Wavelet concept to communications and radar.

~~CONTENTS~~

~~BACKGROUND ART~~

II. Description of the Related Art

Multi-resolution waveforms used for signaling and/or filters and which are addressed in this invention are defined to be waveforms of finite extent in time and frequency, with scale and shift properties of multi-resolution over the time-frequency (t-f) space. These waveforms can also be referred to as multi-scale waveforms, and include multi-rate filtering and the Wavelet as special cases. The emphasis will be on digital design and applications with the understanding that these multi-resolution waveforms are equally applicable to analog design and applications.

Background art consists of the collection of waveform and filtering design techniques which can be grouped into six broad categories. These categories are: C1) least squares (LS) design algorithms for filters and waveforms that design to specifications on their frequency response, C2) analytic filters and waveforms which are specified by a few free design parameters that can be sub-categorized into current applications and primarily theorectical studies, C3) combinations of C1 and C2 for greater flexibility in meeting communications and radar performance goals, C4) special design techniques to control the noise levels from intersymbol interference (ISI) and adjacent channel interference (ACI) in the presence of timing offsets for multiple channel applications, C5) Wavelet filter design using scaling functions (iterated filter banks) as the set of design coordinates or basis functions, C6) filter and waveform design techniques for non-linear channels and in particular for operation in the non-linear and saturation regions of a high power amplifier (HPA) such as a traveling wave tube (TWT) or a solid state amplifier, and C7) LS dynamic filters derived from discrete filtering and tracking algorithms that include adaptive equalization for communications, adaptive antenna filters,

Wiener filters, Kalman filters, and stochastic optimization filters.

Category C1 common examples of LS digital filter design are the eigenvalue algorithm in "A New Approach to Least-Squares FIR Filter Design and Applications Including Nyquist Filters" ~~[7]~~ and the Remez-Exchange algorithm in "A Computer Program for Designing Optimum FIR Linear Phase Filters'. ~~[8].~~ The eigenvalue algorithm is a direct LS minimization and the Remez-Exchange can be reformulated as an equivalent LS gradient problem through proper choice of the cost function. Both LS algorithms use the FIR (finite impulse response) digital samples as the set of design coordinates. LS design metrics are the error residuals in meeting their passband and stopband ideal performance as shown in FIG. **3**. Category C2 common examples of analytical waveforms and filters for system applications are the analog Chebyshev, Elliptic, Butterworth, and the digital raised-cosine, and square-root raised-cosine. For theorectical studies, common examples are polyphase multirate filters, quadrature mirror filters (QMF), and perfect reconstruction filters. Although these theorectical studies have yet to yield realizable useful filters for system applications, their importance for this invention lies in their identification and application of ideal performance metrics for filter designs. Category C3 common digital example is to start with the derivation of a Remez-Exchange ~~finite impulse response (FIR)~~ filter and then up-sample and filter with another bandwidth limiting filter. This results in an FIR over the desired frequency band that is larger than available with the Remez-Exchange algorithm and with sidelobes that now drop off with frequency compared to the flat sidelobes of the original Remez-Exchange FIR. A category C4 common example is to select the free parameters of the category C3 filter in order to minimize the signal to noise power ratio of the data symbol (SNR) losses from the ISI, ACI, and the non-ideal demodulation. A second common example is start with a truncated pulse whose

length is short enough compared to the symbol repetition interval, to accommodate the timing offsets without significant impact on the ISI and ACI SNR losses. This shortened pulse can then be shaped in the frequency domain.

Category C5 Wavelet filter design techniques discussed in the next section will serve as a useful reference in the disclosure of this invention. Category C6 common example is the Gaussian minimum shift keying (GMSK) waveform. This is a constant amplitude phase encoded Gaussian waveform which has no sidelobe re-growth through a non-linear or saturating HPA. Category C7 common examples are the adaptive equalization filter for communication channels, the adaptive antenna filter, and the Kalman filter for applications including target tracking and prediction as well as for equalization and adaptive antennas.

Minimizing excess bandwith in the waveform and filter design is a key goal in the application of the C1,…,C6 design techniques for communications and radar. Excess bandwith is identified as the symbol α in the bandwidth-time product $BT_s=1+\alpha$ where the two-sided available frequency band is B and the symbol repetition interval is T_s. Current performance capability is represented by the use of the square-root raised cosine (sq-rt rc) waveform with α= 0.22 to 0.4 as shown in FIG. **4<u>6</u>**. The goal is to design a waveform with α=0 within the performance constraints of ISI, ACI, passband, sideband, and passband ripple. This goal of eliminating the excess bandwidth corresponds to the symbol rate equal to the available frequency band $1/T_s = B/(1+\alpha) = B$ for α=0. This symbol rate $1/T_s=B$ is well known to be the maximum possible rate for which orthogonality between symbols is maintained. A fundamental performance characteristic of our new waveform designs is the ability to eliminate excess bandwidth for many applications.

Scope of this invention will include all of the waveform and filter categories with the exception of category C4 special design techniques and category C7 LS dynamic filters. Emphasis will be on the category C5 Wavelets to establish the background art since Wavelets are multi-resolution waveforms that can eliminate the excess bandwidth and have known design algorithms for FIR waveforms and filters. However, they do not have a design mechanism that allows direct control of the ISI, ACI, passband, sideband, and passband ripple. Category C2 theorectical studies also eliminate the excess bandwidth. However, ——they are not multi-resolution waveforms and do not have realizable FIR design algorithms. So the emphasis in background art will be on Wavelets whose relevant properties we briefly review.

Wavelet background art relevant to this invention consists of the discrete Waveform equations and basic properties, application of Wavelets to cover a discrete digital time-frequency (t-f) signal space, and the design of Wavelets using the iterated filter construction. Wavelets are waveforms of finite extent in time (t) and frequency (f) over the t-f space, with multi-resolution, scaling, and translation properties. Wavelets over the analog and digital t-f spaces respectively are defined by equations **(1)** and **(2)** as per Daubechies's "Ten Lectures on Wavelets", Philadelphia:SIAM, 1992 ~~reference [1].~~

Continuous wavelet

$$\psi_{a,b}(t) = |a|^{-1/2}\psi(\frac{t-b}{a}) \qquad \textbf{(1)}$$

Discrete wavelet

$$\psi_{a,b}(n) = |a|^{-1/2}\psi(\frac{n-b}{a}) \qquad \textbf{(2)}$$

where the two index parameters "a,b" are the Wavelet dilation and translation respectively or equivalently are the scale and shift.

The ψ is the "mother" wavelet and is a real and symmetric localized function in the t-f space used to generate the doubly indexed Wavelet ψ_{ab}. The scale factor "$|a|^{-1/2}$" has been chosen to keep the norm of the Wavelet invariant under the parameter change "a,b". Norm is the square root of the energy of the Wavelet response. The Wavelets $\psi_{a,b}$ and ψ are localized functions in the t-f space which means that both their time and frequency lengths are bounded. The discrete Wavelet has the time "t" replaced by the equivalent digital sample number "n" assuming the waveform is uniformly sampled at "T" second intervals.

Wavelets in digital t-f space have an orthogonal basis that is obtained by restricting the choice of the parameters "a,b" to the values $a=2^{-p}$, $b=qM2^{p}$ where 'p,q" are the new scale and translation parameters and "M" is the spacing or repetition interval $T_s=MT$ of the Wavelets (which from a communications viewpoint are symbols) at the same scale "p". Wavelets at "p,q" are related to the mother Wavelet by the equation ~~[1]~~

$$\psi_{p,q}(\mathbf{n}) = 2^{-p/2}\psi(2^{-p}\mathbf{n} - \mathrm{qM}) \qquad (3)$$

where the mother Wavelet is a real and even function of the sample coordinates. The orthonormality property means that these Wavelets satisfy the orthogonality equation with a correlation value equal to "1".

$$\sum_{\mathbf{n}} \psi_{p,q}\psi_{k,m} = 1 \text{ iff both } p = k \text{ and } q = m$$
$$= 0 \text{ otherwise} \qquad (4)$$

Wavelet representation of a digital t-f space starts with selecting an N sample time window of a uniform stream of digital samples at the rate of 1/T Hz (1/second) equivalent to a "T" second sampling interval. The N point or sample t-f space in FIG. **1** illustrates a Wavelet representation or "tiling" with Wavelets that are designed analytically or by an iterated filter construction.

The t-f space in FIG. **1** is partitioned or covered or tiled by a set of Wavelet subspaces $\{W_p, p = 0,1,...,m-1\}$ **1** where $N=2^m$. Each Wavelet subspace W_p **1** at scale "p" consists of the set of Wavelet time translations {q = 0,1,…, $N/2^{p+1}-1$} over this subspace. These Wavelet subspaces are mutually orthogonal and the Wavelets within each subspace are mutually orthogonal with respect to the time translates. This N-point t-f space extends over the time interval from 0 to (N-1)T **2** ~~where T is the digital sampling interval,~~ and over the frequency interval from 0 to (N-1) **3** in units of the normalized frequency fNT **4**.

The iterated filter bank in FIG. **2** is used to generate the Wavelets which cover the t-f space in FIG. **1**. Each filter stage **5** consists of a high pass filter (HPF) and a low pass filter (LPF). Output **6** of the LPF is subsampled by 2 which is equivalent to decimation by 2. This t-f space space is an N-dimensional complex vector metric space V **7**. At stage m in the iterated filter bank, the remaining t-f space V_{m-1} **8** is partitioned into V_{m+1} **9** and the Wavelet subspace W_{m+1} **10** .

Scaling functions and Wavelets at each stage of this filter bank satisfy the following equations

$$\varphi(\mathbf{n}) = 2^{-1/2}\sum_{\mathbf{q}}\mathbf{h}_{\mathbf{q}}\,\varphi(2\mathbf{n}-\mathbf{q}) \quad \forall q$$
$$\psi(\mathbf{n}) = 2^{-1/2}\sum_{\mathbf{q}}\mathbf{g}_{\mathbf{q}}\,\varphi(2n-q) \quad \forall \mathbf{q} \qquad \textbf{(5)}$$

where φ is the scaling function, ψ is the Wavelet, HPF_p coefficients are $\{h_q, \forall q\}$, LPF_p coefficients are $\{g_q, \forall q\}$, and the equations apply to the stages 0,1,…,m-1. Identifying the scale parameter and using the previous Wavelet formulations enable these equations to be rewritten for stages p=0,1,…,m-1 as

$$\varphi_p = \sum_{q}\mathbf{h}_q\,\varphi_{p-1,q} \quad \forall p$$
$$\psi_p = \sum_{q}g_q\,\varphi_{p-1,q} \quad \forall p \qquad \textbf{(6)}$$

For our application the HPF_p and LPF_p are quadrature mirror filters (QMF) with perfect reconstruction. This means they cover the subspace V_p with flat responses over the subband frequency including the edges of the frequency subband, and the HPF_p coefficients are the frequency translated coefficients for the LPF_p: $\{g_q=(-1)^q h_q\,,\ \forall q\}$.

Wavelet design using iterated filter bank starts with the selection of the scaling functions. Starting with a primative scaling function such as the one proposed by Daubechies ~~[1],~~ one can use the iterated filter construction given by equations **(5)** and **(6)** to derive successive approximations to a desired scaling function which has properties that have been designed into it by the selection of the filter coefficients $\{g_q, \forall q\}$ at each level of iteration. The Wavelets can be derived from these scaling functions using the iterated filter construction or scaling equations **(5)** and **(6)**.

Another use of the iterated filter construction is to design the scaling functions as Wavelets thereupon ending up with a larger set of Wavelets for multi-resolution analysis and synthesis as illustrated by Coifman's Wavelets in "Wavelet analysis and signal processing". ~~[2]. Design examples abound in the open literature and the recent publications [3], [4], [5], [6] are representative illustrations of the diverse applications of Wavelets.~~

~~SUMMARY OF INVENTION~~

SUMMARY OF THE INVENTION

~~This invention is a new and novel design of Wavelet multi-resolution waveforms and filters in the frequency domain with a property which provides a single waveform design for all of the waveforms at multiple resolutions and scales. Wavelets are designed to meet the specific application requirements, are complex, are defined by frequency harmonics, include a frequency translation parameter in addition to the scale and translation parameters in current Wavelets, and have the property that the set of design coefficients in the frequency domain remain invariant for all possible multi-resolution scales, and time-frequency translations. Frequency design harmonics and the frequency translation capability enable the waveform at multiple resolution scales to be derived from the single waveform design by scaling the dilation, translation, and frequency translation parameters using the set of frequency design harmonics. Wavelet waveform design is illustrated by Matlab 5.0 code to design a linear filter waveform using an iterative least-squares eigenvalue approach to minimize the non-linear least-squares cost function, and to scale this waveform design for multi-resolution application specified by the dilation, time translation, and~~

~~frequency translation parameters. Additional results are given for a constant amplitude minimum-shift-keying bandwidth-efficient modulation waveform and for a synthetic aperture radar waveform.~~

This invention ~~is a new approach to~~ for the design of multi-resolution Wavelet waveforms ~~that~~ improves their performance for engineering and scientific applications, and in particular for applications to communications and radar. Current practice is to 1) design traditional multi-resolution waveforms in the time domain using metrics which specify frequency performance and without consideration of Wavelet properties~~, and~~ or to 2) design Wavelet multi-resolution waveforms using the time-domain iterated multi-resolution filtering approach with a set of scaling functions used to perform the filtering and without direct considerations of the frequency performance. These two separate design approaches yield fundamentally different waveforms. ~~Our new~~This invention provides a means to combine these two approaches to generate a new multi-resolution Wavelet waveform with the best properties of the traditional multi-resolution waveforms and the Wavelet multi-resolution waveform.

~~Our~~ This invention introduces ~~the new~~ innovations for the design of our ~~new~~ Wavelet waveform that 1) include the ISI (intersymbol interference), ACI (adjacent channel interference), and QMF (quadrature mirror filter) requirements into the design algorithm along with non-linear modifications to the traditional passband and stopband frequency requirements which are used in the Remez-Exchange and eigenvalue LS algorithms~~ in references [8], [7] respectively~~, 2) select the frequency harmonics as the design coordinates, 3) use an appropriate subset of the available Fourier domain frequency harmonics as the design coordinates with the property that this subset of coordinates is a basis for the multi-resolution Wavelet waveform design, and 4)

design the multi-resolution Wavelet waveform for no excess bandwidth $\alpha=0$.

These innovations support the development of our new waveforms 1) that are generalizations of Wavelets in the frequency domain using a means which makes them useful for communications and radar over their t-f space, 2) that can be designed to be an orthonormal basis or orthonormal set of coordinates over the available frequency bandwidth with the implicit property that the excess bandwidth vanishes $\alpha=0$, to within the accuracies allowed by communication and radar design implementations, and 3) that have multi-scale properties which allow a single dc waveform design to be used to uniquely define the complete set of ~~new~~ waveforms over the t-f space for multi-scale applications Specific design algorithm examples developed in this invention disclosure are the LS design algorithms that use eigenvalue and gradient search techniques in the frequency domain to find the best waveform design which minimizes the corresponding LS error residual cost function that is a weighted linear sum of the residual error metrics.

Wavelet ~~Waveform~~ waveform performance calculated in this invension disclosure from the application of these LS design algorithms, demonstrates the capability of this invention to provide a means to design waveforms that are improved over current practice. There are other algorithmic design algorithms which can be realized by modifications to this invention. An example given in this invention disclosure is the modification of these LS algorithms for application to constant amplitude bandwidth efficient (BEM) waveforms for communications.

BRIEF DESCRIPTION OF THE DRAWINGS AND THE PERFORMANCE DATA

~~**BRIEF DESCRIPTION OF DRAWINGS AND PERFORMANCE DATA**~~

The above-mentioned and other features, objects, design algorithms, and performance advantages of the present invention will become more apparent from the detailed description set forth below when taken in conjunction with the drawings and performance data wherein like reference characters and numerals denote like elements, and in which:

FIG. **1** is a Wavelet ~~an~~ N-point t-f space extending over the time interval (0, (N-1)T] and the frequency interval (0, (N-1)/NT], which is tiled or covered by a set of orthonormal Wavelets at the scales p=0,1,…,m-1.

FIG. **2** is a Wavelet iterated filter bank used to generate the set of Wavelets which tile or cover the t-f space in FIG. **1**.

FIG. **3** illustrates the power spectral density (PSD) of our ~~new~~ Wavelet waveform at dc, and the set of stopband and passband design requirements.

~~FIG. 3 is the power spectral density (PSD) template for the the stopband and passband used to construct the LS error metrics,~~

FIG. **4** is the flow diagram of the LS metrics and cost functions and the final cost function used to find the optimal LS solution for our ~~the~~ Wavelet waveform.

FIG. **5** is flow diagram for the LS recursive solution algorithm to find the optimal harmonic coordinates that define the LS solution for our Wavelet waveform.

~~FIG. 5 is the Matlab 5.0 code for the LS algorithm used to design the Wavelet waveform in FIG. 6.~~

FIG. **6** plots the dc PSD in dB units for the frequency response of ~~the~~ our mother Wavelet at dc and the square-root raised-cosine (sq-rt r-c) waveforms with excess bandwidth parameter α= 0.22, 0.40 vs. the normalized frequency in units of symbol rate $1/T_s$.

FIG. **7** plots the dc PSD in dB units for our waveforms vs. the normalized frequency fT_s for ~~the~~ our ~~new~~ Wavelet waveform designed with modifications to the LS algorithms for application to constant amplitude BEM communications, and for a Gaussian minimum shift keying (GMSK) waveform.

~~FIG. 7 plots the dc PSD in dB units for the frequency response of the mother Wavelet at dc and an optimized Gaussian minimum shift keying (GMSK) waveform vs. the normalized frequency fT_s.~~

FIG. **8** plots the amplitude of the dc radar ambiguity function vs. the normalized frequency fT_p and normalized time tT_c where the pulse time T_p and chip time T_c are both equal to the communications symbol interval T_s for this example, for the new waveform and an unweighted chirp waveform.

~~DISCLOSURE OF INVENTION~~

DISCLOSURE OF THE INVENTION

~~Wavelet multi-resolution waveforms incorporate a frequency translation, are complex, are designed in frequency harmonic coordinates, a single mother Wavelet design is used for all scales, and in the t-f space are realized as FIR filters and waveforms.~~

New~~These~~ Wavelet waveforms in this invention disclosure are generalizations of Wavelets in t-f space which enable them to be useful for communications and radar applications. This generalization is accomplished by 1) the ~~addition~~ introduction of a frequency translation, by 2) ~~relaxing~~ changing the orthonormality condition in equation **(4)** to apply to waveforms within the same space {q} and over the scales {p} with the inclusion of the frequency translation, and 3) by their characterization and design in the Fourier domain. With frequency translation the analytical formulation of these new waveforms as a function of the baseband or mother waveform centered at dc(dc refers to the origin f=0 of the frequency space) becomes

~~New waveform as a function of dc waveform~~

$$\psi_{p,q,r}(n) = 2^{-p/2}\psi(2^{-p}n - qM)\,e^{i2\pi f_c(p,r)nT} \qquad (7)$$

where $f_c(p,r)$ is the center frequency of the frequency translated dc waveform, at scale "p" and frequency index "r". The purpose of the frequency index "r" is to identify the center frequencies of the waveforms at the scale "p" in the t-f space. ~~The dc or baseband or mother waveform is the generalization of the mother Wavelet for multi-resolution waveforms.~~

These waveforms satisfy the complex orthonormality equations

~~Orthogonality equations~~

$$\sum_{n} \psi_{p,q,r} \psi^{*}_{k,m,v} = 1 \text{ iff } p = k \text{ and } q = m \text{ and } r = v$$
$$= 0 \text{ otherwise} \qquad (8)$$

where "*" is conjugation, and are generalizations of the orthonormality equations for the analytical Wavelets in **(4)**.

The new waveforms in equation **(7)** expand the Wavelet analytical formulation to include a frequency variable. Wavelets are functions of the scale and translation parameters "p,q". ~~The concept of an additional parameter to provide an added degree of flexibility in their tabulation was first introduced by the Coifman library of Wavelets [2] which use an oscillaton parameter for tabulation that roughly corresponds to the frequency of oscillation of the Wavelets.~~ The frequency variable together with the Fourier domain design are entirely new means for deriving these new waveforms as generalization of the traditional Wavelets ~~and their modification with the added parameter in [2].~~

~~New~~ These waveforms are generalizations of Wavelets in the frequency domain using a means which makes them useful for communications and radar in the t-f space. The basis vectors for this metric space V consist of a subset of the admissible set of scaled and translated waveforms $\{\psi_{p,q,r}, \forall p,q,r\}$ derived from the dc waveform ψ as per equation **(7)**. An admissible waveform is any combination that covers V=t-f space. We are interested in the Fourier domain representation of the dc waveform ψ in V,

and in particular in a subset of the discrete Fourier transform (DFT) harmonic coefficients over the Fourier domain which we intend to use as the design coordinates. Starting with the z-transform and continuous Fourier transform, the DFT harmonic coefficients are defined by the following equations

DFT Harmonic Coefficients **(9)**

$$\psi(z) = \sum_n \psi(n)\, z^{-n} \quad \textit{z-transform}$$

$$\psi(\omega) = \sum_n \psi(n)\, e^{-i\omega n} \quad \textit{Fourier transform}$$

$$\psi_k = \sum_n \psi(n)\, W_{N'}^{-kn} \quad \textit{DFT harmonic coefficients for } \forall k$$

where

$$\psi(\omega) = (1/N') \sum_k \Psi_k \sum_n e^{i(2\pi k/N' - \omega)n}$$

$$= \sum_k \psi_k \sin((\omega/2 - \pi k/N')N') / N\sin(\omega/2 - \pi k/N')$$

$$= \sum_k \psi_k \,[\text{Harmonic interpolation for "k"}]$$

$$W_{N'}^{kn} = e^{i2\pi kn/N'}$$

$\{k\}$ = **DFT frequency or harmonic coefficients such that $f_k = k/N'T$ where f_k is the harmonic frequency corresponding to "k"**

N' = **length of** $\psi(n)$

where $\Psi(\omega) = |\psi(\omega)|^2$ is the power spectral density of the dc waveform. These equations define the frequency representation of our new waveforms in terms of the available set of harmonic coefficients, which set is considerable larger than required for most applications.

~~New~~ Our new waveforms are an orthonormal basis with no excess bandwidth, ~~are properties that we will demonstrate. Orthomality and no excess bandwidth are~~ which properties ~~which~~

are asymptoticly approached by our new waveforms to within design accuracies inherent in communications and radar. To ~~proceed~~ demonstrate these properties we need to identify the structure of the dc waveform in V. We start with definitions for the parameters and coordinates in the following equation **(10)**. The waveforms derived from the dc waveform will be designed to be orthogonal over both time translates "MT" and frequency translates "1/~~LT~~MT" which respectively correspond to the Wavelet symbol spacing T_s=MT and the adjacent channel spacing $1/T_s$. This means the orthogonal spacing of the waveforms in V are at the time-frequency increments (MT, 1/~~LT~~MT) = (T_s. $1/T_s$). In the interests of constructing our ~~new~~ orthonormal multi-resolution waveforms to cover V it will be convenient to assume that M,L are powers of 2. We need the following definitions for the parameters and coordinates.

N' = Length of ψ which is an even function about the center and which spans an odd number of points or samples
= ML + 1 where M, L are assumed to be even functions for convenience of this analysis
= Number of points of ψ

M = Sampling interval for ψ
= Spacing of ψ for orthogonality

L = Length of ψ in units of the sample interval M
= Stretching of ψ over L sample intervals

$n = n_0 + n_1 M$
= partitioning into an index n_0 over the sample length $n_0 = 0,1,...,M-1$ and an index $n_1 = 0,1...,L-1$ over the sample intervals

$k = k_0 + k_1 L$
= partitioning into an index k_0 over the harmonic frequencies $k_0 = 0,1,...,L-1$ corresponding to the stretching and an index $k_1 = 0,1,...,M$ over the harmonics frequencies corresponding to the admissible frequency slots for ψ

The harmonic design coordinates are selected using the following observation. For most applications and in the following development it is assumed that the waveforms are spectrally contained in the frequency interval $1/\text{~~LT~~}$ MT corresponding to the frequency spacing. This suggests the harmonic design coordinates be restricted to the subset of L harmonics $\{k_0=0,1,...,L-1\}$ covering this spacing. These L harmonics correspond to the stretching of the mother waveform over the L repetition intervals.

Obviously, for some applications as will be demonstrated later, the spectral containment is spread out over several 1/LT frequency increments whereupon one must increase the subset of design harmonics to possibly 2L, 3L or larger.

~~Pursuing this application using L design harmonics~~, The ~~the~~DFT equations for the dc waveform in **(9)** when rewritten in terms of the L harmonic design coordinates $\{\psi_{k_o}, \forall k_0\}$ become:

DFT equations for dc waveform

$$\psi_{k_0} = \sum_{n} \psi(n)\, W_N^{k_o n} \quad \text{harmonic design coordinates}$$

$$\psi(n) = (1/N') \sum_{k_0} \Psi_{k_0}\, W_N^{k_o n} \quad \text{new waveform defined in terms of the L harmonic design coordinates } \{\psi_{k_0}, \forall k_0\} \qquad \textbf{(11)}$$

It will now be shown that ~~It will be proven that~~ the use of these L harmonic design coordinates is sufficient ~~for our new waveform~~ under time translates to be a basis for the corresponding subspace of V. ~~This~~ which means these waveforms provide a complete set of coordinates to describe this subspace. ~~We will use~~ the will use the theorems of Karhunen-Loeve and Mercer and will limit the demonstration to the dc waveform for simplicity and without loss of generality. We start by considering ~~Consider~~ the expansion of a random complex sequence {z(n), $\forall$n} in a series of waveform coordinates consisting of time translates of the mother waveform ψ. The sequence {z(n), $\forall$n} is a zero-mean stationary random process which is orthonormal over the sample interval "M" and has a frequency spectrum which is flat and extends over the

frequency range 1/LT which is centered at baseband corresponding to a zero frequency. This means the {z(n), $\forall$n} cover the subspace of V corresponding to the scale of our ~~new~~ dc waveform ψ and its time translates $\{\psi(n-qM)=\psi_q(n), \forall q\}$. In addition, the V is now considered to be extended over a time interval which is relatively large compared to the N-dimensional t-f space in FIG. —**1,2** to avoid end-effects on the analysis. We start by approximating the sequence {z(n), $\forall$n} by the $\{\hat{z}(n), \forall n\}$ where:

$$\hat{\mathbf{z}}(\mathbf{n}) = \sum_{\mathbf{q}} \mathbf{Z}_{\mathbf{q}}\, \psi(\mathrm{n}-\mathrm{qM}) = \sum_{\mathbf{q}} \mathbf{Z}_{\mathbf{q}}\, \psi(\mathbf{n}_0 + (\mathbf{n}_1 - \mathbf{q})\mathbf{M})$$

where the complex coefficients $\{Z_q\}$ are derived from the original sequence using the orthogonality properties of ψ **(12)**

$$Z_q = \sum_{\mathrm{n}} \mathrm{z(n)}\, \psi^*(\mathrm{n}-\mathrm{qM}) = \sum_{\mathrm{n}} \mathrm{z(n)}\, \psi_q(\mathbf{n})$$

The following equations prove that the coefficients $\{Z_q, \forall q\}$ are orthonormal:

$$\mathbf{Z_q Z_{q'}}^* = \sum_{\Delta \mathbf{n}} \mathbf{z}(\Delta\mathbf{n}-\mathbf{qM})\mathbf{z}^*(\Delta\mathbf{n}-\mathbf{q'M})\psi_{\mathbf{q}}(\Delta\mathbf{n})\psi_{\mathbf{q'}}{}^*(\Delta\mathbf{n}) \qquad \textbf{(13)}$$

$$= \delta_{qq'} \sum_{\mathrm{n}} |\psi_q(\mathbf{n})|^2 \quad \text{since the sequence } \{z\} \text{ is orthonormal for qM time translates}$$

$$= \delta_{qq'} \quad \text{with normalization of the energy of } \psi$$

Equations **(12)** and **(13)** together prove the Karhunen-Loeve's theorem which proves the following equation for the

accuracy in approximating the stochastic sequence {z(n), $\forall$n} by $\{\hat{z}(n), \forall n\}$. This accuracy is expressed by the expected "E(o)" squared error "(o)" in this approximation:

$$E\left\{\left|z(n)-\hat{z}(n)\right|^2\right\} = 1 - \sum_{n_1}\left|\psi(n_0+n_1M)\right|^2 \qquad \textbf{(14)}$$

We need to prove that the right hand side of this equation is zero which then proves that the approximating sequence is equal to the original sequence in the mean-square sense. In turn this proves that the new waveform coordinates $\{\psi_q, \forall q\}$ are a basis for the original sequence {z(n), $\forall$n} which is our goal.

The right hand side of equation **(14)** when set equal to zero expresses Mercer's theorem so our goal is to prove Mercer's theorem. To do this we use the DFT of ψ in equation **(11)** and the coordinates in **(10)** to evaluate the right hand side of equation **(14)**. We find

$$1 - \sum_{n_1}\left|\psi(n+n_1M)\right|^2 = 1 - \sum_{k_0}\sum_{k_0'}\Psi_{k_0}\Psi_{k_0'}\,W_N^{\Delta k_0 n_0}\,\Gamma$$

$$\textit{where} \quad \Gamma = (1/L)\sum_{n_1} W_L^{\Delta k_0 n_1}$$

$$= \sin(\pi\,\Delta k_0)/L\sin(\pi\,\Delta k_0/L)$$

$$= 1 \text{ for } \Delta k_0 = 0 \qquad \textbf{(15)}$$

$$= 0 \text{ otherwise}$$

This proves that

$$1 - \sum_{n_1}\left|\psi(n+n_1M)\right|^2 = 0 \quad \forall n_0$$

which proves that equation **(~~18~~14)** reduces to

$$E\left\{\left|z(n)-\hat{z}(n)\right|^2\right\} = 0 \qquad \text{(16)}$$

which as per the above proves that the set of multi-resolution waveforms is a basis. This proof easily generalizes to the multi-resolution waveforms at all of the scales {p} and time translates {q}, and to the expansion of the harmonic design coordinates over 2L, 3L, … as required by the application.

~~New~~ Next we demonstrate that these waveforms have multi-scale properties. that we will demonstrate. We start with the observation that the ~~The~~ Fourier domain design for the new waveforms provides a natural and easy way to derive the complete set of waveforms $\{\psi_{p,q}, \forall p,q\}$ for the space V from the design of the dc waveform ψ by using the same invariant set of Fourier domain harmonic design coordinates $\{\Psi_{k_o}, \forall k_0\}$ derived for the dc multi-resolution waveform. This demonstration requires that we show 1) how the multi-scale transformations are implemented with the design in the Fourier domain, and 2) how the waveform design remains invariant under scale changes.

First consider the multi-scale transformation which derives the waveforms at the scale and shift parameters "p,q" ~~for~~ from the dc waveform at scale "p=0" and centered at the origin "q=0". We begin by extending the parameters and coordinates in equation **(10)**, to include both scaling and subsampling or decimation in a form that is equivalent to the iterated filter bank construction which is used to derive the current Wavelet waveform using the filter scaling functions. Starting with the coordinates at scale "p=0" the parameters and coordinates at scale "p=p" are given by the equations:

~~p~~=0 parameters and coordinates

$$n = n_0 + n_1 M \quad (17)$$

$$n_0 = a_0 + a_1 2 + \ldots + a_{m-1} 2^{m-1}$$

$$= M \text{ points}$$

$$M = 2^m$$

$$n_1 = b_0 + b_1 2 + \ldots + b_{l-1} 2^{l-1}$$

$$= L \text{ points spaced at } M \text{ sample intervals}$$

~~L = 2~~

p=p parameters and coordinates

$2^{-p}\, n(\downarrow 2^p)$ = scaled by "2^{-p}"

and subsampled or decimated by 2^p:1

$= n_0(p) + n_1(p)M$

$2^{-p}\, n_0(\downarrow 2^p)$ = scaled by "2^{-p}"

and subsampled or decimated by 2^p:1

$= n_0(p)$

$= a_p + a_{p-1}2 + \ldots + a_{p+m-1} 2^{p+m-1}$

$= M$ points spaced at 2^p sample intervals

$2^{-p}\, n_1(\downarrow 2^p)$ = scaled by "2^{-p}"

and subsampled or decimated by 2^p:1

$= n_1(p)$

$= b_p + b_{p+1}\, 2 + \ldots + b_{p+l-1}\, 2^{p+l-1}$

$= L$ points spaced at $M2^p$ sample intervals

together with the observation that the sampling interval "T" is increased to "2^pT" under the scale change from "p=0" to "p=p" and subsampling or decimation from "1:1" to "2^p:1". Combining these

equations with the analytical formulation in **(7)** and the Fourier domain representation in **(11)** enables the waveforms at the parameters "p,q" to be written as a function of the Fourier domain harmonic design coordinates:

$$\psi_{p,q,r}(n) = 2^{-p/2}\psi(2^{-p}n - qM)\, e^{i2\pi f_c(p,r)nT}$$
$$= (2^{-p/2}/N') \sum_{k_0} \Psi_{k_0} W_{N'}^{k_0(n(p)-qM)}\, e^{i2\pi f_c(p,r)n(p)2^pT} \qquad \textbf{(18)}$$

for all admissible scale, translation, and frequency index parameters "p,q,r".

Next we need to demonstrate that the frequency domain design in **(11)** remains invariant for all parameter changes and in particular for all scale changes. This multi-scale property expresses the accordion behavior of the design in that the Wavelets at different scales are simply the stretched and compressed versions of the mother waveform with the appropriate frequency translation indices. This multi-scale invariancy means that the design for a M=16 channel filter bank remains the same for M=100 or M=10,000 channel filter banks, when the overlap L and the performance goals remain constant. To demonstrate this invariant property across scales, we consider the ~~mr~~ multi-resolution waveform at scale "p" with the other parameters set equal to zero for convenience "q=0, r=0" and without loss of generality. The Fourier domain frequency response $\Psi(f)$ can be evaluated starting with the original formulation in equation **(7)**:

DFT at "p, q=0, r=0" **(19)**

$$\Psi_p(f) = (1/N')\sum_{k_0}\Psi_{k_0}\sum_{n(p)}W_{N'}^{-(fN'2^pT\ -k_0)\,n(p)}$$

$$= \sum_{k_0}\Psi_{k_0}\left[\frac{\sin(\pi\ (fN'2^pT - k_0))}{N'\sin(\pi\ (fN'2^pT - k_0)/N')}\right]$$

$$= \sum_{k_0}\Psi_{k_0}\ \left[\text{Harmonic interpolation for "}k_0\text{"}\right]$$

This only differs from the harmonic representation in equation **(9)** in the restriction of the design coordinates to the subset of harmonic coefficients $\{\psi_{k_0}, \forall k_0\}$ and the stretching of the time interval to "2^pT" corresponding to the scale "p=p". The harmonic interpolation functions are observed to remain invariant over scale changes upon observing that the frequency scales as "$f\sim 1/2^pT$" which means the "frequency*time" product remains invariant with scale changes as per the fundamental property of the waveforms. This means the harmonic interpolation functions remain invariant with scale change and therefore the frequency response remains an invariant. This demonstrates the waveform design is an invariant across the waveform scales which means we only need a single design for all scales or resolutions of interest.

LS design algorithms for new waveform will be described to illustrate the advantages our ~~new~~ waveform has over current designs. The two LS algorithms described are the eigenvalue and

the gradient search which respectively can be reduced to algorithms which are equivalent to ~~the original~~ current eigenvalue ~~[7]~~ and Remez-exchange ~~[8]~~ waveform design algorithms for application to a uniform filter bank. We consider the t-f space which is spanned by a uniform polyphase filter bank consisting of M channels at the frequency spacing f_w=1/MT where T is the digital sampling interval, and the filter waveform FIR time response is stretched over L sampling time intervals T_s. This polyphase filter bank is ideally decimated which means the filter ouput sample rate $1/T_s$ is equal to the channel-to-channel spacing T_s=MT, equivalent to stating that there is no excess bandwidth α=0. Our design for this topology is immediately applicable to an arbitrary set of multi-resolution filters through the scaling equation **(18)** which gives the design of our waveform at arbitrary scales in terms of our design of the dc waveform.

For this polyphase filter bank used to construct the dc waveform or filter impulse response, our LS example design algorithms will use 5 metrics consisting of the 2 prior art passband and stopand metrics, and the 3 new metrics consisting of the ISI, ACI, and QMF, and solve the LS minimization problem using as design coordinates the subset of harmonic coordinates which are a basis. Since our ~~2~~ two example LS design algorithms only differ in the use of an eigenvalue LS optimization and the use of a gradient search LS optimization, the flow diagrams for the construction of the cost functions and the solution for the optimal waveform will be identical. However, there are differences in the construction of the cost functions from the respective metrics and in the iterative solution mathematics. Both LS solutions for the harmonic design coordinates minimize the weighted sum of the error residuals or cost functions from the 5 metrics. These design coordinates ~~for~~ are the Fourier harmonics $\{\psi_{k_o}, \forall k_0\}$ for $\{k_0 = 0,1,\ldots,L-1\}$. Resulting algorithms

are easily extended to the applications requiring the design coordinates to cover 2L, 3L, … harmonics.

Frequency domain design coordinates are related to the waveform time domain digital samples or coordinates as follows.

Mappings of ~~time ⇔~~ frequency to time ____(20)

Time domain design coordinates $\{\psi(n), \forall n\}$ are real and symmetric and can be represented by the reduced set $\{h_t(n), n=0,1,\ldots,ML/2\}$

$h_t(n) = \psi(0)$ for n=0

$= 2\psi(n)$ for n=1,2,…,ML/2

= time domain design coordinates

Frequency domain harmonic design coordinates $\{\psi_{k_o}, \forall k_0\}$ are real and symmetric and can be represented by the reduced set $\{h_f(k), k=0,1,,\ldots,L-1\}$

$h_f(k) = \psi_{k_0}$ for $k=k_0=0$

$= 2\psi_{k_0}$ for $k=k_0=1,2,\ldots,L-1$

= frequency domain design coordinates

Mapping of the frequency coordinates $\{h_f(k), k=0,1,\ldots,L-1\}$ into the time coordinates $\{h_t(n), n=0,1,\ldots,ML/2\}$ is defined by the matrix transformation to within a scale factor

$h_t = B\ h_f$

where

$h_f = (h_f(0), \ldots, h_f(ML/2))^t$ transpose of column vector

$h_t = (h_t(0), \ldots, h_t(ML/2))^t$ transpose of column vector

B = (ML/2 +1) x L matrix

= [B_{kn}] matrix of row k and column n elements B_{kn}

$B_{kn} = 1$ ~~/ML~~ for n=1

$= 2\cos(2\pi kn/ML)$ otherwise

~~Mappings of the frequency coordinates $\{h_f(k),\ k=0,1,\ldots,L-1\}$ into the time coordinates $\{h_t(n),\ n=0,1,\ldots,ML/2\}$ and vice versa are defined by the matrix transformations~~

~~$h_t = B\ h_f$~~

~~$h_f = B^{-1}\ h_t$~~

~~where~~

~~$h_f = (h_f(0), \ldots, h_f(ML/2))^t$ transpose of column vector~~

~~$h_t = (h_t(0), \ldots, h_t(ML/2))^t$ transpose of column vector~~

~~$B = (ML/2+1) \times L$ matrix~~

~~$= [B_{kn}]$ matrix of row k and column n elements B_{kn}~~

~~$B_{kn} = 1/ML+1$ for n=1~~

~~$= 2\cos(2\pi kn/ML+1)$ otherwise~~

~~$B^{-1} = L \times (ML/2+1)$ matrix~~

~~$= [\mathbf{B}^{-1}_{kn}]$ matrix of row k and column n elements $\mathbf{B}^{-1}_{kn}$~~

~~$\mathbf{B}^{-1}_{kn} = 1$ for n=1~~

~~$= 2\cos(2\pi kn/ML+1)$ otherwise~~

~~and~~

~~$B^{-1}B = I$ L x L identify matrix~~

~~$B\ B^{-1} = I$ (ML/2+1) x (ML/2+1) identity matrix~~

wherein the N′=ML+1 has been replaced by ML since a single end point has been added to the the FIR to make it symmetrical for ease of implementation for the example Wavelet being considered with a sample at the mid-point that makes the number of samples N′ an odd number.

Passband and stopband metrics and cost functions are derived with the aid of FIG. **3** which defines the po~~wer spectral density (PSD)~~ parameters of interest for the passband and stopband of the PSD $\Psi(\omega)$ for communications applications.

Requirements for radar applications include these listed for communications. Referring to FIG. **3** the passband **11** of the waveform PSD is centered at dc (f=0) since we are designing the dc or baseband waveform, and extends over the frequency range ω_p extending from $-\omega_p/2$ to $+\omega_p/2$ **12** in units of the radian frequency variable $\omega=2\pi fT$ **13** ~~where T is the digital sampling interval defined in FIG. 1~~. The frequency space extends over the range of f=-1/2T to f=+1/2T which is the frequency range in FIG **1** translated by -1/2T so that the dc waveform is at the center of the frequency band. Quality of the PSD over the passband is expressed by the passband ripple **14**. Stopband **15** starts at the edge **16** of the passbands of the adjacent channels $+/-\omega_a/2$ **16** and extends to the edge of the frequency band $\omega=+/-\pi$ **17** respectively. Stopband attenuation **18** at $+/-\omega_a/2$ measures the PSD isolation between the edge of the passband for the dc waveform and the start of the passband for the adjacent channels centered at $+/-\omega_s$ **19**. Rolloff **20** of the stopband is required to mitigate the spillover of the channels other than the adjacent channels, onto the dc channel. Deadband or transition band **21** is the interval between the passbands of contiguous channels, and is illustrated in FIG. **3** by the interval from $\omega_p/2$ to $\omega_a/2$ between the dc channel and adjacent channel at ω_a. Waveform sample rate ω_s **22** is the waveform repetition rate. For the LS example algorithms, the waveform sample rate is equal to the channel-to-channel spacing for zero excess bandwidth. Therefore, $1/T_s= \omega_s/2\pi T=1/MT$ which can be solved to give $\omega_s=2\pi/M$ for the radian frequency sampling rate of the filter bank which is identical to the waveform repetition rate.

We start by rewriting the DFT equations for the dc waveform in (11) as a function of the $\{h_f(k), k=0,1,\ldots,L-1\}$

$$\psi(\omega) = \sum_{n} \psi(n)\cos(n\omega)$$

$$= c^t B h_f \quad \text{using (21) and the definition of the vector "c"} \qquad \textbf{(21)}$$

$$c = (1, \cos(\omega), \ldots, \cos((ML/2)\omega))^t \quad \text{transpose of column vector}$$

which is equivalent to the equation for $\psi(\omega)$ in **(9)** expressed as a linear function of the $\{h_f(k),\ k=0,1,\ldots,L-1\}$. ~~However, this functional form suggested by the eigenvalue formulation [7] is more convenient to analyze.~~ An ideal "c" vector "c_r" will be introduced for the passband and the stopband in FIG. ~~3~~ in order to identify the error residual $\delta\psi(\omega)$ at the frequency "ω" in meeting the ideal passband and stopband requirements. The ideal PSD is flat and equal to "1" for the passband, and equal to "0" for the stopband. We find

Error residuals for passband and stopband **(22)**

$$c_r = (1,1,\ldots,1)^t \quad \text{passband ideal "c"}$$

$$= (0,0,\ldots,0)^t \quad \text{stopband ideal "c"}$$

$$\delta c = c_r - c \quad \text{error vector}$$

$$\delta\psi(\omega) = \delta c^t B h_f$$

$$= \text{Residual error in meeting the ideal spectrum at "}\omega\text{"}$$

The LS metric for the passband and stopband can now be constructed as follows for the eigenvalue and the LS optimization (or equivalently, the LS algorithm) design algorithms.

Passband and stopband metrics **(23)**

$$J(\text{band}) = \frac{1}{band}\int_{band}\left|\delta\psi(\omega)\right|^2 d\omega \qquad \text{Eigenvalue}$$

$$= h_f^t \mathbf{R}\ h_f \qquad \text{Eigenvalue}$$

$$= \left\|\delta\psi\right\|^2 \qquad \text{LS}$$

~~(23) continued~~

where

band = $[0, \omega_p)$ passband

= $(\omega_s, \pi]$ stopband

$$\mathbf{R} = \frac{1}{band}\int_{band}(B^t\,\delta c\,\delta c^t\,B)\,d\omega$$

= L x L matrix

$\delta\psi$ = $(\delta\psi(\omega_1), \ldots, \delta\psi(\omega_u))^t$

= vector of error residuals at the frequencies $\omega_1, \ldots, \omega_u$ across the band

$\|(o)\|$ = norm or length of the vector (o) and which includes a cost function for the errors of the individual components

where it is observed that the eigenvalue approach requires that the LS metrics be given as quadratic forms in the design coordinates $\{h_f(k), k=0,1,\ldots,L-1\}$ whereas with the LS approach it is sufficient to give the LS metrics as vector norms with imbedded cost functions or an equivalent formulation.

QMF metrics express the requirements on the deadband that the PSD's from the contiguous channels in FIG. **3** add to unity across the deadband $[\omega_p, \omega_s]$ in order that the filters be QMF filters. By suitable modification of the error vector δc, the

previous construction of the passband and stopband metrics can be modified to apply to the deadband. ~~This is a Wavelet requirement on the frequency coverage of the Wavelet basis as observed in Table 1.~~ We find

Deadband metrics **(24)**

$$J(\text{deadband}) = \frac{1}{deadband} \int_{\text{deadband}} \left|\delta\psi(\omega)\right|^2 d\omega \quad \text{Eigenvalue}$$

(24) continued

$$= h_f' \mathbf{R}\ h_f \quad \text{Eigenvalue}$$

$$= \left\|\delta\psi\right\|^2 \quad \text{LS}$$

where

$$\delta c = c_r - c(\omega) - c(\pi/M - \omega)$$

where $c(\omega)=c$ as defined in **(22)** and **(23)**, and $c(\pi/M - \omega) = c$ at the offset frequency "$\pi/M - \omega$" corresponding to the overlap of the contiguous filters over the deadband.

Orthonormality metrics measure how close we are able to designing the set of waveforms to be orthonormal over the t-f space, with the closeness given by the ISI and the ACI. ~~ISI is the non-orthogonality error between channel output samples separated by multiples of the sampling interval 1/MT seconds where T is the sample time and M is the interval of contiguous samples. ACI is the non-orthogonality error between between channel output samples within a channel and the samples in adjacent channels at the same sample time and at sample times separated by multiples of the sample interval. As observed as~~

~~noise contributions within each sample in a given channel, the ISI is the noise contribution due to the other received waveforms at the different timing offsets corresponding to multiples of the sampling interval. Likewise, the ACI is the noise contribution due to the other waveforms in adjacent channels at the same sampling time and at multiples of the sampling interval.~~

ISI and ACI errors are fundamentally caused by different mechanisms and therefore have separate metrics and weights to specify their relative importance to the overall sum of the LS metrics. ISI is a measure of the non-orthogonality between the stream of waveforms within a channel as per the construction in FIG. **3**. On the other hand, ACI is a measure of the non-orthogonality between the waveform within a channel and the other waveforms in adjacent channels. This means the stopband performance metric has a significant impact on the ACI due to the sharp rolloff in frequency of the adjacent channel, and the ACI metric is then a measure of the residual non-orthogonality due to the inability of the stopband rolloff in frequency from completely eliminating the ACI errors.

We assume that the received waveform is identical to the filter waveforms and is transmitted at the filter output sample intervals equal to ~~1/~~MT seconds. The second assumption means we are assuming the receiver is synchronized with the received signal. Since there is no information lost by sampling asynchronously with the received waveform, we are free to make this synchronization assumption without loss of generality. ISI metrics are derived in the following set of equations.

ISI metrics **(25)**

Mapping of h_f into ψ

$\psi = (\psi(-ML/2), \ldots, \psi(ML/2))^t$ transpose of column vector

$= H\ h_f$

H = (ML+1) x L matrix of elements H_{kn}

H_{kn} = 1 for n=1

= 0.5 cos(2πkn/ML+1) otherwise

Offset matrix A

A = L x (ML+1) matrix of elements A_{kn}

A_{kn} = 0 for row vector k=1

= [0 0 ... ψ(-ML/2) ... ψ((L-k)M+1)] row vector k

~~(25) continued~~

1 2 kM LM+1 **column elements**

ISI error vector δE

δE = L x 1 column vector

= A H h_f

ISI metric

$J(ISI) = \delta E^t \delta E$ Eigenvalue

= Non-linear quadratic function of h_f

$= \|\delta E\|^2$ LS

ACI metrics are derived using the ISI metric equations with the following modifications.

ACI metrics **(26)**

Mapping of h_f into ψ is the same as developed for ISI

Offset matrix A elements are changed as follows to apply to Channel 1:

A_{kn} = 0 for row vector k=1

= [0 0 ... $\psi(-ML/2)\,W_M^0$ ... $\psi((L-k)M+1)\,W_M^{(L-k)}$]

1 2 kM+1 LM+1

which means the ACI error vector δE is

δE = L x 1 column vector

= A H h_f ——————————— h_f

ACI metric for the two contiguous channels

$J(ISI) = 2\ \delta E^t\ \delta E$ Eigenvalue

= Non-linear quadratic function of h_f

$= 2\ \|\delta E\|^2$ LS

where the factor "2" takes into account there are two contiguous channels or one on either side of the reference channel 0 in FIG. **3**. Because of the fast rolloff of the frequency spectrum the addition of more channels into the ACI metric is not considered necessary, although the functional form of the ACI metric in **(26)** allows an obvious extension to any number of adjacent channels which could contribute to the ACI.

Cost function J for the LS algorithms is the weighted sum of the LS metrics derived in **(23)**, **(24)**, **(25)**, **(26)**. The LS algorithms minimize J by selecting the optimal set of frequency coordinates $\{h_f(k), \forall k\}$ for the selected set of parameters used to specify the characteristics of the dc waveform, frequency design coordinates, LS metrics, and weights. Cost function and optimization techniques are given by the equations

Cost function J **(27)**

$$J = \sum_x w(metrics)\, J(metrics)$$

= weighted sum of the LS metrics J(metrics)

where

metrics = passband, stopband, deadband, ISI, ACI

$\{w(metrics), \forall metrics\}$ = set of weights

$$\sum_x w(metrics) \quad = 1 \quad \text{normalization}$$

Optimization goal

Goal: minimize J with respect to the selection of the $\{h_f(k), \forall k\}$

Optimization algorithms

Two algorithms are the Eigenvalue and the LS optimization where the eigenvalue optimization algorithm uses the non-linear quadratic formulations of the LS metrics and the LS optimization algorithm uses the norm formulations for the LS metrics.

FIG. **4** is a summary of the LS metrics and the construction of the cost function J. Design parameters **23** are ~~the input and output design parameters. Input parameters are the number of polyphase channels M or equivalently the number of digital samples at spacing T over the symbol interval T_s=MT, the length of the FIR time response for the waveform in units of~~ L, ~~which are the number of digital samples per waveform repetition interval T_s so that the total number of digital samples for the symmetric FIR time response is equal to~~ N'=ML+1, number of DFT samples per FIR length n_fft for implementation of the LS algorithms, passband radian frequency ω_p, stopband radiam frequency ω_a, waveform repetition rate in radian frequency ω_s, selection of the set of design coordinates $\{h_f\}$ to be used in the optimization, and the metric weights {w(metrics)}. Output parameters are the set of harmonic design coordinates $\{h_f\}$ that minimize J. Band metrics **24** are the passband, stopband, and deadband metrics defined in equations **(23)**, **(23)**, **(24)** respectively. Interference metrics **25** are the ISI and ACI

metrics defined in equations **(25)** and **(26)** respectively. LS cost function J **26** is the weighted linear sum of the metrics defined for the band **24** and the interference **25** as defined in equation **(27)**.

FIG. **5** is a flow diagram of the LS recursive solution algorithm. There are two loops with the topology constructed so that the outer loop **27** is an iteration over the set of metric weights {w(metrics)}, and the inner nested loop **28** is the recursive or iterative LS solution to find the optimal $\{h_f\}$ for the given design parameters and weights where each step refers to an iteration step in the solution. A recursive LS solution is required to be able to solve the highly non-linear interference metrics as well as the band metrics when one chooses to use non-linear techniques to construct these metrics.

Consider the inner nested loop **28**. The recursive LS solution starts with the initial step i=0 **29** which begins with the selection of the input design parameters and weights and the selection of an initial set of values for the $\{h_f\}$ **30**. Next the band metrics are calculated **31**. Since this is the initial step i=0 **32** the cost function J is restricted to the linear band metrics in order to fine the linear approximation to $\{h_f\}$ **33** to initialize the non-linear solution starting with step i=1 **34** wherein the highly non-linear interference metrics are included in J. Following the signal flow, for step i=1 the band metrics **31** and interference metrics **35** are calculated, weighted, and summed to form the cost function J **36**. An iterative solution algorithm **37** finds the best approximation in step i=1 to the $\{h_f\}$ which minimizes J using the approximation to $\{h_f\}$ from the previous step i=0 to linearize the search algorithm coefficients for the eigenvalue and LS step i=1 iteration. If there is no convergence to the correct solution for $\{h_f\}$ this recursive sequence of calculations is repeated for step i=2 **34**. This recursive solution technique is repeated for subsequent steps

until there is convergence **38** whereupon one exits this inner loop.

Consider the outer loop. After exiting the inner loop **38** the solution for $\{h_f\}$ is tested to see if it meets the performance goals **39**. If not, a new set of metric weights is selected and the inner loop is initialized i=0 **40** and the inner loop is used to find the next solution for $\{h_f\}$. This process continues until the performance goals are met or adequated approximated **39** whereupon the algorithm is exited with the final solution set $\{h_f\}$ **41.**

~~FIG. **5A,5B**,. . .,,are the Matlab 5.0 code for the LS recursive eigenvalue solution algorithm used to design the Wavelet Wavelet in FIG.**6**. Included are a listing of the frequency domain design harmonics, time response, and data plotting software used in the optimization, and an example of the scaling of this mother Wavelet into a Wavelet with new scaling (dilation), time translation, frequency translation parameters, and the functions used in the code. The Matlab code uses an iterative approach to find the optimal frequency domain eigenvector solution to the quadratic form for the LS error whose error matrix is the weighed sum of the error matrices for the stopband, passband, deadband metrics and the error matrices for the ISI and ACI metrics which are functions of the eigenvectors. For each iteration the ISI and ACI error matrices are constructed with the frequency domain eigenvectors from the previous iteration. The iteration finds the new frequency domain eigenvectors which are then used to update the ISI and ACI metrics for the next iteration. This iteration is repeated until there is convergence. The Matlab code allows the operator to update the metric weights as well as the scenario parameters to find the optimal choice for the performance goals.~~

FIG **5A** Matlab code starts with the selection of the design parameters in **29** Step **1**. Step **1.1** lists the scenario parameters which are M=16 digital samples per Wavelet ψ sample interval, L=16 nominal length of Wavelet ψ in units of M, N=ML+1 Wavelet ψ length which is represented by N' in equations **(10)**, fs=1 is the normalized channel spacing equal to the Wavelet ψ sample rate, fp=0.8864 is the passband frequency interval, n f=16 is the number of design frequency harmonics, n fft=1024 is the number of digital samples used for calculation of the frequency spectrum centered at 0 frequency. ebno=E_b/N_o=6.0 dB is the design value of the energy per bit E_b to noise power density N_0 ratio, and x imbal aci=6.0 dB is the assumed channel-to-channel power imbalance used in the calculation of the ACI errors. Step **1.2** derives the software parameters from the design parameters in Step **1.1**. Step **1.3** lists the optimization parameters which are the number of iterations n iteration = 10, and the metric weights w(metric) from equation **(27)** and in FIG. **4** equal to w(pass)= alpha 1=1.e-2 for passband, w(stop)=alpha 2=0.80 for stopband, w(ISI)=alpha 3=2.e-3 for ISI, w(ACI)=alpha 4=0.5 for ACI, and w(dead)=alpha 5=0 for deadband. The number of iterations was selected to provide a convergent solution for the weighted LS error metrics w(metric)J(metric) in FIG. **5K 38** Step **10** figure(2) and for their sum J in figure(1). Weight values were selected to optimize the Wavelet ψ filter performance in FIG. **6** and in figure(**3**) in FIG. **5L 39** Step **11**, Wavelet ψ ripple, ISI, ACI signal-to-noise SNR power ratio losses in figure(4), and Wavelet ψ time response in figure(5).

FIG. **5B 30** Step **2** are the initialization calculations prior to the start of the iteration loop. Step **2.1** calculates the one-sided Wavelet ψ length parameter m=128. Step **2.2** calculates the matrix transformation bw matrix which maps the ψ frequency domain design eigenvectors into the one-sided ψ time response. Step **2.3**

refers to the function pmn in FIG. **5P,5Q 41** in Step **13.1** which computes the LS error matrix which is the sampled data integral $\Sigma[\delta c \bullet \delta c']d\omega$ over the band in equation **(23)** for the the passband and stopband metrics J(pass),J(stop). The function pmn d computes the corresponding integral over the deadband in equation **(24)** and is not listed since it was not used for FIG. **6.** Step **2.4** constructs a structural matrix c matrix used in the ISI and ACI calculations. Step **2.5** constructs the sample rate templates for the passband upper edge, sample rate marker, and passband lower edge for frequency performance evaluation.

FIG. **5C 31** Step **3** uses the function pmn to compute the LS error matrices passband and stopband in Step **3.1, 3.2**. Deadband LS error matrix deadband is set equal to a null matrix in Step **3.3.** Step **3.4** computes the matrix p total equal to the weighted sum of these matrices. Step **3.5** maps this LS error matrix p total in the time domain into the LS error matrix pw t in the frequency domain using the matrix transformation bw matrix.

FIG. **5C,5D 32** Step **4** initializes matrices used in the iteration loop and starts the iteration loop for the iterations i iteration=1,…,10. Step **4.1** calculates the eigenvalue and eigenvector which minimize the cost function J in equations **(27)** and FIG. **4** whose LS error matrix is pw t. Step **4.2** uses the bw matrix to map the eigenvector in frequency into the Wavelet time response ψ=hn and stores the eigenvector as the set of Wavelet ψ design harmonics ψ_k=hw eig(k) for k=0,1,…,15 where ψ_k has been defined in equations **(9)** and in equations **(11)** upon recognizing that there are n f=16=L design harmonics k_o=k=0,1,. . .,15. There is no reason to use the negative harmonics since the spectrum is real and symmetric about the 0 frequency. Step **4.3** computes the passband peak-to-peak ripple as xripple and the stopband attenuation as xstop.

FIG. **5E 33** Step **5** calculates the weighted passband error metric w(pass)J(pass)=beta pass, weighted stopband error metric w(stop)J(stop)=beta stop, and weighted deadband error metric w(dead)J(dead)=beta dead in equations **(27)** using the b vector format for hn and the LS error matrices - passband, stopband, deadband.

FIG. **5E,5F 34** Step **6** calculates the ISI and ACI LS error matrices, their metrics, and their error contributations to the SNR loss. Step **6.1** calculates the ISI LS error matrix w matrix and the corresponding ISI metric J(ISI)=errM isi with Matlab code which implements equations **(25)**, and calculates the ISI residual error errV isi that causes an ISI SNR loss. Step **6.2** calculates the ACI LS error matrix w f matrix and the corresponding ACI metric J(ACI)= errM aci with Matlab code which implements equations **(26)**, and calculates the ACI residual error errV aci that causes a ACI SNR loss.

FIG. **5G 35** Step **7** calculates the weighted LS error metrics for ISI and ACI and the LS error matrix pw t for the next iteration. Step **7.1** calculates the weighted ISI LS error metric w(ISI)J(ISI)=beta isi and the weighed ACI LS error metric w(ACI)J(ACI)=beta aci in equations **(27)** and the sum of the weighted LS error metrics J=errM isi. Step **7.2** saves the weighted LS error metrics and their sum J for each iteration. Step **7.3** updates the pw t matrix for the next iteration.

FIG. **5G,5H 36** Step **8** calculates the SNR losses, stores these losses for each iteration, and completes the iteration loop. Step **8.1** computes the SNR loss in dB due to passband ripple as xloss ripple, due to ISI as xloss isi, due to ACI as xloss aci, and the total SNR loss as xloss total. Step **8.2** saves these SNR losses for each iteration and completes the iteration loop.

FIG. 5H,5I,5J,5K 37 Step 9 documents the Wavelet ψ frequency design harmonics and time response generated by the Matlab code for the Wavelet in FIG. ψ 6. Step 9.1 lists the Wavelet ψ frequency domain harmonic design coordinates $\psi_k(k)=hw\ eig(k)$ for harmonics k=0,1,…,15. Only the positive harmonics are listed since the frequency spectrum is real and symmetric about k=0. Step 9.2 lists the Wavelet ψ time response ψ(n)=hn(n) for n=0,1,2,. . . ,128 with the coordinate frame centered at the Wavelet peak. Only the positive digital samples are listed since the time response is real and symmetric about n=0.

FIG. 5K 38 Step 10 plots the total weighted LS error metric J in figure(1) and the individual weighted LS error metrics in figure(2) as functions of the iteration number. After about 6-7 iterations both the total and the individual weighted LS error metrics are observed to stabilize indicating that the selected number of iterations n iteration=10 is sufficient for convergence.

FIG. 5L 39 Step 11 plots the Wavelet ψ frequency response in figure(3) which is the same as the frequency response in FIG. 6, plots the SNR losses due to passband ripple, ISI, ACI and the total loss in figure(4), and plots the time response in figure(5) for use in the optimization of the LS metric weights in Step 1.3 as well as the scenario parameters in Step 1.1.

FIG. 5M 40 Step 12 documents the Matlab code to rescale the mother Wavelet ψ in FIG. 6 which was derived in the previous Matlab code in Steps 1-11, for new scale (dilation) p, time translation q, and frequency translation k parameters compared to the values p=0,q=0,k=0 for the mother Wavelet ψ. An example set

~~of new parameters documented in the code is p=2, q=2, k=3 and with the assumption that the digital sampling rate remains fixed under the parameter change. A constant digital sample rate keeps the frequency band constant under the parameter change.~~

FIG. **4,5** ~~**5M 40** Step **12.1**~~ derive the new multi-resolution Wavelet ψ at baseband. Scaling equations ~~defines the new Wavelet $\Psi_{p,q,k}$ in equations~~ **(7),(18)** can be used to derive the corresponding digital Wavelet at scales p,q,k with parameters M,L wherein the digital frequency parameter "k" replaces the frequency index "r". Equation **(7)** can be rewritten to define the scaling equation which derives this Wavelet $\psi_{p,q,M,L,k}$ from ψ: ~~resulting from these parameter changes, in equations **(28)**~~

New Wavelet scaled from mother Wavelet **(28)**

$$\psi_{p,q,M,L,k}\ \Psi_{p,q,k} = \psi_{p,q,k} \text{ with parameters M,L}$$
$$= 2^{-p/2}\ \psi(2^{-p}n - qM)\ \exp(j2\pi\ k\ 2^{-p}n\ /ML)$$

There are at least two methods of scaling used to implement equation **(28)**. In method **1** corresponding to the standard Wavelet assumption, the subsampling or decimation of n by the factor 2^p stretches the time between contiguous samples by the factor 2^p while keeping constant the number of samples M per Wavelet ψ sample interval, and therefore reduces the frequency band by the factor 2^p. For a uniform filter bank, this means the filter frequency bands are reduced by the factor 2^p. In method **2**, the sampling is held constant corresponding to a constant frequency band assumption. The factor 2^(-p) is divided out in the Wavelet expression which is equivalent to the M being scaled to 2^pM corresponding to increasing the number of samples per Wavelet interval by the factor 2^p. For a uniform filter bank, this

number of channels by the factor 2^p over the same frequency band.

~~Case 1 Scaled (dilated) sampling $2^{-p}n$ with fixed M subsamples (decimates) n by the factor 2^p~~

~~· Represent n as~~

~~$n = n\_0 + 2^p n\_p$~~

~~$n\_0 = 0,1,\ldots, 2^p-1$~~

~~$n\_p = 0, +/-1, +/-2, \ldots$~~

~~· We observe $2^{-p}n = n\_p$~~

~~· This enables the new Wavelet to be written~~

~~$\psi_{p,q,k} = 2^{-p/2}\psi(n\_p - qM)\exp(j2\pi k n\_p /ML)$~~

~~Case 2 Sampling n remains fixed and M is rescaled by the factor 2^p~~

~~· New M is M new~~

~~$M\_new = 2^p M$~~

~~· This enables the new Wavelet to be written~~

~~$\psi_{p,q,k} = 2^{-p/2}\psi(n - qM\_new)\exp(j2\pi kn/M\_newL)$~~

~~wherein the new Wavelet equation from (7),(18) is re-written using the frequency translation parameter k=r and the explicit frequency translation expression exp(j2π k 2^{-p}n /ML) which is recognized as the discrete Fourier transform kernal.~~

~~In Case 1 corresponding to the standard Wavelet assumption, the subsampling or decimation of n by the factor 2^p stretches the time between contiguous samples by the factor 2^p while keeping constant the number of samples M per Wavelet ψ sample~~

interval, and therefore reduces the frequency band by the factor 2^p. The new n can be represented as the sum of the two fields n 0 = 0,1,. . ,(2^p -1) and n p = 0, +/-1, +/-2, . . . Scaling or equivalently subsampling results in the new n equal to n new = 2^-p n = n p corresponding to a stretching of the sample interval by 2^p. The new Wavelet length N new remains constant N new=N using the n p sampling.

In Case **2** which is the communications application being considered, the sampling is held constant corresponding to a constant frequency band assumption. The factor 2^-p is divided out in the Wavelet expression which is equivalent to the M being scaled to M new=2^p M corresponding to increasing the number of samples per Wavelet interval by the factor 2^p. This means Case 2 corresponds to increasing the maximum number of channels by the factor 2^p over the same frequency band. The new Wavelet length is equal to N new=M newL+1 =1025 since M new=2^pM=64.

FIG. **5M 40** Step **12.2** derives the new matrix transformation bw matrix new which maps the ψ frequency domain design eigenvectors into the one-sided ψ time response.

FIG. **5M,5N 40** Step **12.3** uses the matrix transformation bw matrix new to map the design eigenvector hw eig into the new Wavelet in three steps. In the first step, the mother Wavelet is translated into the new baseband Wavelet $\psi_{p,q-0,k-0}$ = hn 0 which is the mother Wavelet scaled by p and with no time and frequency translations q=k=0. The second step translate this baseband Wavelet by qM new to generate $\psi_{p,q,k-0}$ = hn 1. The last step translates this Wavelet $\psi_{p,q,k-0}$ = hn 1 in frequency to give the new Wavelet $\psi_{p,q,k}$ = hn new.

FIG. **5N 40** Step **12.4** plots the Wavelet time responses for the mother Wavelet ψ=hn and the new Wavelet $\psi_{p,q,k}$ = hn new in

figure(6). Step **12.5** plots the Wavelet frequency responses for the mother Wavelet ψ=hn and the new Wavelet $\psi_{p,q,k}$ = hn new in figure(7) versus the normalized frequency/(ψ=hn sample rate) and in figure (8) versus the normalized frequency/($\psi_{p,q,k}$ = hn new sample rate).

FIG. **41** Step **13** documents the functions used in the Matlab code. Step **13.1** is the code for the function pmn which computes the matrix for the J(BAND) in equations **(23)**. FIG. **41** Step **13.2** lists the code for the function freq rsp which computes the Fourier transform of the input hn versus the normalized frequency/(Wavelet ψ=hn sample rate).

Consider the inner nested loop **28**. The recursive LS solution starts with the initial step i=0 **29** which begins with the selection of the input design parameters and weights and the selection of an initial set of values for the $\{h_\ell\}$ **30**. Next the band metrics are calculated **31**. Since this is the initial step i=0 **32** the cost function J is restricted to the linear band metrics in order to fine the linear approximation to $\{h_\ell\}$ **33** to initialize the non-linear solution starting with step i=1 **34** wherein the highly non-linear interference metrics are included in J. Following the signal flow, for step i=1 the band metrics **31** and interference metrics **35** are calculated, weighted, and summed to form the cost function J **36**. An iterative solution algorithm **37** finds the best approximation in step i=1 to the $\{h_\ell\}$ which minimizes J using the approximation to $\{h_\ell\}$ from the previous step i=0 to linearize the search algorithm coefficients for the eigenvalue and LS step i=1 iteration. If there is no convergence to the correct solution for $\{h_\ell\}$ this recursive sequence of calculations is repeated for step i=2 **34**. This recursive solution technique is repeated for subsequent steps until there is convergence **38** whereupon one exits this inner loop.

~~Consider the outer loop. After exiting the inner loop 38 the solution for $\{h_\ell\}$ is tested to see if it meets the performance goals 39. If not, a new set of metric weights is selected and the inner loop is initialized i=0 40 and the inner loop is used to find the next solution for $\{h_\ell\}$. This process continues until the performance goals are met or adequated approximated 39 whereupon the algorithm is exited with the final solution set $\{h_\ell\}$ 41.~~

Applications of this new invention to both communications and radar will be given using these example algorithms and other algorithms supported by this invention. These new waveforms are considered for the applications: 1)to replace the square-root raised cosine waveform (sq-root rc) which is extensively used for the third generation (3G) CDMA communications, 2)to replace the Gaussian minimum shift keying (GMSK) waveform for constant amplitude bandwidth efficient (BEM) applications, and 3) as a candidate waveform for synthetic aperture radar (SAR) and real aperture radar (RAR) applications.

CDMA communications application for the current and the new 3G CDMA considers a waveform designed with this new invention as a possible replacement for the sq-rt rc waveform with bandwidth expansion parameter $\alpha = 0.22$ to $\alpha = 0.40$. This notation means that for $\alpha = 0.22$ the spectral efficiency is (symbol rate/bandwidth) = $1/1+\alpha$ =1/1.22 = 0.82 = 82%. A basic advantage of the waveform is the potential for a symbol rate increase within the same bandwidth with an increase in the spectral efficiency to $\approx 100\%$ depending on the application and operational constraints. The dc power spectral density or power spectrum (PSD) of the waveform is compared to the PSD for the sq-rt r-c in FIG. 6. Plotted are the measured PSD in dB 42 versus the frequency offset from dc expressed in units of the symbol rate 43 Plotted against the

normalized frequency offset are the dc PSD for the new waveform **44**, the sq-rt r-c with α=0.22 **45**, and the sq-rt r-c with α=0.40 **46**. It is observed that the PSD for the new waveform rolls off faster that that for the sq-rt r-c which means that the new mr waveform will support an increased symbol rate for a given available frequency band while satisfying the inherent requirements for low ISI and MAI (multiple access interference).

Constant amplitude BEM application of the new waveform indicates that it is a viable candidate for replacing the current preferred modulation waveform which is the GMSK. The GMSK finds applications for transmitters which operate their HPA(s) amplifiers in a saturation mode in order to maximize their radiated power from the HPA(s), and which require a BEM PSD to avoid excessive spreading of the transmitted power. Simulation data for the dc PSD is plotted in FIG. **7** for the new waveform BEM and the GMSK. Plotted are the measured dc PSD in dB **47** versus the frequency offset from dc expressed in units of the bit rate **48**. Plotted against the normalized frequency offset are the dc PSD for the new waveform BEM **49** and the GMSK **50**, for a length parameter L=10 where L is the length of the phase pulse in terms of the phase pulse repetition rate. The significance of this example data is that the new waveform has the potential to be designed to offer a PSD which is less spread out than the current GMSK, and therefore an improved BEM waveform.

Radar RAR and SAR application of the waveform indicates that it is a viable candidate to replace the current chirp waveforms for wideband signal transmission, when combined with pseudo-random phase codes. Results of the simulation for the new waveform and an unweighted frequency chirp waveform are given in FIG. 8. Plotted are the ambiguity function for the new waveform **51** and the unweighted frequency chirp waveform **52**. The dc 2-dimensional radar ambiguity function **53** is plotted as a function

of the frequency offset in units of fT_p and the time offset in units of t/T_c where T_p is the phase-coded radar pulse length or length of the phase code and T_c is the phase code chip length. The chip length is identical to the waveform repetition interval T_s so that $T_c = T_s$. It is observed that the new waveform has the potential for significant improvements in the ambiguity function and by implication in the performance.

Preferred embodiments in the previous description ~~is~~ are provided to enable any person skilled in the art to make or use the present invention. The various modifications to these embodiments will be readily apparent to those skilled in the art, and the generic principles defined herein may be applied to other embodiments without the use of the inventive faculty. Thus, the present invention is not intended to be limited to the embodiments shown herein ~~but~~and ~~is not~~ to be accorded the wider scope consistent with the principles and novel features disclosed herein.

~~**REFERENCES:**~~

~~[1] I. Daubechies, "Ten Lectures on Wavelets", Philadelphia:SIAM, 1992~~

~~[2] Ronald R. Coifman, Yves Meyer, Victor Wickerhauser, "Wavelet analysis and signal processing", in "Wavelets and Their Applications', Jones & Bartlett Publishers, 1992~~

~~[3] T. Blu, "A new design algorithm for two-band orthonormal rational filter banks and orthonormal rational Wavelets", IEEE Signal Processing, June 1998, pp. 1494-1504~~

~~[4] M. Unser, P. Thevenaz, and A. Aldroubi, "Shift-orthogonal Wavelet bases", IEEE Signal Processing, July 1998, pp. 1827-1836~~

[5] K.C. Ho and Y. T. Chan, "Optimum discrete Wavelet scaling and its application to delay and Doppler estimation", IEEE Signal Processing, Sept. 1998, pp. 2285-2290

[6] Q. Pan, L. Zhang, G. Dai, and H. Zhang, "Two denoising methods by Wavelet transforms", IEEE Signal Processing, Dec. 1999, pp. 3401-3406

[7] P.P. Vaidyanathan and T.Q. Nguyen, "Eigenvalues: A New Approach to Least-Squares FIR Filter Design and Applications Including Nyquist Filters", IEEE Trans. on Circuits and Systems, Vo. CAS-34, No. 1, Jan. 1987, pp 11-23

[8] J.H. Mc.Clellan, T.W. Parks and L.R. Rabiner, "A Computer Program for Designing Optimum FIR Linear Phase Filters', IEEE Trans Audio Electroacoust. Vol. AU-21, Dec. 1973, pp. 506-526

DRAWINGS AND PERFORMANCE DATA

FIG. 1 Wavelet Tiling of an N-Point Digital t-f Space

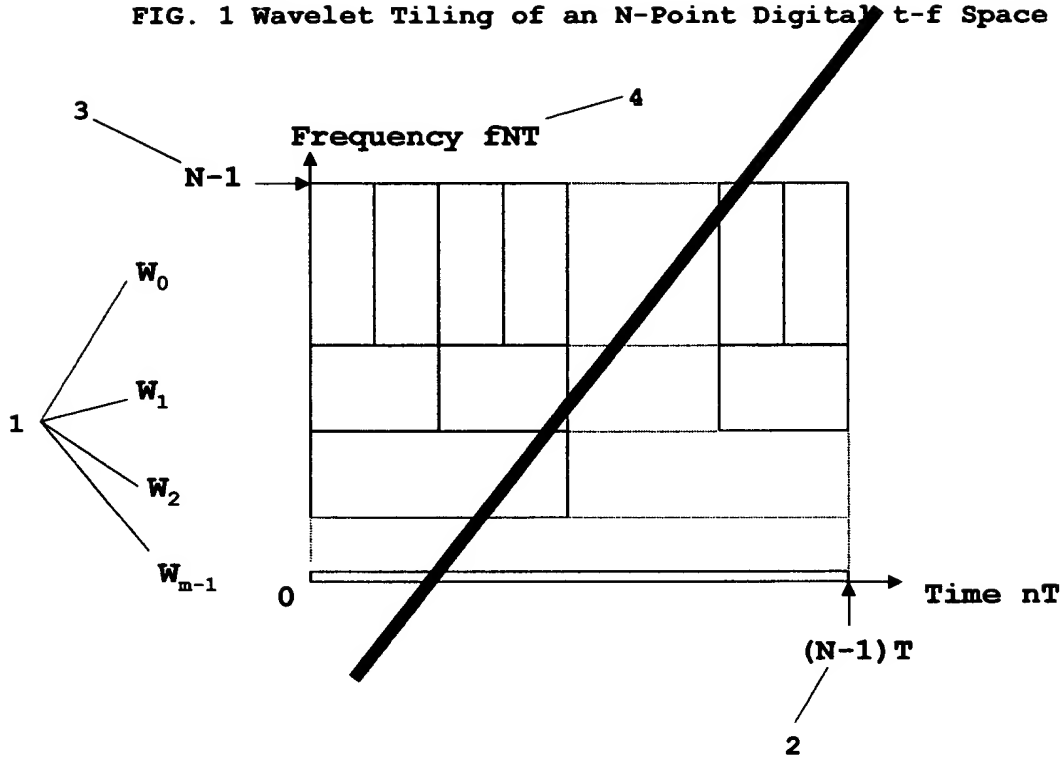

FIG. 2 Wavelet Iterated Filter Bank for Tiling t-f Space in FIG. 1

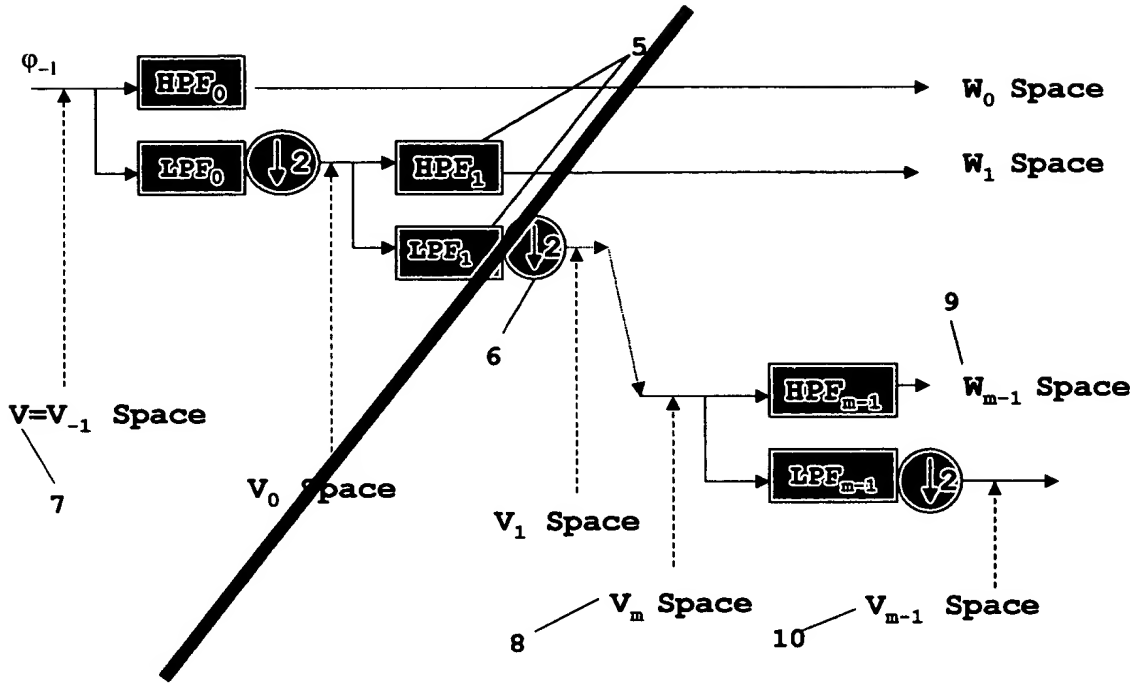

FIG. 3 PSD Requirements for Communications

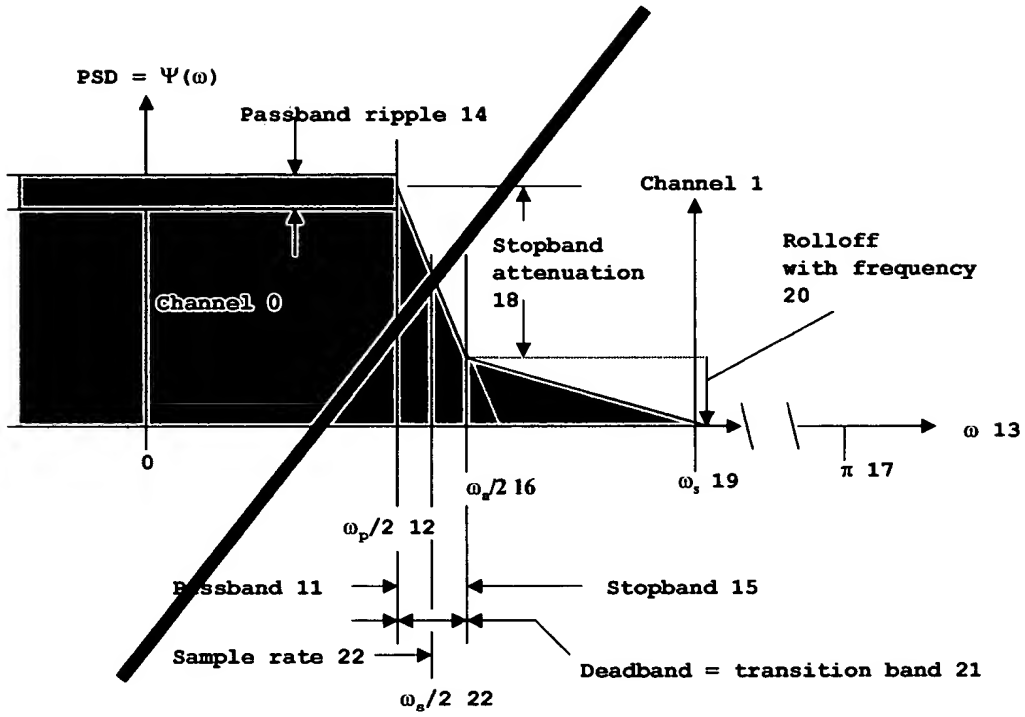

FIG. 4 LS Metrics and Cost Function

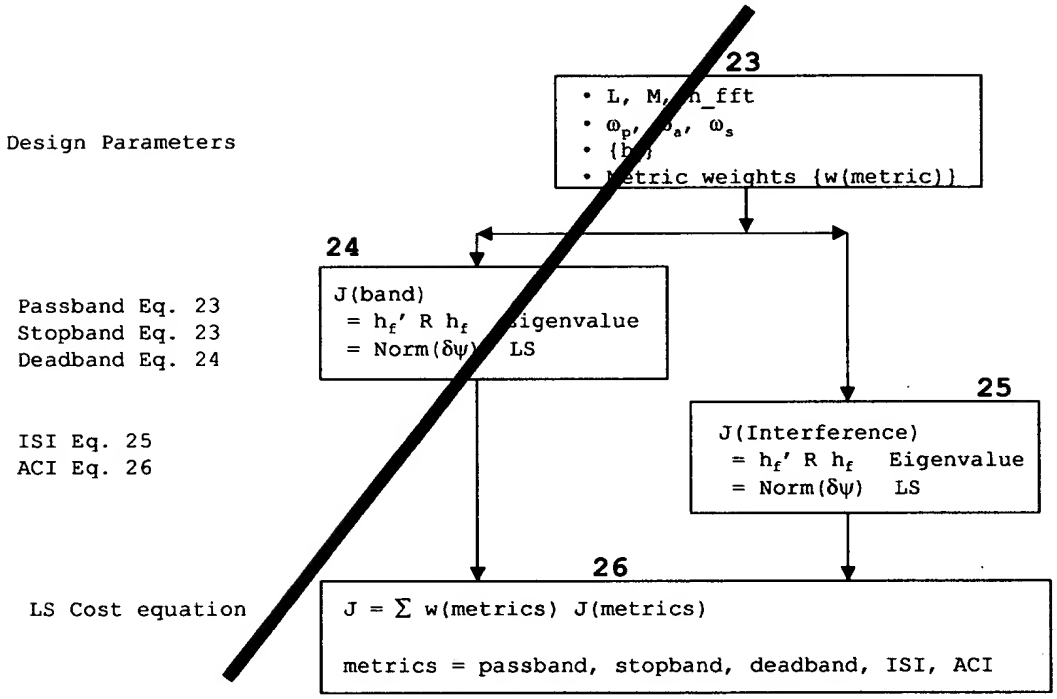

FIG. 5 LS Recursive Solution Algorithm

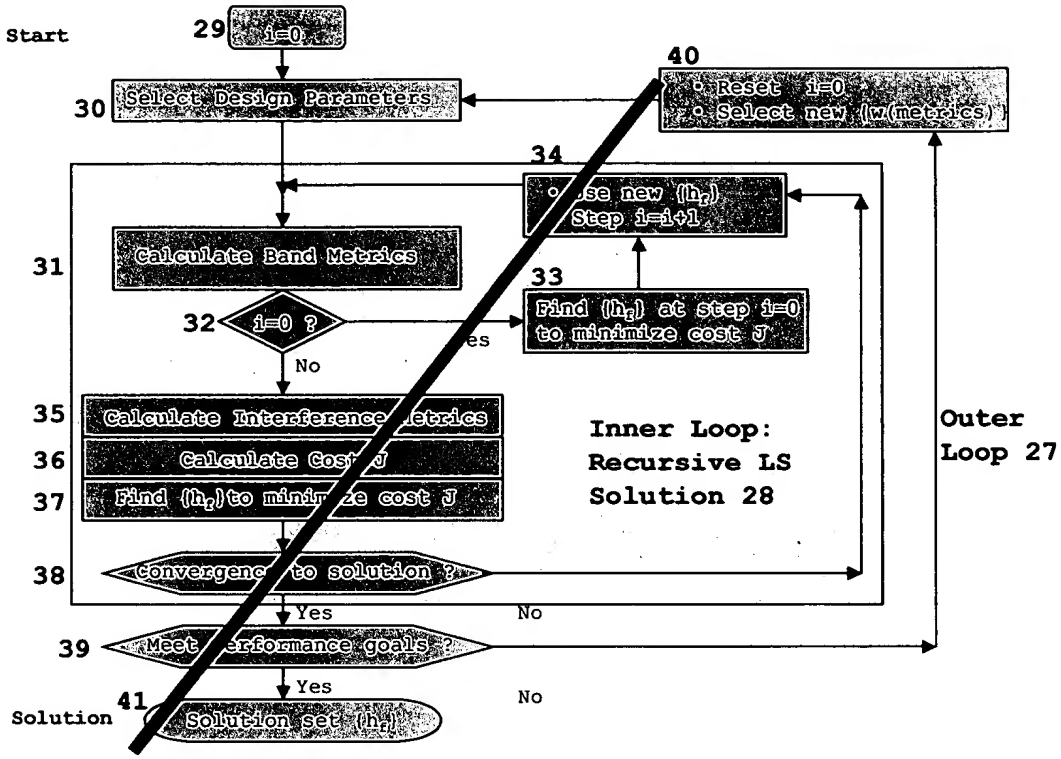

5

FIG. 6 PSD for New Waveform and Square-Root Raised-Cosine

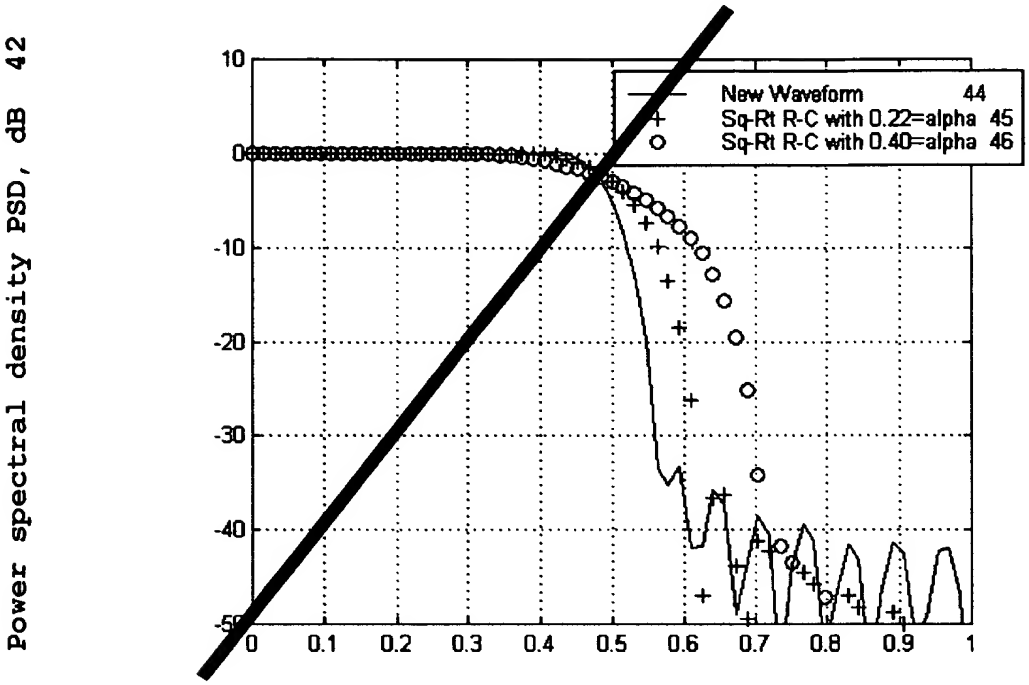

FIG. 7 PSD for New Waveform BEM and GMSK

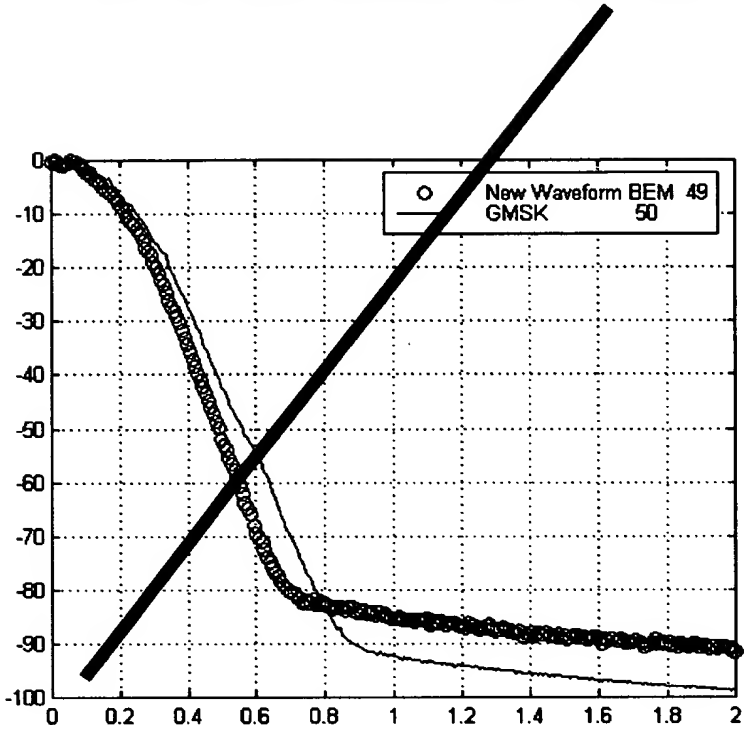

Power spectral density PSD, dB 47

Normalized frequency, bit rate 48

5

10

FIG. 8 Radar Ambiguity Functions of New Waveform and Unweighted Chirp Waveform

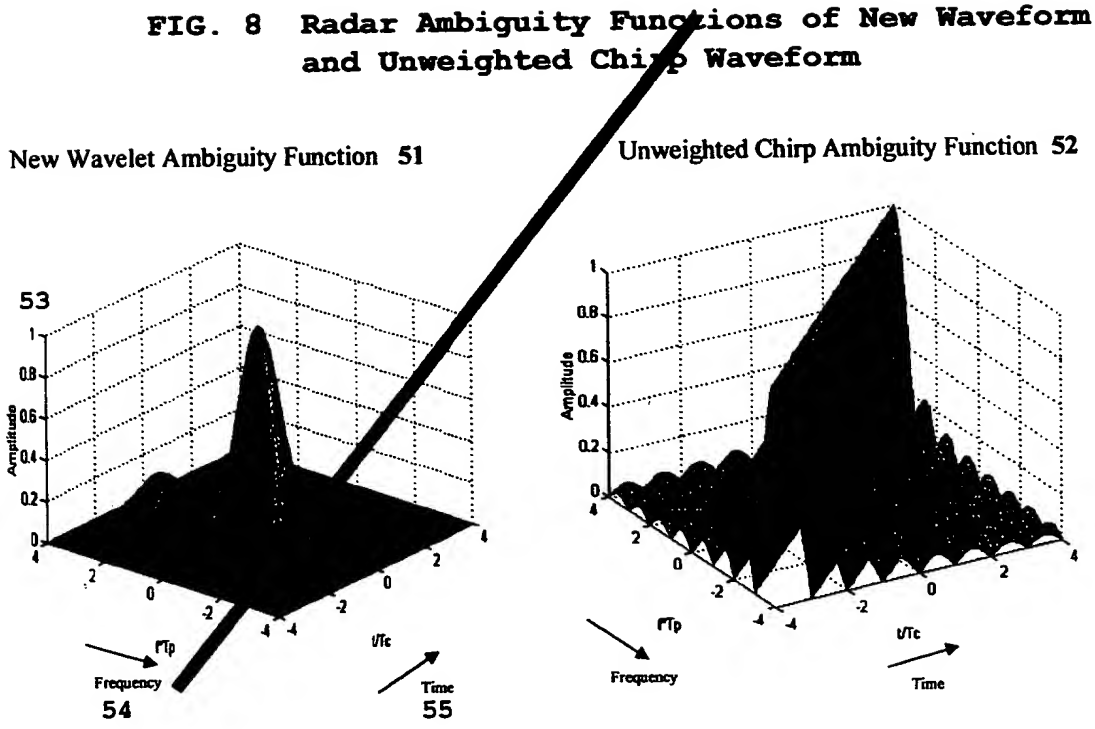

APPLICATION NO. 09/826,118

TITLE OF INVENTION: Wavelet Multi-Resolution Waveforms

INVENTOR: Urbain A. von der Embse

Clean version of how the SPECIFICATION Will read.

APPLICATION NO. 09/826,118
TITLE OF INVENTION: Wavelet Multi-Resolution Waveforms
INVENTOR: Urbain A. von der Embse

BACKGROUND OF THE INVENTION

I. Field of the Invention

The present invention relates to CDMA (Code Division Multiple Access) cellular telephone and wireless data communications with data rates up to multiple T1 (1.544 Mbps) and higher (>100 Mbps), and to optical CDMA. Applications are mobile, point-to-point and satellite communication networks. More specifically the present invention relates to a new and novel approach to the design of waveforms and filters using mathematical formulations which generalize the Wavelet concept to communications and radar.

II. Description of the Related Art

Multi-resolution waveforms used for signaling and/or filters and which are addressed in this invention are defined to be waveforms of finite extent in time and frequency, with scale and shift properties of multi-resolution over the time-frequency (t-f) space. These waveforms can also be referred to as multi-scale waveforms, and include multi-rate filtering and the Wavelet as special cases. The emphasis will be on digital design and applications with the understanding that these multi-resolution waveforms are equally applicable to analog design and applications.

Background art consists of the collection of waveform and filtering design techniques which can be grouped into six broad categories. These categories are: C1) least squares (LS) design algorithms for filters and waveforms that design to specifications on their frequency response, C2) analytic filters and waveforms which are specified by a few free design parameters that can be sub-categorized into current applications and primarily theorectical studies, C3) combinations of C1 and C2 for greater flexibility in meeting communications and radar performance goals, C4) special design techniques to control the noise levels from intersymbol interference (ISI) and adjacent channel interference (ACI) in the presence of timing offsets for multiple channel applications, C5) Wavelet filter design using scaling functions (iterated filter banks) as the set of design coordinates or basis functions, C6) filter and waveform design techniques for non-linear channels and in particular for operation in the non-linear and saturation regions of a high power amplifier (HPA) such as a traveling wave tube (TWT) or a solid state amplifier, and C7) LS dynamic filters derived from discrete filtering and tracking algorithms that include adaptive equalization for communications, adaptive antenna filters, Wiener filters, Kalman filters, and stochastic optimization filters.

Category C1 common examples of LS digital filter design are the eigenvalue algorithm in "A New Approach to Least-Squares FIR Filter Design and Applications Including Nyquist Filters" and the Remez-Exchange algorithm in "A Computer Program for Designing Optimum FIR Linear Phase Filters'. The eigenvalue algorithm is a direct LS minimization and the Remez-Exchange can be reformulated as an equivalent LS gradient problem through proper choice of the cost function. Both LS algorithms use the FIR (finite impulse response) digital samples as the set of design coordinates. LS design metrics are the error residuals in meeting their passband

and stopband ideal performance as shown in FIG. **3**. Category C2 common examples of analytical waveforms and filters for system applications are the analog Chebyshev, Elliptic, Butterworth, and the digital raised-cosine, and square-root raised-cosine. For theorectical studies, common examples are polyphase multirate filters, quadrature mirror filters (QMF), and perfect reconstruction filters. Although these theorectical studies have yet to yield realizable useful filters for system applications, their importance for this invention lies in their identification and application of ideal performance metrics for filter designs. Category C3 common digital example is to start with the derivation of a Remez-Exchange FIR filter and then up-sample and filter with another bandwidth limiting filter. This results in an FIR over the desired frequency band that is larger than available with the Remez-Exchange algorithm and with sidelobes that now drop off with frequency compared to the flat sidelobes of the original Remez-Exchange FIR. A category C4 common example is to select the free parameters of the category C3 filter in order to minimize the signal to noise power ratio of the data symbol (SNR) losses from the ISI, ACI, and the non-ideal demodulation. A second common example is start with a truncated pulse whose length is short enough compared to the symbol repetition interval, to accommodate the timing offsets without significant impact on the ISI and ACI SNR losses. This shortened pulse can then be shaped in the frequency domain.

Category C5 Wavelet filter design techniques discussed in the next section will serve as a useful reference in the disclosure of this invention. Category C6 common example is the Gaussian minimum shift keying (GMSK) waveform. This is a constant amplitude phase encoded Gaussian waveform which has no sidelobe re-growth through a non-linear or saturating HPA. Category C7 common examples are the adaptive equalization filter for communication channels, the adaptive antenna filter,

and the Kalman filter for applications including target tracking and prediction as well as for equalization and adaptive antennas.

Minimizing excess bandwith in the waveform and filter design is a key goal in the application of the C1,…,C6 design techniques for communications and radar. Excess bandwith is identified as the symbol α in the bandwidth-time product $BT_s=1+\alpha$ where the two-sided available frequency band is B and the symbol repetition interval is T_s. Current performance capability is represented by the use of the square-root raised cosine (sq-rt rc) waveform with α= 0.22 to 0.4 as shown in FIG. **6**. The goal is to design a waveform with α=0 within the performance constraints of ISI, ACI, passband, sideband, and passband ripple. This goal of eliminating the excess bandwidth corresponds to the symbol rate equal to the available frequency band $1/T_s = B/(1+\alpha) = B$ for α=0. This symbol rate $1/T_s=B$ is well known to be the maximum possible rate for which orthogonality between symbols is maintained. A fundamental performance characteristic of our new waveform designs is the ability to eliminate excess bandwidth for many applications.

Scope of this invention will include all of the waveform and filter categories with the exception of category C4 special design techniques and category C7 LS dynamic filters. Emphasis will be on the category C5 Wavelets to establish the background art since Wavelets are multi-resolution waveforms that can eliminate the excess bandwidth and have known design algorithms for FIR waveforms and filters. However, they do not have a design mechanism that allows direct control of the ISI, ACI, passband, sideband, and passband ripple. Category C2 theorectical studies also eliminate the excess bandwidth. However, they are not multi-resolution waveforms and do not have realizable FIR design algorithms. So the emphasis in background art will be on Wavelets whose relevant properties we briefly review.

Wavelet background art relevant to this invention consists of the discrete Waveform equations and basic properties, application of Wavelets to cover a discrete digital time-frequency (t-f) signal space, and the design of Wavelets using the iterated filter construction. Wavelets are waveforms of finite extent in time (t) and frequency (f) over the t-f space, with multi-resolution, scaling, and translation properties. Wavelets over the analog and digital t-f spaces respectively are defined by equations **(1)** and **(2)** as per Daubechies's "Ten Lectures on Wavelets", Philadelphia:SIAM, 1992

Continuous wavelet

$$\psi_{a,b}(t) = |a|^{-1/2}\psi(\frac{t-b}{a}) \qquad \textbf{(1)}$$

Discrete wavelet

$$\psi_{a,b}(n) = |a|^{-1/2}\psi(\frac{n-b}{a}) \qquad \textbf{(2)}$$

where the two index parameters "a,b" are the Wavelet dilation and translation respectively or equivalently are the scale and shift. The ψ is the "mother" wavelet and is a real and symmetric localized function in the t-f space used to generate the doubly indexed Wavelet ψ_{ab}. The scale factor "$|a|^{-1/2}$" has been chosen to keep the norm of the Wavelet invariant under the parameter change "a,b". Norm is the square root of the energy of the Wavelet response. The Wavelets $\psi_{a,b}$ and ψ are localized functions in the t-f space which means that both their time and frequency lengths are bounded. The discrete Wavelet has the time "t" replaced by the equivalent digital sample number "n" assuming the waveform is uniformly sampled at "T" second intervals.

Wavelets in digital t-f space have an orthogonal basis that is obtained by restricting the choice of the parameters "a,b" to the values $a=2^{-p}$, $b=qM2^{p}$ where 'p,q" are the new scale and translation parameters and "M" is the spacing or repetition interval $T_s=MT$ of the Wavelets (which from a communications viewpoint are symbols) at the same scale "p". Wavelets at "p,q" are related to the mother Wavelet by the equation

$$\psi_{p,q}(\mathbf{n}) = 2^{-p/2}\psi(2^{-p}n - qM) \qquad (3)$$

where the mother Wavelet is a real and even function of the sample coordinates. The orthonormality property means that these Wavelets satisfy the orthogonality equation with a correlation value equal to "1".

$$\sum_{n} \psi_{p,q}\psi_{k,m} = 1 \text{ iff both } p = k \text{ and } q = m$$
$$= 0 \text{ otherwise} \qquad (4)$$

Wavelet representation of a digital t-f space starts with selecting an N sample time window of a uniform stream of digital samples at the rate of 1/T Hz (1/second) equivalent to a "T" second sampling interval. The N point or sample t-f space in FIG. **1** illustrates a Wavelet representation or "tiling" with Wavelets that are designed analytically or by an iterated filter construction.

The t-f space in FIG. **1** is partitioned or covered or tiled by a set of Wavelet subspaces $\{W_p, p = 0,1,\ldots,m-1\}$ **1** where $N=2^m$. Each Wavelet subspace W_p **1** at scale "p" consists of the set of Wavelet time translations $\{q = 0,1,\ldots, N/2^{p+1}-1\}$ over this subspace. These Wavelet subspaces are mutually orthogonal and the Wavelets within

each subspace are mutually orthogonal with respect to the time translates. This N-point t-f space extends over the time interval from 0 to (N-1)T **2** and over the frequency interval from 0 to (N-1) **3** in units of the normalized frequency fNT **4**.

The iterated filter bank in FIG. **2** is used to generate the Wavelets which cover the t-f space in FIG. **1**. Each filter stage **5** consists of a high pass filter (HPF) and a low pass filter (LPF). Output **6** of the LPF is subsampled by 2 which is equivalent to decimation by 2. This t-f space space is an N-dimensional complex vector metric space V **7**. At stage m in the iterated filter bank, the remaining t-f space V_{m-1} **8** is partitioned into $\mathbf{V}_{m+1}$ **9** and the Wavelet subspace W_{m+1} **10** .

Scaling functions and Wavelets at each stage of this filter bank satisfy the following equations

$$\varphi(\mathbf{n}) = 2^{-1/2}\sum_{\mathbf{q}}\mathbf{h}_{\mathbf{q}}\,\varphi(2\mathbf{n}-\mathbf{q}) \quad \forall \mathrm{q}$$
$$\psi(\mathbf{n}) = 2^{-1/2}\sum_{\mathbf{q}}\mathbf{g}_{\mathbf{q}}\,\varphi(2\mathrm{n}-\mathrm{q}) \quad \forall \mathbf{q} \qquad \textbf{(5)}$$

where φ is the scaling function, ψ is the Wavelet, HPF_p coefficients are $\{h_q, \forall q\}$, LPF_p coefficients are $\{g_q, \forall q\}$, and the equations apply to the stages 0,1,…,m-1. Identifying the scale parameter and using the previous Wavelet formulations enable these equations to be rewritten for stages p=0,1,…,m-1 as

$$\varphi_p = \sum_{\mathrm{q}}\mathrm{h}_{\mathrm{q}}\,\varphi_{\mathrm{p-1,q}} \quad \forall \mathrm{p}$$
$$\psi_{\mathrm{p}} = \sum_{\mathrm{q}}\mathrm{g}_{\mathrm{q}}\,\varphi_{p-1,q} \quad \forall \mathrm{p} \qquad \textbf{(6)}$$

For our application the HPF_p and LPF_p are quadrature mirror filters (QMF) with perfect reconstruction. This means they cover the subspace V_p with flat responses over the subband frequency including the edges of the frequency subband, and the HPF_p coefficients are the frequency translated coefficients for the LPF_p: $\{g_q=(-1)^q h_q\ ,\ \forall q\}$.

Wavelet design using iterated filter bank starts with the selection of the scaling functions. Starting with a primative scaling function such as the one proposed by Daubechies'one can use the iterated filter construction given by equations **(5)** and **(6)** to derive successive approximations to a desired scaling function which has properties that have been designed into it by the selection of the filter coefficients $\{g_q, \forall q\}$ at each level of iteration. The Wavelets can be derived from these scaling functions using the iterated filter construction or scaling equations **(5)** and **(6)**.

Another use of the iterated filter construction is to design the scaling functions as Wavelets thereupon ending up with a larger set of Wavelets for multi-resolution analysis and synthesis as illustrated by Coifman's Wavelets in "Wavelet analysis and signal processing".

SUMMARY OF THE INVENTION

This invention for the design of multi-resolution Wavelet waveforms improves their performance for engineering and scientific applications, and in particular for applications to communications and radar. Current practice is to 1) design

traditional multi-resolution waveforms in the time domain using metrics which specify frequency performance and without consideration of Wavelet properties or to 2) design Wavelet multi-resolution waveforms using the time-domain iterated multi-resolution filtering approach with a set of scaling functions used to perform the filtering and without direct considerations of the frequency performance. These two separate design approaches yield fundamentally different waveforms. This invention provides a means to combine these two approaches to generate a new multi-resolution Wavelet waveform with the best properties of the traditional multi-resolution waveforms and the Wavelet multi-resolution waveform.

This invention introduces innovations for the design of our Wavelet waveform that 1) include the ISI (intersymbol interference), ACI (adjacent channel interference) , and QMF (quadrature mirror filter) requirements into the design algorithm along with non-linear modifications to the traditional passband and stopband frequency requirements which are used in the Remez-Exchange and eigenvalue LS algorithms, 2) select the frequency harmonics as the design coordinates, 3) use an appropriate subset of the available Fourier domain frequency harmonics as the design coordinates with the property that this subset of coordinates is a basis for the multi-resolution Wavelet waveform design, and 4) design the multi-resolution Wavelet waveform for no excess bandwidth $\alpha=0$.

These innovations support the development of our new waveforms 1) that are generalizations of Wavelets in the frequency domain using a means which makes them useful for communications and radar over their t-f space, 2) that can be designed to be an orthonormal basis or orthonormal set of coordinates over the available frequency bandwidth with the implicit property that the excess bandwidth vanishes $\alpha=0$, to

within the accuracies allowed by communication and radar design implementations, and 3) that have multi-scale properties which allow a single dc waveform design to be used to uniquely define the complete set of waveforms over the t-f space for multi-scale applications Specific design algorithm examples developed in this invention disclosure are the LS design algorithms that use eigenvalue and gradient search techniques in the frequency domain to find the best waveform design which minimizes the corresponding LS error residual cost function that is a weighted linear sum of the residual error metrics.

Wavelet waveform performance calculated in this invension disclosure from the application of these LS design algorithms, demonstrates the capability of this invention to provide a means to design waveforms that are improved over current practice. There are other algorithmic design algorithms which can be realized by modifications to this invention. An example given in this invention disclosure is the modification of these LS algorithms for application to constant amplitude bandwidth efficient (BEM) waveforms for communications.

BRIEF DESCRIPTION OF THE DRAWINGS AND THE PERFORMANCE DATA

The above-mentioned and other features, objects, design algorithms, and performance advantages of the present invention will become more apparent from the detailed description set forth below when taken in conjunction with the drawings and performance data wherein like reference characters and numerals denote like elements, and in which:

FIG. **1** is a Wavelet N-point t-f space extending over the time interval (0, (N-1)T] and the frequency interval (0, (N-1)/NT], which is tiled or covered by a set of orthonormal Wavelets at the scales p=0,1,…,m-1.

FIG. **2** is a Wavelet iterated filter bank used to generate the set of Wavelets which tile or cover the t-f space in FIG. **1**.

FIG. **3** illustrates the power spectral density (PSD) of our Wavelet waveform at dc, and the set of stopband and passband design requirements.

FIG. **4** is the flow diagram of the LS metrics and cost functions and the final cost function used to find the optimal LS solution for our Wavelet waveform.

FIG. **5** is flow diagram for the LS recursive solution algorithm to find the optimal harmonic coordinates that define the LS solution for our Wavelet waveform.

FIG. **6** plots the dc PSD in dB units for the frequency response of our mother Wavelet at dc and the square-root raised-cosine (sq-rt r-c) waveforms with excess bandwidth parameter α= 0.22, 0.40 vs. the normalized frequency in units of symbol rate $1/T_s$.

FIG. **7** plots the dc PSD in dB units for our waveforms vs. the normalized frequency fT_s for our Wavelet waveform designed with modifications to the LS algorithms for application to constant amplitude BEM communications, and for a Gaussian minimum shift keying (GMSK) waveform.

FIG. **8** plots the amplitude of the dc radar ambiguity function vs. the normalized frequency fT_p and normalized time tT_c where the pulse time T_p and chip time T_c are both equal to the communications symbol interval T_s for this example, for the new waveform and an unweighted chirp waveform.

DISCLOSURE OF THE INVENTION

New Wavelet waveforms in this invention disclosure are generalizations of Wavelets in t-f space which enable them to be useful for communications and radar applications. This generalization is accomplished by 1) the introduction of a frequency translation, by 2) changing the orthonormality condition in equation **(4)** to apply to waveforms within the same space {q} and over the scales {p} with the inclusion of the frequency translation, and 3) by their characterization and design in the Fourier domain. With frequency translation the analytical formulation of these new waveforms as a function of the baseband or mother waveform centered at dc(dc refers to the origin f=0 of the frequency space) becomes

$$\psi_{p,q,r}(n) = 2^{-p/2}\psi(2^{-p}n - qM)\,e^{i2\pi f_c(p,r)nT} \qquad (7)$$

where $f_c(p,r)$ is the center frequency of the frequency translated dc waveform, at scale "p" and frequency index "r". The purpose of the frequency index "r" is to identify the center frequencies of the waveforms at the scale "p" in the t-f space.

These waveforms satisfy the complex orthonormality equations

$$\sum_{n} \psi_{p,q,r} \psi^{*}_{k,m,v} = 1 \text{ iff } p = k \text{ and } q = m \text{ and } r = v$$
$$= 0 \text{ otherwise} \qquad (8)$$

where "*" is conjugation, and are generalizations of the orthonormality equations for the analytical Wavelets in **(4)**.

The new waveforms in equation **(7)** expand the Wavelet analytical formulation to include a frequency variable. Wavelets are functions of the scale and translation parameters "p,q". The frequency variable together with the Fourier domain design are entirely new means for deriving these new waveforms as generalization of the traditional Wavelets

These waveforms are generalizations of Wavelets in the frequency domain using a means which makes them useful for communications and radar in the t-f space. The basis vectors for this metric space V consist of a subset of the admissible set of scaled and translated waveforms $\{\psi_{p,q,r}, \forall p,q,r\}$ derived from the dc waveform ψ as per equation **(7)**. An admissible waveform is any combination that covers V=t-f space. We are interested in the Fourier domain representation of the dc waveform ψ in V, and in particular in a subset of the discrete Fourier transform (DFT) harmonic coefficients over the Fourier domain which we intend to use as the design coordinates. Starting with the z-transform and continuous Fourier transform, the DFT harmonic coefficients are defined by the following equations

DFT Harmonic Coefficients **(9)**

$$\psi(z) = \sum_n \psi(n)\, z^{-n} \quad \textit{z-transform}$$

$$\psi(\omega) = \sum_n \psi(n)\, e^{-i\omega n} \quad \textit{Fourier transform}$$

$$\psi_k = \sum_n \psi(n)\, W_{N'}^{-kn} \quad \textit{DFT harmonic coefficients for } \forall k$$

where

$$\psi(\omega) = (1/N') \sum_k \Psi_k \sum_n e^{i(2\pi k/N' - \omega)n}$$

$$= \sum_k \psi_k \sin((\omega/2 - \pi k/N')N') / N\sin(\omega/2 - \pi k/N')$$

$$= \sum_k \psi_k \,[\text{Harmonic interpolation for "k"}]$$

$$W_{N'}^{kn} = e^{i2\pi kn/N'}$$

{k} = DFT frequency or harmonic coefficients such that $f_k = k/N'T$ where f_k is the harmonic frequency corresponding to "k"

N' = length of $\psi(n)$

where $\Psi(\omega) = |\psi(\omega)|^2$ is the power spectral density of the dc waveform. These equations define the frequency representation of our new waveforms in terms of the available set of harmonic coefficients, which set is considerable larger than required for most applications.

Our new waveforms are an orthonormal basis with no excess bandwidth, which properties are asymptoticly approached by our new waveforms to within design accuracies inherent in communications and radar. To demonstrate these properties we need to identify the structure of the dc waveform in V. We start with definitions for the parameters and coordinates in the following equation **(10)**. The waveforms derived from the dc waveform will be designed to be orthogonal over both time translates "MT" and frequency translates "1/MT" which respectively correspond to the Wavelet symbol spacing T_s=MT and

the adjacent channel spacing $1/T_s$. This means the orthogonal spacing of the waveforms in V are at the time-frequency increments $(MT, 1/MT) = (T_s, 1/T_s)$. In the interests of constructing our orthonormal multi-resolution waveforms to cover V it will be convenient to assume that M,L are powers of 2. We need the following definitions for the parameters and coordinates.

Parameters and Coordinates **(10)**

N' = Length of ψ which is an even function about the center and which spans an odd number of points or samples
= ML + 1 where M, L are assumed to be even functions for convenience of this analysis
= Number of points of ψ

M = Sampling interval for ψ
= Spacing of ψ for orthogonality

L = Length of ψ in units of the sample interval M
= Stretching of ψ over L sample intervals

n $= n_0 + n_1 M$
= partitioning into an index n_0 over the sample length $n_0 = 0,1,...,M-1$ and an index $n_1 = 0,1...,L-1$ over the sample intervals

k $= k_0 + k_1 L$
= partitioning into an index k_0 over the harmonic frequencies $k_0 = 0,1,...,L-1$ corresponding to the stretching and an index $k_1 = 0,1,...,M$ over the harmonics frequencies corresponding to the admissible frequency slots for ψ

The harmonic design coordinates are selected using the following observation. For most applications and in the following development it is assumed that the waveforms are spectrally

contained in the frequency interval 1/MT corresponding to the frequency spacing. This suggests the harmonic design coordinates be restricted to the subset of L harmonics $\{k_0=0,1,\ldots,L-1\}$ covering this spacing. These L harmonics correspond to the stretching of the mother waveform over the L repetition intervals.

Obviously, for some applications as will be demonstrated later, the spectral containment is spread out over several 1/LT frequency increments whereupon one must increase the subset of design harmonics to possibly 2L, 3L or larger.

, TheDFT equations for the dc waveform in **(9)** when rewritten in terms of the L harmonic design coordinates $\{\psi_{k_o}, \forall k_0\}$ become:

DFT equations for dc waveform

$$\psi_{k_0} = \sum_n \psi(n)\, W_{N'}^{-k_o n} \quad \text{harmonic design coordinates}$$

$$\psi(n) = (1/N') \sum_{k_0} \Psi_{k_0}\, W_{N'}^{k_o n} \quad \text{new waveform defined in terms of the L harmonic design coordinates } \{\psi_{k_0}, \forall k_0\} \qquad \textbf{(11)}$$

It will now be shown that the use of these L harmonic design coordinates is sufficient under time translates to be a basis for the corresponding subspace of V which means these waveforms provide a complete set of coordinates to describe this subspace. Wethe will use the theorems of Karhunen-Loeve and Mercer and will limit the demonstration to the dc waveform for simplicity and without loss of generality. We start by considering the expansion of a random complex sequence {z(n),

$\forall n\}$ in a series of waveform coordinates consisting of time translates of the mother waveform ψ. The sequence $\{z(n), \forall n\}$ is a zero-mean stationary random process which is orthonormal over the sample interval "M" and has a frequency spectrum which is flat and extends over the frequency range 1/LT which is centered at baseband corresponding to a zero frequency. This means the $\{z(n), \forall n\}$ cover the subspace of V corresponding to the scale of our dc waveform ψ and its time translates $\{\psi(n-qM) = \psi_q(n), \forall q\}$. In addition, the V is now considered to be extended over a time interval which is relatively large compared to the N-dimensional t-f space in FIG. **1,2** to avoid end-effects on the analysis. We start by approximating the sequence $\{z(n), \forall n\}$ by the $\{\hat{z}(n), \forall n\}$ where:

$$\hat{\mathbf{z}}(\mathbf{n}) = \sum_{q} \mathbf{Z}_q \, \psi(\mathbf{n} - \mathbf{qM})$$

$$= \sum_{q} \mathbf{Z}_q \, \psi(\mathbf{n}_0 + (\mathbf{n}_1 - \mathbf{q})\mathbf{M})$$

where the complex coefficients $\{Z_q\}$ are derived from the original sequence using the orthogonality properties of ψ **(12)**

$$Z_q = \sum_{n} z(n) \, \psi^*(n - qM)$$

$$= \sum_{n} z(n) \, \psi_q(n)$$

The following equations prove that the coefficients $\{Z_q, \forall q\}$ are orthonormal:

$$\mathbf{Z_q Z_{q'}}^* = \sum_{\Delta n} \mathbf{z(\Delta n - qM) z^*(\Delta n - q'M)\psi_q(\Delta n)\psi_{q'}^*(\Delta n)} \qquad \textbf{(13)}$$

$$= \delta_{qq'} \sum_{n} \left|\psi_q(\mathbf{n})\right|^2 \quad \text{since the sequence } \{z\} \text{ is orthonormal}$$

$$\text{for qM time translates}$$

$$= \delta_{qq'} \quad \text{with normalization of the energy of } \psi$$

Equations **(12)** and **(13)** together prove the Karhunen-Loeve's theorem which proves the following equation for the accuracy in approximating the stochastic sequence {z(n), $\forall$n} by {$\hat{z}(n)$, $\forall$n}. This accuracy is expressed by the expected "E(o)" squared error "(o)" in this approximation:

$$E\left\{\left|z(n) - \hat{z}(n)\right|^2\right\} = 1 - \sum_{n_1} \left|\psi(n_0 + n_1 M)\right|^2 \qquad \textbf{(14)}$$

We need to prove that the right hand side of this equation is zero which then proves that the approximating sequence is equal to the original sequence in the mean-square sense. In turn this proves that the new waveform coordinates {ψ_q, $\forall$q} are a basis for the original sequence {z(n), $\forall$n} which is our goal.

The right hand side of equation **(14)** when set equal to zero expresses Mercer's theorem so our goal is to prove Mercer's theorem. To do this we use the DFT of ψ in equation **(11)** and the coordinates in **(10)** to evaluate the right hand side of equation **(14)**. We find

$$1 - \sum_{n_1} \left|\psi(n + n_1 M)\right|^2 = 1 - \sum_{k_0} \sum_{k_0'} \Psi_{k_0} \Psi_{k_0'} W_N^{\Delta k_0 n_0} \Gamma$$

where $\Gamma = (1/L) \sum_{n_1} W_L^{\Delta k_0 n_1}$

$= \sin(\pi \Delta k_0) / L \sin(\pi \Delta k_0 / L)$

$= 1$ for $\Delta k_0 = 0$ **(15)**

$= 0$ otherwise

This proves that

$$1 - \sum_{n_1} \left|\psi(n + n_1 M)\right|^2 = 0 \quad \forall n_0$$

which proves that equation **(14)** reduces to

$$E\left\{\left|z(n) - \hat{z}(n)\right|^2\right\} = 0 \qquad \textbf{(16)}$$

which as per the above proves that the set of multi-resolution waveforms is a basis. This proof easily generalizes to the multi-resolution waveforms at all of the scales {p} and time translates {q}, and to the expansion of the harmonic design coordinates over 2L, 3L, … as required by the application.

Next we demonstrate that these waveforms have multi-scale properties. that we will demonstrate. We start with the observation that the Fourier domain design for the new waveforms provides a natural and easy way to derive the complete set of waveforms $\{\psi_{p,q}, \forall p,q\}$ for the space V from the design of the dc waveform ψ by using the same invariant set of Fourier domain harmonic design coordinates $\{\Psi_{k_0}, \forall k_0\}$ derived for the dc multi-resolution waveform. This demonstration requires that we show 1) how the multi-scale transformations are implemented with the

design in the Fourier domain, and 2) how the waveform design remains invariant under scale changes.

First consider the multi-scale transformation which derives the waveforms at the scale and shift parameters "p,q" from the dc waveform at scale "p=0" and centered at the origin "q=0". We begin by extending the parameters and coordinates in equation **(10)**, to include both scaling and subsampling or decimation in a form that is equivalent to the iterated filter bank construction which is used to derive the current Wavelet waveform using the filter scaling functions. Starting with the coordinates at scale "p=0" the parameters and coordinates at scale "p=p" are given by the equations:

p=0 parameters and coordinates

$$n = n_0 + n_1 M \qquad \textbf{(17)}$$

$$n_0 = a_0 + a_1 2 + \ldots + a_{m-1} 2^{m-1}$$

$$= M \text{ points}$$

$$M = 2^m$$

$$n_1 = b_0 + b_1 2 + \ldots + b_{l-1} 2^{l-1}$$

$$= L \text{ points spaced at } M \text{ sample intervals}$$

p=p parameters and coordinates

$$2^{-p}\, n(\downarrow 2^p) = \text{scaled by } "2^{-p}"$$

and subsampled or decimated by 2^p:1

$$= n_0(p) + n_1(p)M$$

$$2^{-p}\, n_0(\downarrow 2^p) = \text{scaled by } "2^{-p}"$$

and subsampled or decimated by 2^p:1

$$= n_0(p)$$

$$= a_p + a_{p-1}2 + \ldots + a_{p+m-1} 2^{p+m-1}$$

$$= M \text{ points spaced at } 2^p \text{ sample intervals}$$

$2^{-p}\ n_1(\downarrow 2^p)$ = scaled by "2^{-p}"
and subsampled or decimated by 2^p:1
= $n_1(p)$
= $b_p + b_{p+1}\ 2 + \ldots + b_{p+l-1}\ 2^{p+l-1}$
= L points spaced at $M2^p$ sample intervals

together with the observation that the sampling interval "T" is increased to "2^pT" under the scale change from "p=0" to "p=p" and subsampling or decimation from "1:1" to "2^p:1". Combining these equations with the analytical formulation in **(7)** and the Fourier domain representation in **(11)** enables the waveforms at the parameters "p,q" to be written as a function of the Fourier domain harmonic design coordinates:

$$\psi_{p,q,r}(n) = 2^{-p/2}\psi(2^{-p}n - qM)\, e^{i2\pi f_c(p,r)nT}$$
$$= (2^{-p/2}/N') \sum_{k_0} \Psi_{k_0}\, W_{N'}^{k_0(n(p)-qM)}\ e^{i2\pi f_c(p,r)n(p)2^pT} \qquad \textbf{(18)}$$

for all admissible scale, translation, and frequency index parameters "p,q,r".

Next we need to demonstrate that the frequency domain design in **(11)** remains invariant for all parameter changes and in particular for all scale changes. This multi-scale property expresses the accordion behavior of the design in that the Wavelets at different scales are simply the stretched and compressed versions of the mother waveform with the appropriate frequency translation indices. This multi-scale invariancy means that the design for a M=16 channel filter bank remains the same for M=100 or M=10,000 channel filter banks, when the overlap L and the performance goals remain constant. To demonstrate this invariant property across scales, we consider the multi-

resolution waveform at scale "p" with the other parameters set equal to zero for convenience "q=0, r=0" and without loss of generality. The Fourier domain frequency response $\Psi(f)$ can be evaluated starting with the original formulation in equation **(7)**:

DFT at "p, q=0, r=0" **(19)**

$$\Psi_p(f) = (1/N')\sum_{k_0}\Psi_{k_0}\sum_{n(p)}W_{N'}^{-(fN'2^pT\ -k_0)n(p)}$$

$$= \sum_{k_0}\Psi_{k_0}\left[\frac{\sin(\pi\ (fN'2^pT - k_0))}{N'\sin(\pi\ (fN'2^pT - k_0)/N')}\right]$$

$$= \sum_{k_0}\Psi_{k_0}\ \left[\text{Harmonic interpolation for "}k_0\text{"}\right]$$

This only differs from the harmonic representation in equation **(9)** in the restriction of the design coordinates to the subset of harmonic coefficients $\{\psi_{k_o}, \forall k_0\}$ and the stretching of the time interval to "2^pT" corresponding to the scale "p=p". The harmonic interpolation functions are observed to remain invariant over scale changes upon observing that the frequency scales as "$f\sim 1/2^pT$" which means the "frequency*time" product remains invariant with scale changes as per the fundamental property of the waveforms. This means the harmonic interpolation functions remain invariant with scale change and therefore the frequency response remains an invariant. This demonstrates the waveform design is an invariant across the waveform scales which means we only need a single design for all scales or resolutions of interest.

LS design algorithms for new waveform will be described to illustrate the advantages our waveform has over current designs. The two LS algorithms described are the eigenvalue and the gradient search which respectively can be reduced to algorithms which are equivalent to current eigenvalue and Remez-exchange waveform design algorithms for application to a uniform filter bank. We consider the t-f space which is spanned by a uniform polyphase filter bank consisting of M channels at the frequency spacing $f_w=1/MT$ where T is the digital sampling interval, and the filter waveform FIR time response is stretched over L sampling time intervals T_s. This polyphase filter bank is ideally decimated which means the filter ouput sample rate $1/T_s$ is equal to the channel-to-channel spacing $T_s=MT$, equivalent to stating that there is no excess bandwidth $\alpha=0$. Our design for this topology is immediately applicable to an arbitrary set of multi-resolution filters through the scaling equation **(18)** which gives the design of our waveform at arbitrary scales in terms of our design of the dc waveform.

For this polyphase filter bank used to construct the dc waveform or filter impulse response, our LS example design algorithms will use 5 metrics consisting of the 2 prior art passband and stopand metrics, and the 3 new metrics consisting of the ISI, ACI, and QMF, and solve the LS minimization problem using as design coordinates the subset of harmonic coordinates which are a basis. Since our two example LS design algorithms only differ in the use of an eigenvalue LS optimization and the use of a gradient search LS optimization, the flow diagrams for the construction of the cost functions and the solution for the optimal waveform will be identical. However, there are differences in the construction of the cost functions from the respective metrics and in the iterative solution mathematics. Both LS solutions for the harmonic design coordinates minimize the weighted sum of the error residuals or cost functions from

the 5 metrics. These design coordinates are the Fourier harmonics $\{\psi_{k_o}, \forall k_0\}$ for $\{k_0 = 0,1,\ldots,L-1\}$. Resulting algorithms are easily extended to the applications requiring the design coordinates to cover 2L, 3L, … harmonics.

Frequency domain design coordinates are related to the waveform time domain digital samples or coordinates as follows.

Mappings of frequency to time **(20)**

Time domain design coordinates $\{\psi(n), \forall n\}$ are real and symmetric and can be represented by the reduced set $\{h_t(n), n=0,1,\ldots,ML/2\}$

$h_t(n) = \psi(0)$ for n=0

$= 2\psi(n)$ for n=1,2,…,ML/2

= time domain design coordinates

Frequency domain harmonic design coordinates $\{\psi_{k_o}, \forall k_0\}$ are real and symmetric and can be represented by the reduced set $\{h_f(k), k=0,1,,\ldots,L-1\}$

$h_f(k) = \psi_{k_0}$ for $k=k_0=0$

$= 2\psi_{k_0}$ for $k=k_0=1,2,\ldots,L-1$

= frequency domain design coordinates

Mapping of the frequency coordinates $\{h_f(k), k=0,1,\ldots,L-1\}$ into the time coordinates $\{h_t(n), n=0,1,\ldots,ML/2\}$ is defined by the matrix transformation to within a scale factor

$h_t = B\ h_f$

where

$h_f = (h_f(0), \ldots, h_f(ML/2))^t$ transpose of column vector

$h_t = (h_t(0), \ldots, h_t(ML/2))^t$ transpose of column vector

B = (ML/2 +1) x L matrix

$$= [\ B_{kn}\ ] \quad \text{matrix of row k and column n elements } B_{kn}$$

$$B_{kn} = 1 \qquad \text{for n=1}$$

$$= 2\cos(2\pi kn/ML) \quad \text{otherwise}$$

wherein the N′=ML+1 has been replaced by ML since a single end point has been added to the the FIR to make it symmetrical for ease of implementation for the example Wavelet being considered with a sample at the mid-point that makes the number of samples N′ an odd number.

Passband and stopband metrics and cost functions are derived with the aid of FIG. **3** which defines the po PSD parameters of interest for the passband and stopband of the PSD $\Psi(\omega)$ for communications applications. Requirements for radar applications include these listed for communications. Referring to FIG. **3** the passband **11** of the waveform PSD is centered at dc (f=0) since we are designing the dc or baseband waveform, and extends over the frequency range ω_p extending from $-\omega_p/2$ to $+\omega_p/2$ **12** in units of the radian frequency variable $\omega=2\pi fT$ **13**. The frequency space extends over the range of f=-1/2T to f=+1/2T which is the frequency range in FIG **1** translated by -1/2T so that the dc waveform is at the center of the frequency band. Quality of the PSD over the passband is expressed by the passband ripple **14**. Stopband **15** starts at the edge **16** of the passbands of the adjacent channels $+/-\omega_a/2$ **16** and extends to the edge of the frequency band $\omega=+/-\pi$ **17** respectively. Stopband attenuation **18** at $+/-\omega_a/2$ measures the PSD isolation between the edge of the passband for the dc waveform and the start of the passband for the adjacent channels centered at $+/-\omega_s$ **19**. Rolloff **20** of the stopband is required to mitigate the spillover of the channels other than the adjacent channels, onto

the dc channel. Deadband or transition band **21** is the interval between the passbands of contiguous channels, and is illustrated in FIG. **3** by the interval from $\omega_p/2$ to $\omega_a/2$ between the dc channel and adjacent channel at ω_a. Waveform sample rate ω_s **22** is the waveform repetition rate. For the LS example algorithms, the waveform sample rate is equal to the channel-to-channel spacing for zero excess bandwidth. Therefore, $1/T_s = \omega_s/2\pi T = 1/MT$ which can be solved to give $\omega_s = 2\pi/M$ for the radian frequency sampling rate of the filter bank which is identical to the waveform repetition rate.

We start by rewriting the DFT equations for the dc waveform in (11) as a function of the $\{h_f(k),\ k=0,1,\ldots,L-1\}$

$$\psi(\omega) = \sum_n \psi(n)\cos(n\omega)$$
$$= c^t B h_f \quad \text{using (21) and the definition of the vector "c"} \qquad \textbf{(21)}$$
$$c = (1, \cos(\omega), \ldots, \cos((ML/2)\omega))^t \quad \text{transpose of column vector}$$

which is equivalent to the equation for $\psi(\omega)$ in **(9)** expressed as a linear function of the $\{h_f(k),\ k=0,1,\ldots,L-1\}$. An ideal "c" vector "$c_r$" will be introduced for the passband and the stopband in FIG. **3** in order to identify the error residual $\delta\psi(\omega)$ at the frequency "ω" in meeting the ideal passband and stopband requirements. The ideal PSD is flat and equal to "1" for the passband, and equal to "0" for the stopband. We find

Error residuals for passband and stopband **(22)**

$$c_r = (1,1,\ldots,1)^t \quad \text{passband ideal "c"}$$
$$= (0,0,\ldots,0)^t \quad \text{stopband ideal "c"}$$
$$\delta c = c_r - c \quad \text{error vector}$$

$$\delta\psi(\omega) = \delta c^t \, B \, h_f$$

= Residual error in meeting the ideal spectrum at "ω"

The LS metric for the passband and stopband can now be constructed as follows for the eigenvalue and the LS optimization (or equivalently, the LS algorithm) design algorithms

Passband and stopband metrics **(23)**

$$J(\text{band}) = \frac{1}{band} \int_{band} |\delta\psi(\omega)|^2 \, d\omega \qquad \text{Eigenvalue}$$

$$= h_f' \mathbf{R} \; h_f \qquad \text{Eigenvalue}$$

$$= \|\delta\psi\|^2 \qquad \text{LS}$$

where

band = $[0, \omega_p)$ passband

= $(\omega_s, \pi]$ stopband

$$\mathbf{R} = \frac{1}{band} \int_{band} (B^t \, \delta c \, \delta c^t \, B) \, d\omega$$

= L x L matrix

$\delta\psi$ = $(\delta\psi(\omega_1), \ldots, \delta\psi(\omega_u))^t$

= vector of error residuals at the frequencies $\omega_1, \ldots, \omega_u$ across the band

$\|(o)\|$ = norm or length of the vector (o) and which includes a cost function for the errors of the individual components

where it is observed that the eigenvalue approach requires that the LS metrics be given as quadratic forms in the design

coordinates $\{h_f(k),\ k=0,1,\ldots,L-1\}$ whereas with the LS approach it is sufficient to give the LS metrics as vector norms with imbedded cost functions or an equivalent formulation.

QMF metrics express the requirements on the deadband that the PSD's from the contiguous channels in FIG. **3** add to unity across the deadband $[\omega_p\ ,\ \omega_s]$ in order that the filters be QMF filters. By suitable modification of the error vector δc, the previous construction of the passband and stopband metrics can be modified to apply to the deadband. We find

Deadband metrics **(24)**

$$J(\text{deadband}) = \frac{1}{deadband}\int_{\text{deadband}} |\delta\psi(\omega)|^2\, d\omega \qquad \text{Eigenvalue}$$

(24) continued

$$= h_f' \mathbf{R}\ h_f \qquad \text{Eigenvalue}$$

$$= \|\delta\psi\|^2 \qquad \text{LS}$$

where

$$\delta c = c_r - c(\omega) - c(\pi/M - \omega)$$

where $c(\omega)=c$ as defined in **(22)** and **(23)**, and $c(\pi/M - \omega) = c$ at the offset frequency "$\pi/M - \omega$" corresponding to the overlap of the contiguous filters over the deadband.

Orthonormality metrics measure how close we are able to designing the set of waveforms to be orthonormal over the t-f space, with the closeness given by the ISI and the ACI. ISI and ACI errors are fundamentally caused by different mechanisms and therefore have separate metrics and weights to specify their relative importance to the overall sum of the LS metrics. ISI

is a measure of the non-orthogonality between the stream of waveforms within a channel as per the construction in FIG. **3**. On the other hand, ACI is a measure of the non-orthogonality between the waveform within a channel and the other waveforms in adjacent channels. This means the stopband performance metric has a significant impact on the ACI due to the sharp rolloff in frequency of the adjacent channel, and the ACI metric is then a measure of the residual non-orthogonality due to the inability of the stopband rolloff in frequency from completely eliminating the ACI errors.

We assume that the received waveform is identical to the filter waveforms and is transmitted at the filter output sample intervals equal to MT seconds. The second assumption means we are assuming the receiver is synchronized with the received signal. Since there is no information lost by sampling asynchronously with the received waveform, we are free to make this synchronization assumption without loss of generality. ISI metrics are derived in the following set of equations.

ISI metrics **(25)**

Mapping of h_f into ψ

$\psi = (\psi(-ML/2), \ldots, \psi(ML/2))^t$ transpose of column vector

$= H\ h_f$

$H = (ML+1) \times L$ matrix of elements H_{kn}

$H_{kn} = 1$ for n=1

$= 0.5 \cos(2\pi kn/ML+1)$ otherwise

Offset matrix A

$A = L \times (ML+1)$ matrix of elements A_{kn}

$A_{kn} = 0$ for row vector k=1

$= [0 \quad 0 \quad \ldots \quad \psi(-ML/2) \ldots \psi((L-k)M+1)]$ row vector k

$1 \quad 2 \qquad kM \qquad\qquad LM+1$ column elements

ISI error vector δE

$\delta E = L \times 1$ column vector

$= A H h_f$

ISI metric

$J(ISI) = \delta E^t \delta E$ Eigenvalue

$=$ Non-linear quadratic function of h_f

$= \|\delta E\|^2$ LS

ACI metrics are derived using the ISI metric equations with the following modifications.

ACI metrics **(26)**

Mapping of h_f into ψ is the same as developed for ISI Offset matrix A elements are changed as follows to apply to Channel 1:

$A_{kn} = 0$ for row vector k=1

$= [0 \quad 0 \quad \ldots \quad \psi(-ML/2) W_M^0 \quad \ldots \quad \psi((L-k)M+1) \; W_M^{(L-k)}]$

$1 \quad 2 \qquad kM+1 \qquad\qquad LM+1$

which means the ACI error vector δE is

$\delta E = L \times 1$ column vector

$= A H h_f$

ACI metric for the two contiguous channels

$J(ISI) = 2\ \delta E^t \delta E$ Eigenvalue

$=$ Non-linear quadratic function of h_f

$= 2\ \|\delta E\|^2$ LS

where the factor "2" takes into account there are two contiguous channels or one on either side of the reference channel 0 in FIG. **3**. Because of the fast rolloff of the frequency spectrum the addition of more channels into the ACI metric is not considered necessary, although the functional form of the ACI metric in **(26)** allows an obvious extension to any number of adjacent channels which could contribute to the ACI.

Cost function J for the LS algorithms is the weighted sum of the LS metrics derived in **(23)**, **(24)**, **(25)**, **(26)**. The LS algorithms minimize J by selecting the optimal set of frequency coordinates $\{h_f(k), \forall k\}$ for the selected set of parameters used to specify the characteristics of the dc waveform, frequency design coordinates, LS metrics, and weights. Cost function and optimization techniques are given by the equations

Cost function J **(27)**

$$J = \sum_{x} w(metrics)\, J(\text{metrics})$$

= weighted sum of the LS metrics J(metrics)

where

metrics = passband, stopband, deadband, ISI, ACI

$\{w(\text{metrics}), \forall metrics\}$ = set of weights

$$\sum_{x} w(metrics) = 1 \quad \text{normalization}$$

Optimization goal

Goal: minimize J with respect to the selection of the $\{h_f(k), \forall k\}$

Optimization algorithms

Two algorithms are the Eigenvalue and the LS optimization

where the eigenvalue optimization algorithm uses the non-linear quadratic formulations of the LS metrics and the LS optimization algorithm uses the norm formulations for the LS metrics.

FIG. **4** is a summary of the LS metrics and the construction of the cost function J. Design parameters **23** are L, N'=ML+1, number of DFT samples per FIR length n_fft for implementation of the LS algorithms, passband radian frequency ω_p, stopband radiam frequency ω_a, waveform repetition rate in radian frequency ω_s, selection of the set of design coordinates $\{h_f\}$ to be used in the optimization, and the metric weights {w(metrics)}. Output parameters are the set of harmonic design coordinates $\{h_f\}$ that minimize J. Band metrics **24** are the passband, stopband, and deadband metrics defined in equations **(23)**, **(23)**, **(24)** respectively. Interference metrics **25** are the ISI and ACI metrics defined in equations **(25)** and **(26)** respectively. LS cost function J **26** is the weighted linear sum of the metrics defined for the band **24** and the interference **25** as defined in equation **(27)**.

FIG. **5** is a flow diagram of the LS recursive solution algorithm. There are two loops with the topology constructed so that the outer loop **27** is an iteration over the set of metric weights {w(metrics)}, and the inner nested loop **28** is the recursive or iteratived LS solution to find the optimal $\{h_f\}$ for the given design parameters and weights where each step refers to an iteration step in the solution. A recursive LS solution is required to be able to solve the highly non-linear interference metrics as well as the band metrics when one chooses to use non-linear techniques to construct these metrics.

Consider the inner nested loop **28**. The recursive LS solution starts with the initial step i=0 **29** which begins with the selection of the input design parameters and weights and the selection of an initial set of values for the $\{h_f\}$ **30**. Next the band metrics are calculated **31**. Since this is the initial step i=0 **32** the cost function J is restricted to the linear band metrics in order to fine the linear approximation to $\{h_f\}$ **33** to initialize the non-linear solution starting with step i=1 **34** wherein the highly non-linear interference metrics are included in J. Following the signal flow, for step i=1 the band metrics **31** and interference metrics **35** are calculated, weighted, and summed to form the cost function J **36**. An iterative solution algorithm **37** finds the best approximation in step i=1 to the $\{h_f\}$ which minimizes J using the approximation to $\{h_f\}$ from the previous step i=0 to linearize the search algorithm coefficients for the eigenvalue and LS step i=1 iteration. If there is no convergence to the correct solution for $\{h_f\}$ this recursive sequence of calculations is repeated for step i=2 **34**. This recursive solution technique is repeated for subsequent steps until there is convergence **38** whereupon one exits this inner loop.

Consider the outer loop. After exiting the inner loop **38** the solution for $\{h_f\}$ is tested to see if it meets the performance goals **39**. If not, a new set of metric weights is selected and the inner loop is initialized i=0 **40** and the inner loop is used to find the next solution for $\{h_f\}$. This process continues until the performance goals are met or adequated approximated **39** whereupon the algorithm is exited with the final solution set $\{h_f\}$ **41**.

FIG. **4,5** derive the new multi-resolution Wavelet ψ at baseband. Scaling equations **(7),(18)** can be used to derive the corresponding digital Wavelet at scales p,q,k with parameters M,L wherein the digital frequency parameter "k" replaces the frequency index "r". Equation **(7)** can be rewritten to define the scaling equation which derives this Wavelet $\psi_{p,q,M,L,k}$ from ψ:

New Wavelet scaled from mother Wavelet **(28)**

$$\psi_{p,q,M,L,k} = \psi_{p,q,k} \quad \text{with parameters } M,L$$

$$= 2^{-p/2}\, \psi(2^{-p}n - qM)\, \exp(j2\pi\, k\, 2^{-p}n\, /ML)$$

There are at least two methods of scaling used to implement equation **(28)**. In method **1** corresponding to the standard Wavelet assumption, the subsampling or decimation of n by the factor 2^p stretches the time between contiguous samples by the factor 2^p while keeping constant the number of samples M per Wavelet ψ sample interval, and therefore reduces the frequency band by the factor 2^p. For a uniform filter bank, this means the filter frequency bands are reduced by the factor 2^p. In method **2**, the sampling is held constant corresponding to a constant frequency band assumption. The factor 2^(-p) is divided out in the Wavelet expression which is equivalent to the M being scaled to 2^pM corresponding to increasing the number of samples per Wavelet interval by the factor 2^p. For a uniform filter bank, this means method **2** corresponds to increasing the maximum number of channels by the factor 2^p over the same frequency band.

Applications of this new invention to both communications and radar will be given using these example algorithms and other

algorithms supported by this invention. These new waveforms are considered for the applications: 1)to replace the square-root raised cosine waveform (sq-root rc) which is extensively used for the third generation (3G) CDMA communications, 2)to replace the Gaussian minimum shift keying (GMSK) waveform for constant amplitude bandwidth efficient (BEM) applications, and 3) as a candidate waveform for synthetic aperture radar (SAR) and real aperture radar (RAR) applications.

CDMA communications application for the current and the new 3G CDMA considers a waveform designed with this new invention as a possible replacement for the sq-rt rc waveform with bandwidth expansion parameter $\alpha = 0.22$ to $\alpha = 0.40$. This notation means that for $\alpha = 0.22$ the spectral efficiency is (symbol rate/bandwidth) = $1/1+\alpha$ =1/1.22 = 0.82 = 82%. A basic advantage of the waveform is the potential for a symbol rate increase within the same bandwidth with an increase in the spectral efficiency to $\approx 100\%$ depending on the application and operational constraints. The dc power spectral density or power spectrum (PSD) of the waveform is compared to the PSD for the sq-rt r-c in FIG. **6**. Plotted are the measured PSD in dB **42** versus the frequency offset from dc expressed in units of the symbol rate **43** Plotted against the normalized frequency offset are the dc PSD for the new waveform **44**, the sq-rt r-c with α=0.22 **45**, and the sq-rt r-c with α=0.40 **46**. It is observed that the PSD for the new waveform rolls off faster that that for the sq-rt r-c which means that the new mr waveform will support an increased symbol rate for a given available frequency band while satisfying the inherent requirements for low ISI and MAI (multiple access interference).

Constant amplitude BEM application of the new waveform indicates that it is a viable candidate for replacing the current preferred modulation waveform which is the GMSK. The GMSK finds applications for transmitters which operate their HPA(s)

amplifiers in a saturation mode in order to maximize their radiated power from the HPA(s), and which require a BEM PSD to avoid excessive spreading of the transmitted power. Simulation data for the dc PSD is plotted in FIG. **7** for the new waveform BEM and the GMSK. Plotted are the measured dc PSD in dB **47** versus the frequency offset from dc expressed in units of the bit rate **48**. Plotted against the normalized frequency offset are the dc PSD for the new waveform BEM **49** and the GMSK **50**, for a length parameter L=10 where L is the length of the phase pulse in terms of the phase pulse repetition rate. The significance of this example data is that the new waveform has the potential to be designed to offer a PSD which is less spread out than the current GMSK, and therefore an improved BEM waveform.

Radar RAR and SAR application of the waveform indicates that it is a viable candidate to replace the current chirp waveforms for wideband signal transmission, when combined with pseudo-random phase codes. Results of the simulation for the new waveform and an unweighted frequency chirp waveform are given in FIG. 8. Plotted are the ambiguity function for the new waveform **51** and the unweighted frequency chirp waveform **52**. The dc 2-dimensional radar ambiguity function **53** is plotted as a function of the frequency offset in units of fT_p and the time offset in units of t/T_c where T_p is the phase-coded radar pulse length or length of the phase code and T_c is the phase code chip length. The chip length is identical to the waveform repetition interval T_s so that $T_c = T_s$. It is observed that the new waveform has the potential for significant improvements in the ambiguity function and by implication in the performance.

Preferred embodiments in the previous description are provided to enable any person skilled in the art to make or use the present invention. The various modifications to these embodiments will be readily apparent to those skilled in the art, and the generic principles defined herein may be applied to other

embodiments without the use of the inventive faculty. Thus, the present invention is not intended to be limited to the embodiments shown herein andis to be accorded the wider scope consistent with the principles and novel features disclosed herein.

APPLICATION NO. 09/826,118

TITLE OF INVENTION: Wavelet Multi-Resolution Waveforms

INVENTOR: Urbain A. von der Embse

Marked up version of amended ABSTRACT OF THE DISCLOSURE

APPLICATION NO. 09/826,118

TITLE OF THE INVENTION: ~~New~~ Wavelet Multi-Resolution Waveforms

INVENTORS: Urbain ~~Alfred~~ A. von der Embse

ABSTRACT OF THE DISCLOSURE

~~**ABSTRACT**~~

~~The present invention describes a new method for the design of multi-resolution waveforms to improve system performance, design flexibility, applicability, and reduce the costs of implementation, compared to the current art. The multi-resolution waveform designs are a generalization of Wavelets to the Fourier domain. This generalization uses design algorithms which include application metrics to improve system performance, allows a single design to be used for all scales, and allows each design to be characterized by a relatively few parameters. Preliminary simulations indicate that waveform and filter performance can be significantly improved compared to current techniques for communications applications to code division multiple access (CDMA) waveforms and filters, communications constant-amplitude bandwidth efficient waveforms, and radar system applications.~~

~~Wavelets for multi-resolution waveforms and filters are designed to meet specific application requirements, are defined by a relatively small number of frequency harmonics, are complex, include a frequency translation, and can be designed to be orthogonal with no excess bandwidth for communications applications. Frequency design harmonics and frequency translation capability enable the waveforms at multiple resolutions to be derived from a single design by scaling the dilation, translation, and frequency translation parameters. Design is illustrated by Matlab 5.0 code to generate a linear filter waveform using an iterative least-squares eigenvalue approach to minimize the non-linear least-squares cost function,~~

~~and to scale this waveform design for multi-resolution application specified by the dilation, time translation, and frequency translation parameters. Additional results are given for a constant amplitude minimum-shift-keying bandwidth-efficient modulation waveform and for a synthetic aperture radar waveform.~~

A method for designing Wavelets for communications and radar which combines requirements for Wavelets and finite impulse response FIR filters including no excess bandwidth, linear performance metrics for passband, stopband, quadrature mirror filter QMF properties, intersymbol interference, and adjacent channel interference, polystatic filter design requirements, and non-linear metrics for bandwidth efficient modulation BEM and synthetic aperture radar SAR. Demonstrated linear design methodology finds the best design coordinates to minimize the weighted sum of the contributing LS error metrics for the respective performance requirements. Design coordinates are mapped into the optimum FIR symbol time response. Harmonic design coordinates provide multi-resolution properties and enable a single design to generate Wavelets for arbitrary parameters which include dilation, down-sampling, up-sampling, time translation, frequency translation, sample rate, symbol rate, symbol length, and set of design harmonics. Non-linear applications introduce additional constraints. Performance examples are linear communications, BEM, and SAR.

APPLICATION NO. 09/826,118

TITLE OF INVENTION: Wavelet Multi-Resolution Waveforms

INVENTOR: Urbain A. von der Embse

Clean version of how the ABSTRACT OF THE DISCLOSURE will read.

APPLICATION NO. 09/826,118

TITLE OF THE INVENTION: Wavelet Multi-Resolution Waveforms

INVENTOR: Urbain A. von der Embse

ABSTRACT OF THE DISCLOSURE

A method for designing Wavelets for communications and radar which combines requirements for Wavelets and finite impulse response FIR filters including no excess bandwidth, linear performance metrics for passband, stopband, quadrature mirror filter QMF properties, intersymbol interference, and adjacent channel interference, polystatic filter design requirements, and non-linear metrics for bandwidth efficient modulation BEM and synthetic aperture radar SAR. Demonstrated linear design methodology finds the best design coordinates to minimize the weighted sum of the contributing LS error metrics for the respective performance requirements. Design coordinates are mapped into the optimum FIR symbol time response. Harmonic design coordinates provide multi-resolution properties and enable a single design to generate Wavelets for arbitrary parameters which include dilation, down-sampling, up-sampling, time translation, frequency translation, sample rate, symbol rate, symbol length, and set of design harmonics. Non-linear applications introduce additional constraints. Performance examples are linear communications, BEM, and SAR.

APPLICATION NO. 09/826,118

TITLE OF INVENTION: Wavelet Multi-Resolution Waveforms

INVENTOR: Urbain A. von der Embse

Currently amended DRAWINGS AND PERFORMANCE DATA

APPLICATION NO. 09/826,118
INVENTION: Wavelet Multi-Resolution Waveforms
INVENTOR: Urbain Alfred von der Embse

DRAWINGS AND PERFORMANCE DATA

DELETED SHEET

FIG. 1 Wavelet Tiling of an N-Point Digital t-f Space

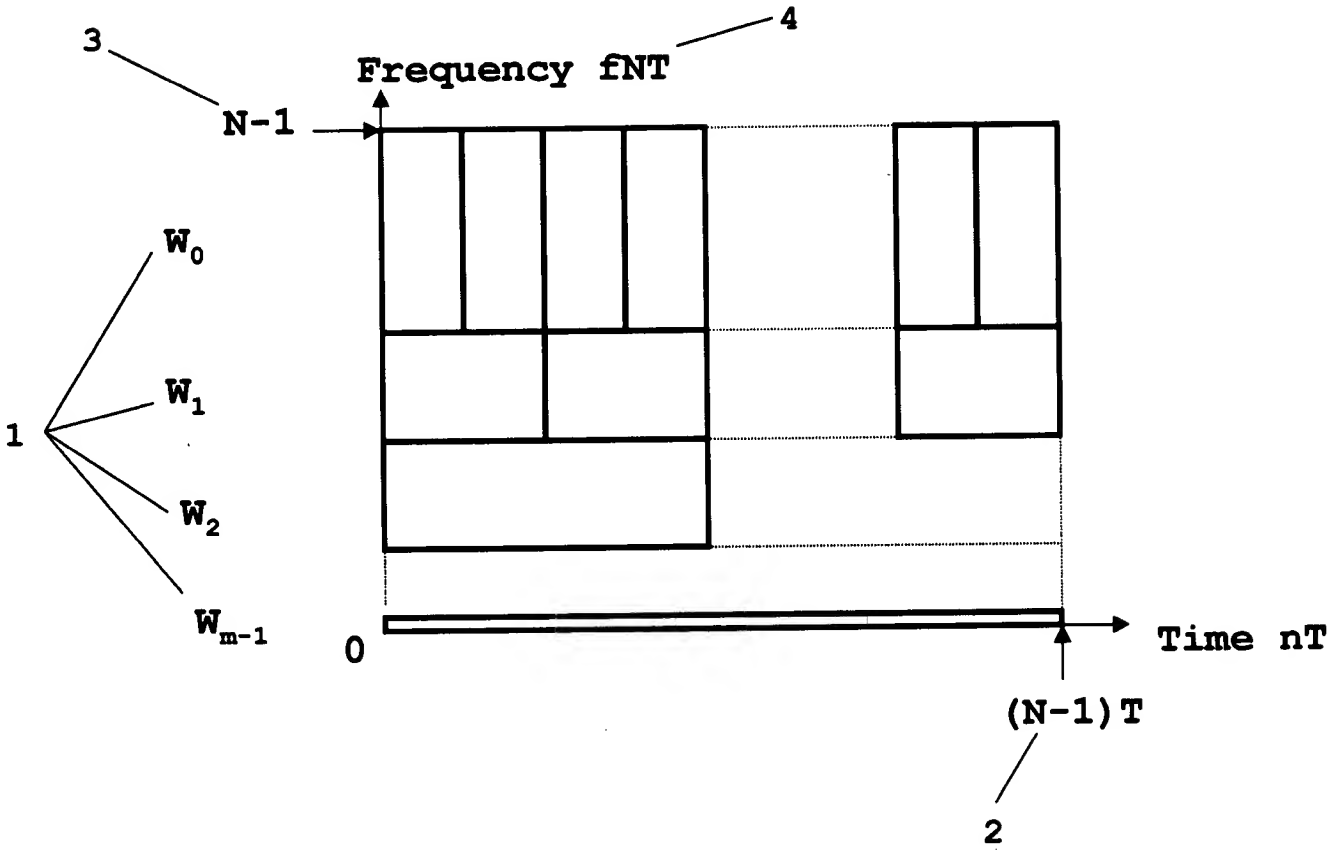

REPLACEMENT SHEET

FIG. 1 Prior Art: Wavelet Tiling of an N-Point Digital t-f Space

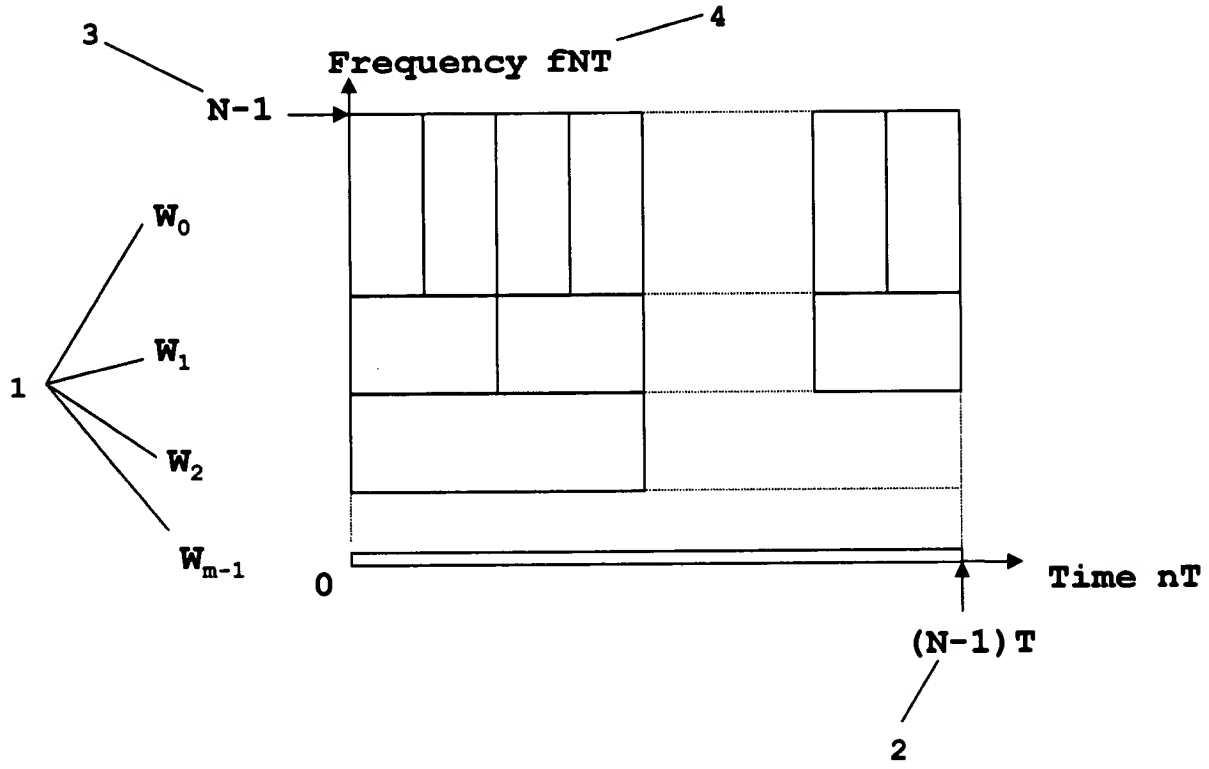

DELETED SHEET

FIG. 2 Wavelet Iterated Filter Bank for Tiling t-f Space in FIG. 1

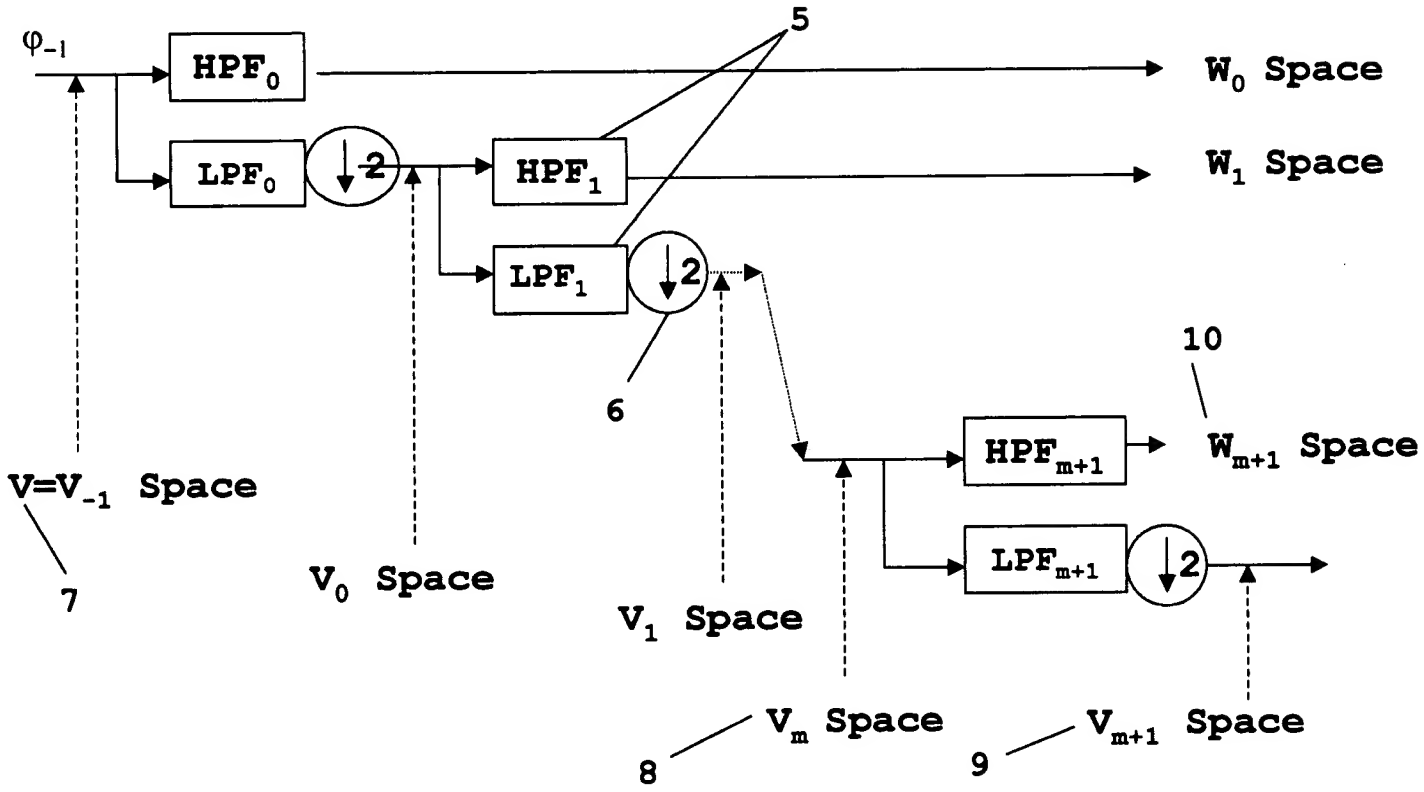

FIG. 2 Prior Art: Wavelet Iterated Filter Bank for Tiling t-f Space in FIG. 1

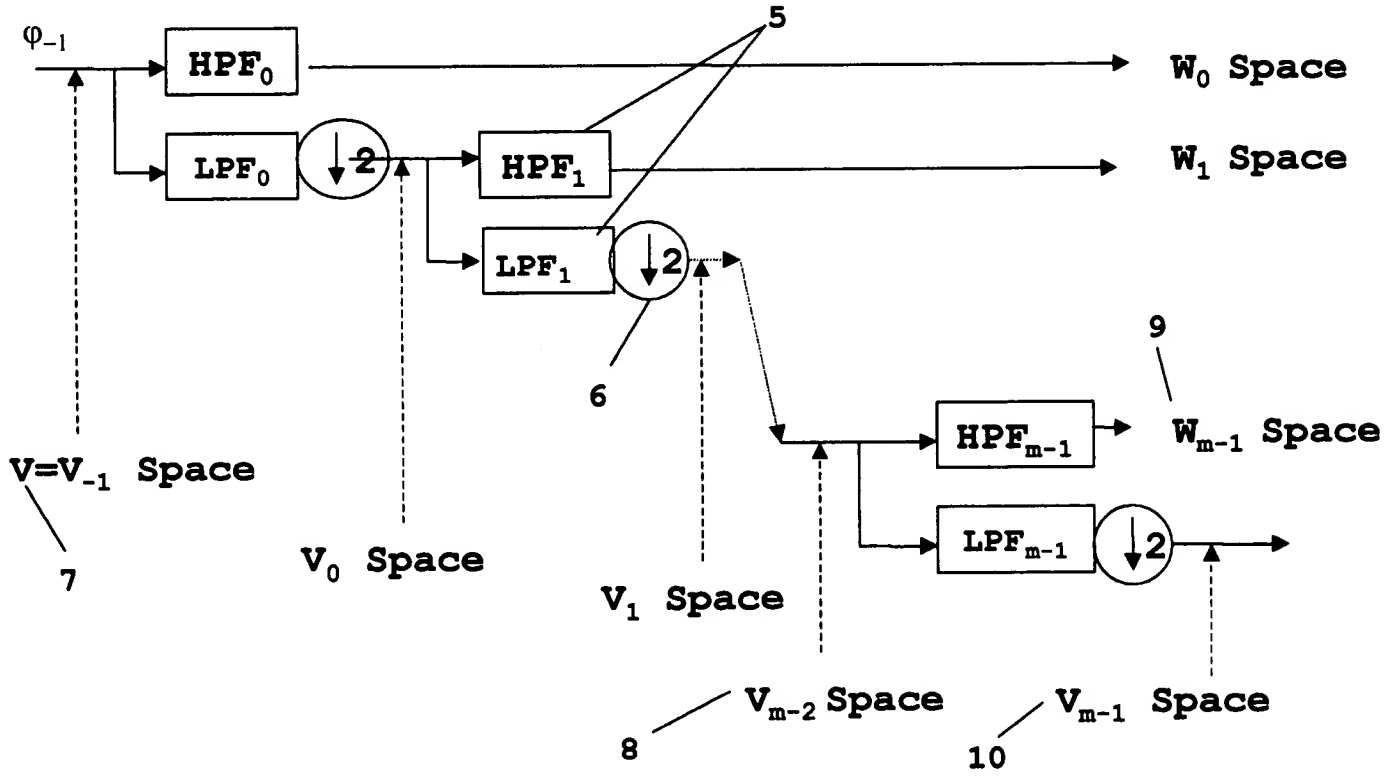

DELETED SHEET

FIG. 3 PSD Requirements for Communications

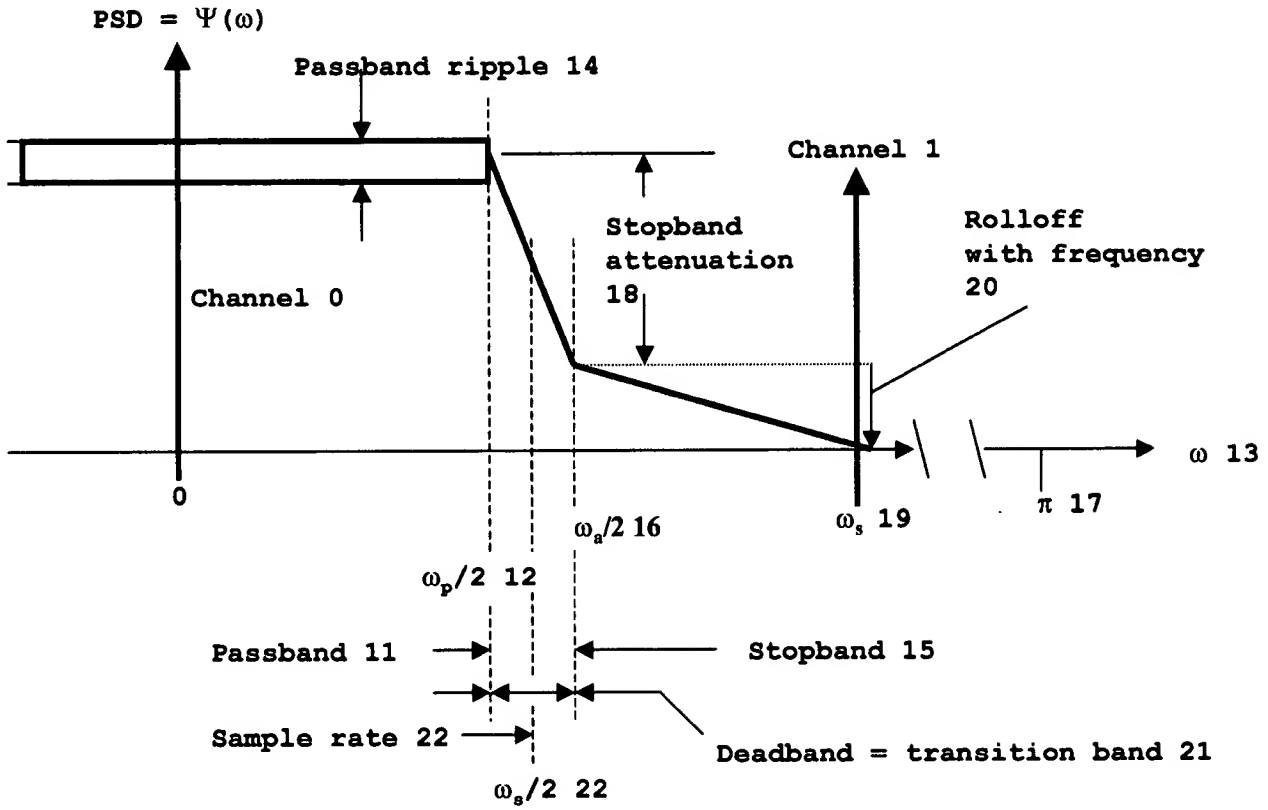

FIG. 3 PSD Requirements for Communications

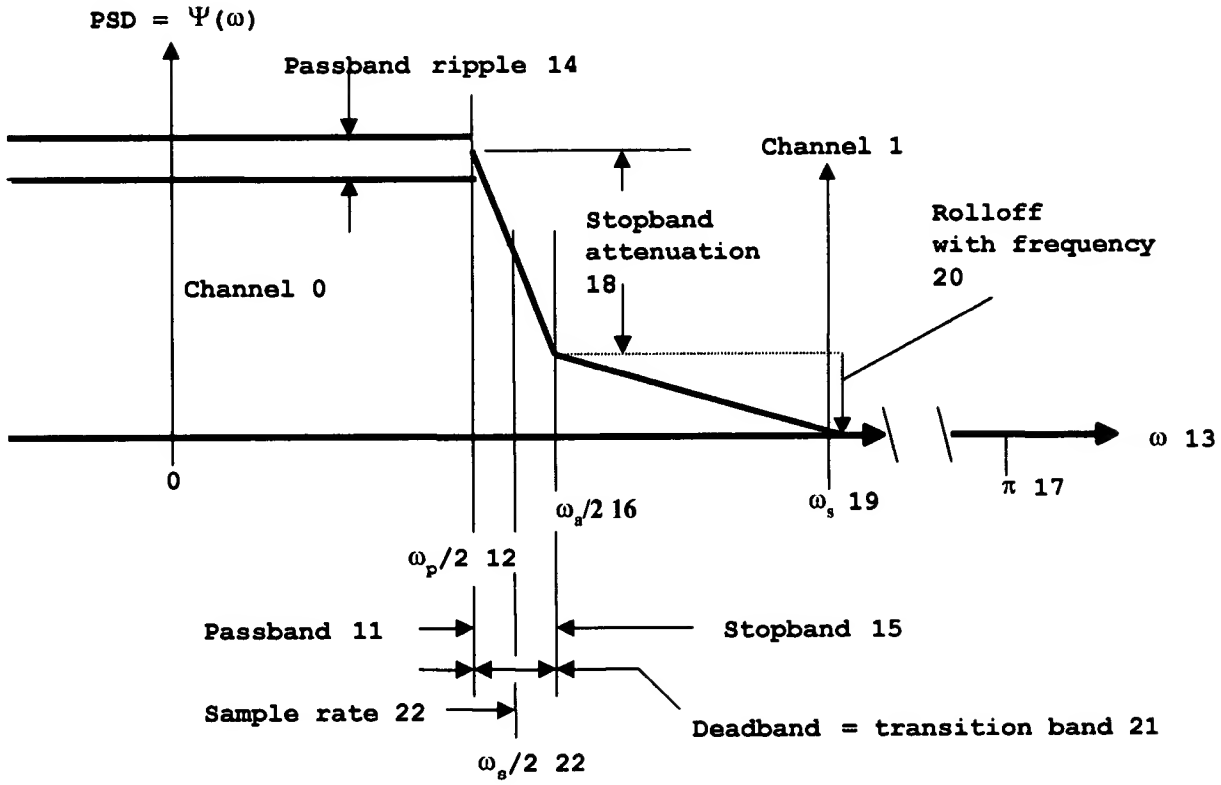

DELETED SHEET

FIG. 4 LS Metrics and Cost Function

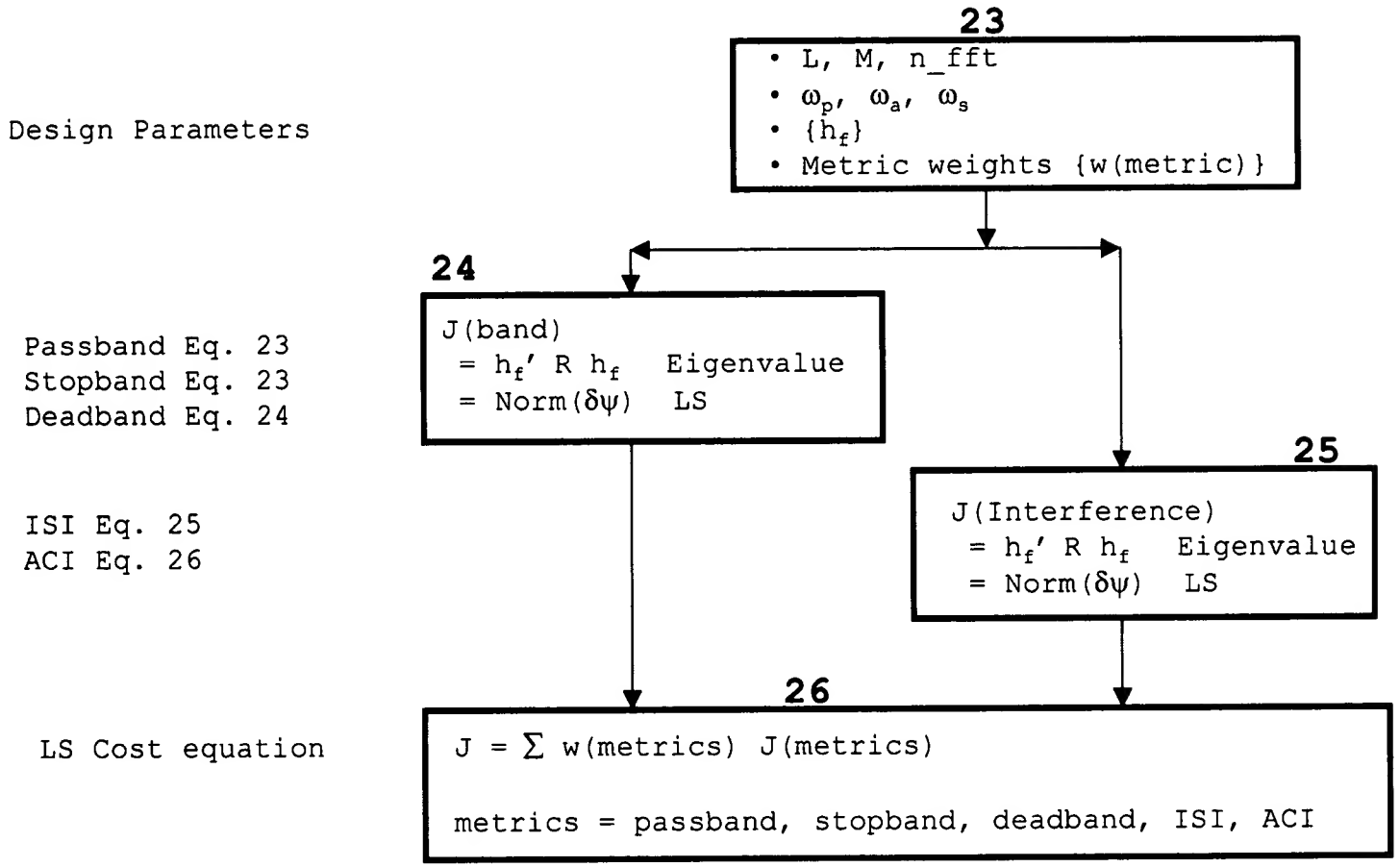

FIG. 4 LS Metrics and Cost Function

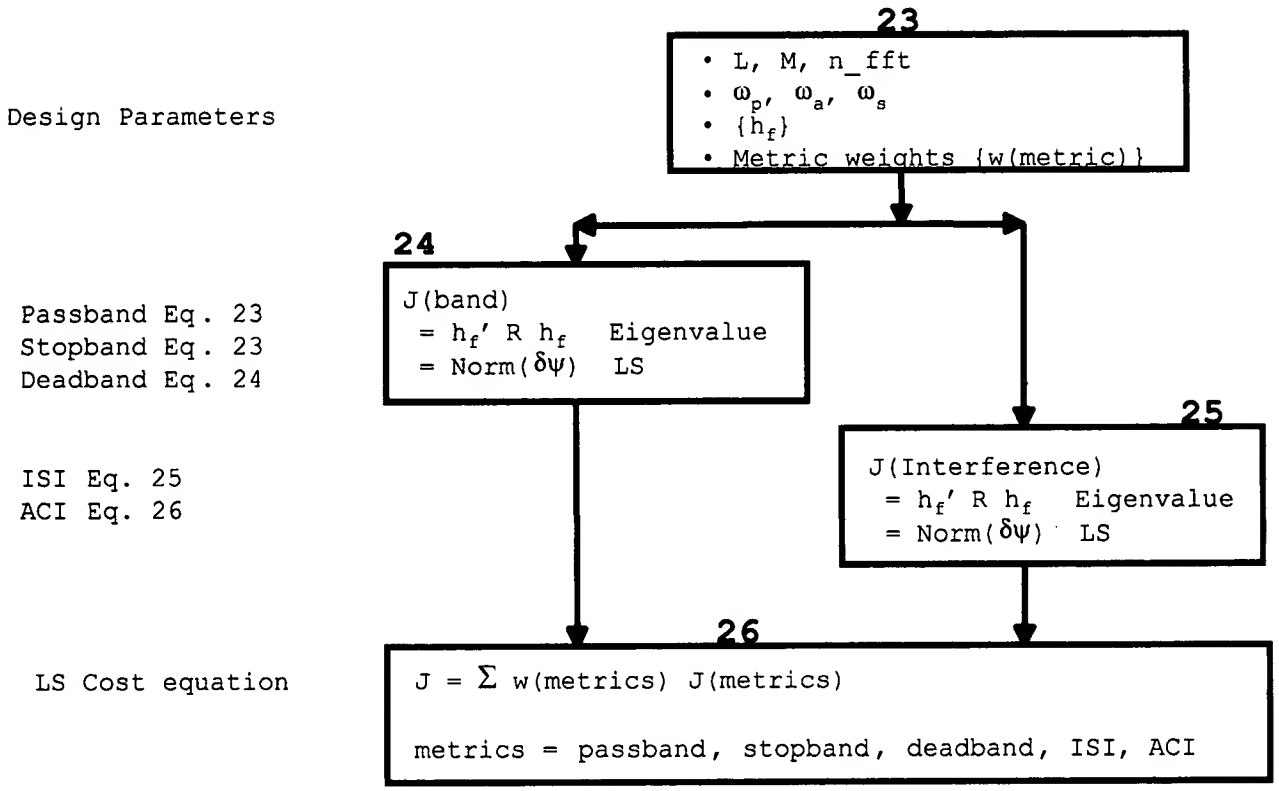

DELETED SHEET

FIG. 5 LS Recursive Solution Algorithm

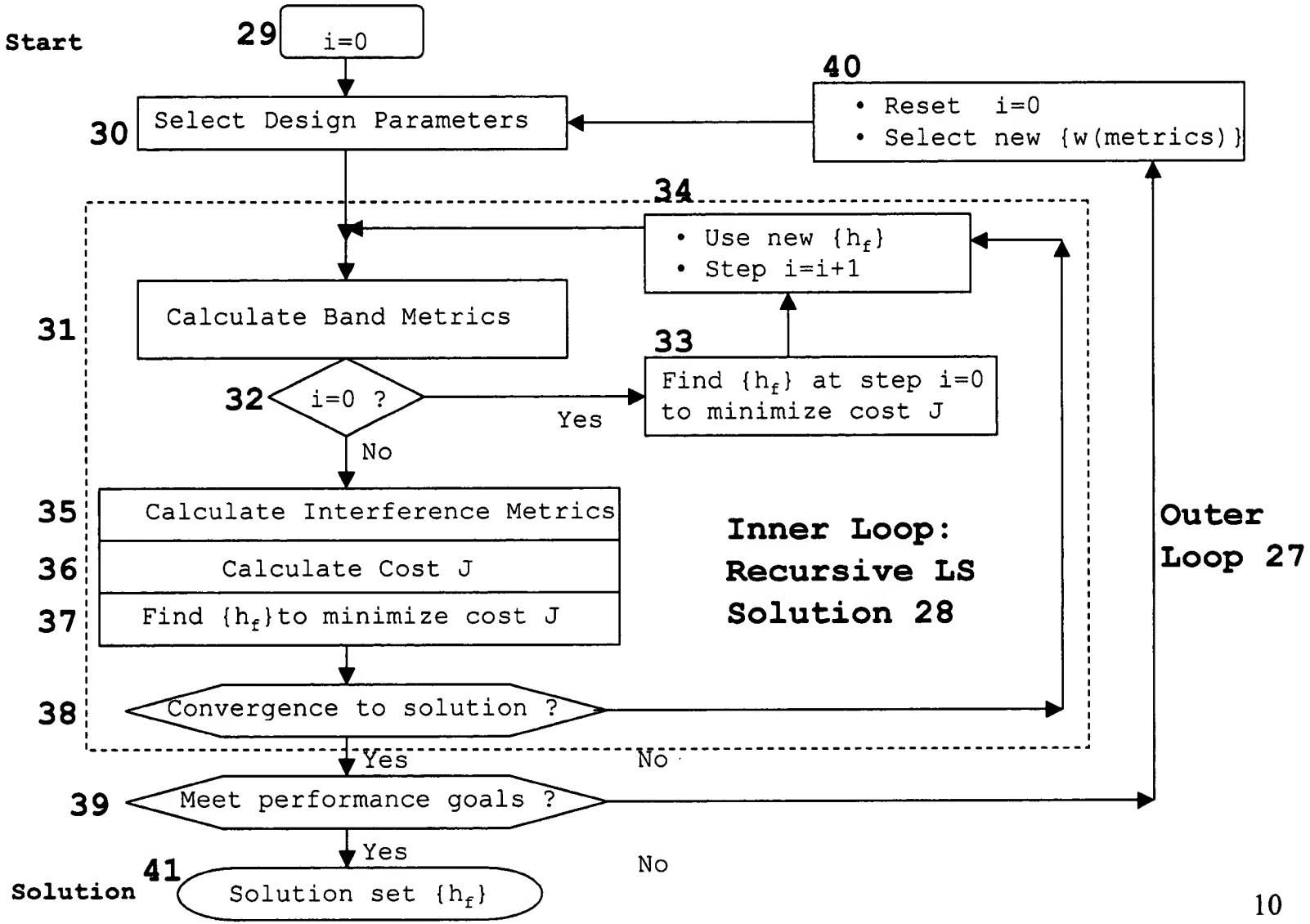

FIG. 5 LS Recursive Solution Algorithm

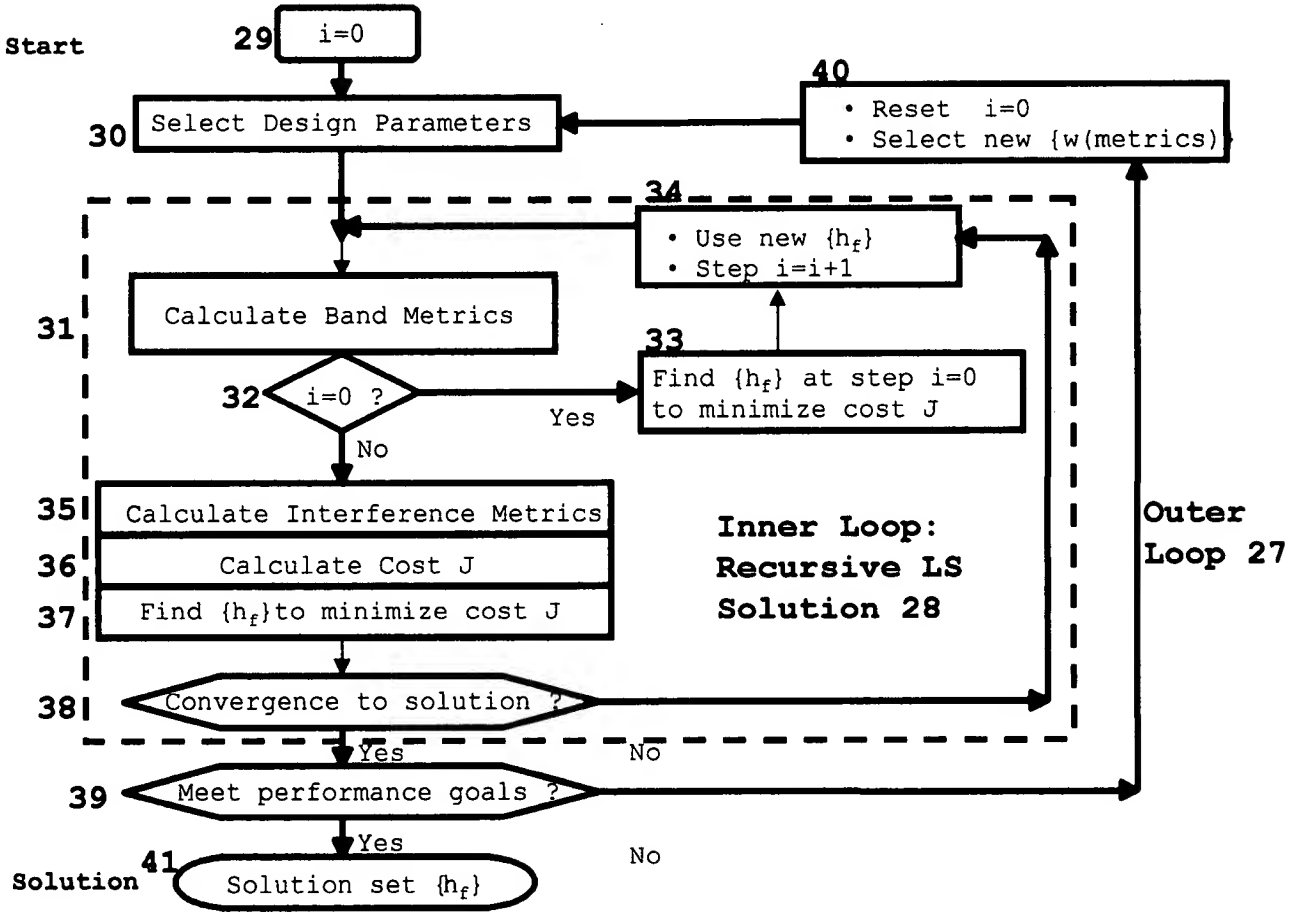

DELETED SHEET

FIG. 5A LS RECURSIVE DESIGN ALGORITHM IN MATLAB 5.0 CODE TO DESIGN:

- **MOTHER WAVELET IN FIG. 6**
- **NEW WAVELET FROM MOTHER WAVELET**
- **PERFORMANCE DATA AND PLOTS**

29

```
% STEP 1 DESIGN PARAMETERS
%============================================================
% STEP 1.1 SCENARIO PARAMETERS
%====
M           = 16;       % Wavelet sample interval
L           = 16;       % nominal Wavelet length in units of M
N           = M*L+1 ;   % Wavelet length N =ML+1
fs          = 1;        % normalized channel spacing
                        % = normalized Wavelet sample rate
fp          = 0.8864;   % normalized channel passband
n_f         = 16        % number of design harmonics
n_fft       = 1024 ;    % FFT size for spectrum centered at 0
ebno        = 6.0 ;     % dB, Eb/No
x_imbal_aci = 6.0 ;     % dB, channel-to-channel imbalance
%============================================================
% STEP 1.2 DERIVED PARAMETERS
twopi       = pi*2 ;    % definition
nc          = M;        % maximum number of channels allowed
nfft_wsr    = (n_fft/M) % 0.5 * Wavelet sample rate
f_pass      = fp/(M*fs)           % wp/2pi edge of passband
f_stop      = (2-fp)/(M*fs)       % ws/2pi edge of stopband
nfft_pass   = floor(f_pass*n_fft) % edge of passband
%nfft_stop====floor(f_stop*n_fft) % edge of stopband==========
% STEP 1.3 OPTIMIZATION PARAMETERS
%====
n_iteration = 10;       % number of iterations for LS design
alpha_1     = 1.e-2     % weighting for passband
alpha_2     = 0.80      % weighting for stopband
alpha_3     = 2.e-3     % weighting for ISI
alpha_4     = 0.5       % weighting for ACI
alpha_5     = 0         % weighting for deadband
%============================================================
```

DELETED SHEET

FIG. 5B

30

```
% STEP 2 INITIALIZATION CALCULATIONS
%=================================================================
% STEP 2.1 WAVELET LENGTH PARAMETERS
%====
nodd= fix( N/2 );
nodd = N - 2 * nodd ;
if ( nodd == 1)
  m = (N - 1 ) /2    %  N is odd
  nrow = m+1;
else
   m = N/2 ;    %     N is even
   nrow = m;
end
%=================================================================
% STEP 2.2 MATRIX "bw_matrix" MAPS WAVELET FREQUENCY DESIGN
%          HARMONICS INTO WAVELET TIME RESPONSE
%===
bw_matrix = zeros(m,n_f);
for i_r=1:m              % freq
   ang = 2*pi* rem( (i_r)*(0:n_f-1)/(N-1),1); % time
   bw_matrix(i_r + 1, :) = 2 * cos(ang);
end
bw_matrix(1,:) = ones(1,n_f);
%=================================================================
% STEP 2.3 FUNCTION "pmn" CALCULATES PASSBAND, STOPBAND LS
%          ERROR MATRICES FOR THE METRICS J(PASS), J(STOP) IN
%          EQ. 23 AND FUNCTION "pmn_d" CACULATES ERROR MATRIX
%          FOR J(DEAD)IN EQ. 24
%=================================================================
% STEP 2.4 MATRIX "c_matrix" USED FOR ISI,ACI LS ERROR METRICS
%          J(ISI)IN EQ. 25 AND J(ACI) IN EQ. 26
%===
au=eye(m+1,m+1);     % identity matrix
bb=rot90(au);        % rotation
c_matrix=[bb; flipud(bb(1:m,1:(m+1)))]/2;
c_matrix(m+1,1)=c_matrix(m+1,1)*2;
%=================================================================
% STEP 2.5 PASSBAND,STOPBAND, WAVELET SAMPLE RATE TEMPLATES
%====
%====set up passband and stopband templet
v_1 = 1:nfft_pass+1;
v_2 = nfft_pass+2:nfft_stop;
v_3 = nfft_stop+1:nfft_stop+nfft_pass;
hw_ref= [zeros(size(v_1))  -110*ones(size(v_2)) ...
         zeros(size(v_3))];
%====set up wavelet sample rate templet
v_1b = 1:nfft_wsr;
v_2b = nfft_wsr+1:nfft_wsr+1;
v_3b = nfft_wsr+2:nfft_wsr+nfft_pass+nfft_stop;
hw_wsr= [-110*ones(size(v_1b))  zeros(size(v_2b)) ...
      -110*ones(size(v_3b))];
%=================================================================
```

DELETED SHEET

FIG. 5C

31

% STEP 3 PASSBAND, STOPBAND, DEADBAND LS ERROR MATRICES

```
%=================================================================
% STEP 3.1 J(PASSBAND) LS ERROR MATRIX "passband"
%====
omega_l = 0.0 * pi;
omega_u = f_pass  * pi ;   % 0.0554
an=ones(1,nrow);
passband = pmn( omega_l, omega_u, N, an) ;
%=================================================================
% STEP 3.2 J(STOPBAND) LS ERROR MATRIX "stopband"
%====
omega_l = f_stop * pi;   %
omega_u = pi ;
an=zeros(1,nrow);
stopband = pmn( omega_l, omega_u, N, an) ;
%=================================================================
% STEP 3.3 J(DEADBAND) LS ERROR MATRIX "deadband"
%====
omega_l = f_pass  * pi;   %
omega_u = f_stop * pi;
an=ones(1,nrow);
%deadband = pmn_d( omega_l, omega_u, N, an) ;
deadband = zeros(nrow,nrow);
%=================================================================
% STEP 3.4 WEIGHTED LS ERROR MATRIX "p_total" FOR THE WEIGHTED
%          SUM OF J(PASSBAND), J(STOPBAND), J(DEADBAND)
%====
p_total= alpha_1*passband+alpha_2*stopband+alpha_5*deadband;
%=================================================================
% STEP 3.5 CONVERT LS ERROR MATRIX IN TIME "p_total" TO LS
%          ERROR MATRIX IN FREQUENCY "pw_t"
%====
pw_total = bw_matrix'*(p_total*bw_matrix);
pw_t = pw_total;
%=================================================================
```

32

% STEP 4 ITERATIVE EIGENVALUE SOLUTION

```
%====
hn_data           = [];
hw_data           = [];
err_LS            = [];
loss_LS           = [];
for i_iteration = 1:n_iteration
    i_iteration
%====
```

DELETED SHEET

FIG. 5D

```
%============================================================
% STEP 4.1 FOR EACH ITERATION "i_iteration" FIND EIGENVECTOR
%          IN FREQUENCY THAT MINIMIZES THE COST FUNCTION J IN
%          EQ. 27 WHOSE LS  ERROR MATRIOX IS  "pw_t"
%====
eig_val = eig(pw_t);
  [eig_vec eigval] = eig(pw_t);
  [eigval_min,min_index] = min(eig_val);
%============================================================
% STEP 4.2 MAP EIGENVECTOR INTO:
%          - WAVELET FREQUENCY DESIGN HARMONICS "hw_eig"
%          - WAVELET IMPULSE RESPONE IN TIME "hn"
%====
b_vector = bw_matrix * eig_vec(:,min_index);
hw_eig   = eig_vec(:,min_index);
hw_eig(1)= 2*hw_eig(1);
hw_max   = max(hw_eig);
hw_eig   = hw_eig/hw_max;
if ( nodd == 1)    % N is odd
   hn(1:m) = 0.5*b_vector((m+1):-1:2);
   hn(m+1) = b_vector(1);
   hn(m+2:N) = hn(m:-1:1);
else
   hn(m:-1:1)= 0.5 * b_vector(1:m);
   hn( m+1:1:2*m) = hn(m:-1:1);
end  % nodd
 hmax = max( abs(hn) ) ;
 scale_ww = 1. / (hmax^2);
% normalized hn is the normalized Wavelet response
hn = hn/ hmax;
%============================================================
% STEP 4.3 PASSBAND RIPPLE "xripple" AND
%          STOPBAND ATTENUATION "xstop"
%====
%Fourier transform of hn & hn in the next channel
ich = 0;
arg_rot = twopi* rem( (0:N-1)*ich /nc , 1 );
[freq, hw_db] = freq_rsp(hn, arg_rot, n_fft);
%        hn_data = [hn_data hn'];
%        hw_data = [hw_data hw_db'];
%====
%===== peak_to_peak ripple in passband
max_ripple = max( hw_db(1: nfft_pass+1));
min_ripple = min( hw_db(1: nfft_pass+1));
xripple = max_ripple - min_ripple ;
%=== stopband atttenuation
  xstop = max(hw_db(nfft_stop+1:nfft_stop+nfft_pass+1) );
%============================================================
```

DELETED SHEET

FIG. 5E

33

```
% STEP 5 WEIGHTED LS ERROR METRICS FOR:
%        - J(PASSBAND) = "beta_pass"
%        - J(STOPBAND) = "beta_stop"
%        - J(DEADBAND) = "beta_dead"
%=============================================================
  err_pass = b_vector' * passband * b_vector;
  err_stop = b_vector' * stopband * b_vector;
  err_dead = b_vector' * deadband * b_vector;
  beta_pass = alpha_1 * err_pass;
  beta_stop = alpha_2 * err_stop;
  beta_dead = alpha_5 * err_dead;
%=============================================================
```

34

```
% STEP 6 ISI AND ACI LS:
%     - MATRICES "w_matrix" AND "w_f_matrix"
%     - METRICS  J(ISI)="errM_isi" AND J(ACI)="errM_aci"
%     - SNR ERROR CONTRIBUTORS "errV_isi" AND "errV_aci"
%=============================================================
% STEP 6.1 J(ISI):
%             - LS ERROR MATRIX "w_matrix"
%             - J(ISI) = "errM_isi"
%             - SNR LOSS ISI ERROR "errV_isi"
%=====
for k_wave = 0:M
  n_i = N - 1 - k_wave*nc;
  w_vector(k_wave+1) = 0.;
  for ii = 0:n_i
% ISI error residual vector w_vector
  w_vector(k_wave+1)=w_vector(k_wave+1)+hn(ii+1)*hn(ii+1+ ...
                     nc*k_wave);
 end
end
scale_isi_aci = 1/w_vector(1) ;
w_vector = w_vector * scale_isi_aci;      % normalize
errV_isi = sum(w_vector(2:M) .*w_vector(2:M)); %ISI LS error
%2-sided power summation of isi residual errors
      errV_isi = 2. * errV_isi;
      errV_isiMax = max( abs(w_vector(2:M)) );
 %=====a_matrix = m+1  x 2m+1 = A
a_matrix= zeros(m+1,2*m+1);
for i_r = 0:m
  n_cc = i_r * nc;
  if ( i_r>=1 & i_r<=M)
      nic = (n_cc+1):(2*m+1);
      a_matrix(i_r+1, nic) = hn(nic  - n_cc) ;
  end
end
%====
```

DELETED SHEET

FIG. 5E

33

```
% STEP 5 WEIGHTED LS ERROR METRICS FOR:
%        - J(PASSBAND) = "beta_pass"
%        - J(STOPBAND) = "beta_stop"
%        - J(DEADBAND) = "beta_dead"
%============================================================
  err_pass = b_vector' * passband * b_vector;
  err_stop = b_vector' * stopband * b_vector;
  err_dead = b_vector' * deadband * b_vector;
  beta_pass = alpha_1 * err_pass;
  beta_stop = alpha_2 * err_stop;
  beta_dead = alpha_5 * err_dead;
%============================================================
```

34

```
% STEP 6 ISI AND ACI LS:
%     - MATRICES "w_matrix" AND "w_f_matrix"
%     - METRICS  J(ISI)="errM_isi" AND J(ACI)="errM_aci"
%     - SNR ERROR CONTRIBUTORS "errV_isi" AND "errV_aci"
%============================================================
% STEP 6.1 J(ISI):
%             - LS ERROR MATRIX "w_matrix"
%             - J(ISI) = "errM_isi"
%             - SNR LOSS ISI ERROR "errV_isi"
%=====
for k_wave = 0:M
  n_i = N - 1 - k_wave*nc;
  w_vector(k_wave+1) = 0.;
  for ii = 0:n_i
% ISI error residual vector w_vector
  w_vector(k_wave+1)=w_vector(k_wave+1)+hn(ii+1)*hn(ii+1+ ...
                     nc*k_wave);
 end
end
scale_isi_aci = 1/w_vector(1) ;
w_vector = w_vector * scale_isi_aci;      % normalize
errV_isi = sum(w_vector(2:M) .*w_vector(2:M)); %ISI LS error
%2-sided power summation of isi residual errors
      errV_isi = 2. * errV_isi;
      errV_isiMax = max( abs(w_vector(2:M)) );
 %=====a_matrix = m+1  x 2m+1 = A
a_matrix= zeros(m+1,2*m+1);
for i_r = 0:m
  n_cc = i_r * nc;
  if ( i_r>=1 & i_r<=M)
      nic = (n_cc+1):(2*m+1);
      a_matrix(i_r+1, nic) = hn(nic  - n_cc) ;
  end
end
%====
```

DELETED SHEET

FIG. 5G

35

```
% STEP 7  - WEIGHTED LS ERROR METRICS
%          - UPDATE LS ERROR MATRIX "pw_t" FOR NEXT
%            ITERATION
%============================================================
% STEP 7.1 WEIGHTED LS ERROR METRICS FOR ISI, ACI, TOTAL
%                - WEIGHTED ISI LS ERROR METRIC   "beta_isi"
%                - WEIGHTED ACI LS ERROR METRIC   "beta_aci"
%                - TOTAL LS ERROR METRIC J =  "errM_LS"
%====
beta_isi = alpha_3*errM_isi;
beta_aci = alpha_4*errM_aci;
errM_LS = beta_pass+beta_stop+beta_dead+beta_isi+beta_aci;
%============================================================
% STEP 7.2 SAVE WEIGHTED LS ERROR METRICS FOR EACH ITERATION
%====
if i_iteration==1
   scale_err = errM_LS;
end
beta_pass_1 = beta_pass * 1./errM_LS;  % in fraction
beta_stop_1 = beta_stop * 1./errM_LS;  % in fraction
beta_dead_1 = beta_dead * 1./errM_LS;  % in fraction
beta_isi_1  = beta_isi  * 1./errM_LS;  % in fraction
beta_aci_1 =  beta_aci  * 1./errM_LS;  % in fraction
%errM_LS = errM_LS / (alpha_1+alpha_2+alpha_3+alpha_4+alpha_5);
errM_LS = errM_LS /scale_err;
err_LS  =[err_LS ; i_iteration ....
beta_pass_1 beta_stop_1 beta_dead_1 beta_isi_1 beta_aci_1  errM_LS];
%============================================================
% STEP 7.3 UPDATE J LS ERROR MATRIX "pw_t" FOR NEXT ITERATION
%====
p_t  = p_total+ alpha_3 * w_matrix+ alpha_4 * w_f_matrix ;
pw_t =  bw_matrix'*p_t*  bw_matrix;
%============================================================
```

36

```
% STEP 8 SIGNAL-TO-NOISE SNR LOSS
%          - PASSBAND RIPPLE LOSS "xloss_ripple", dB
%          - ISI LOSS             "xloss_isi",    dB
%          - ACI LOSS             "xloss_aci".    dB
%          - TOTAL LOSS           "xloss_total",  dB
%====
% STEP 8.1 SNR LOSSES DUE TO PASSBAND RIPPLE, ISI, ACI, AND
%          THE TOTAL SNR LOSS
%=====     passband ripple loss
x_delta  = 10.^( xripple/2. /20.) - 1.;
xloss_ripple = -10. * log10( 1.0 - x_delta^2 );
%=====     isi loss
xebno  = 10.^( ebno / 10.0 );
xx_isi = xebno  * errV_isi ;
xloss_isi = 10. * log10( 1.0 + xx_isi );
%====
```

DELETED SHEET

FIG. 5H

```
%====    aci loss
x_g_aci   = 10.^( x_imbal_aci / 10. ) ;
xx_aci    = xebno * errV_aci * x_g_aci ;
%====
xloss_aci = 10. * log10( 1. + xx_aci );
% ====   total loss
xloss_total =  10.* log10( 1.+ xx_isi + xx_aci ) + xloss_ripple;
%=================================================================
% STEP 8.2 SAVE SNR LOSSES FOR EACH ITERATION
%====
loss_LS  =[loss_LS ; i_iteration  xloss_total ....
     xloss_ripple  xloss_isi  xloss_aci ];
%====
%==== end of iterations
end
%=================================================================
```

37

```
% STEP 9 WAVELET DESIGN FOR FIG. 6
%=================================================================
% STEP 9.1 WAVELET FREQUENCY DESIGN HARMONICS "hn_eig
%====
'Harmonic number  Harmonic value'
[(0:n_f-1)'         hw_eig]
%=================================================================
         0    0.9651
    1.0000    0.9499
    2.0000    0.9842
    3.0000    0.9485
    4.0000    0.9869
    5.0000    0.9434
    6.0000    1.0000
    7.0000    0.8428
    8.0000    0.2266
    9.0000   -0.0018
   10.0000    0.0019
   11.0000   -0.0006
   12.0000    0.0003
   13.0000    0.0001
   14.0000   -0.0000
   15.0000    0.0002
%=================================================================
% STEP 9.2 WAVELET TIME RESPONSE "hn"
%====
'Sample index   Wavelet response'
[(0:m)'         hn(m+1:2*m+1)']
%=================================================================
      0       1.0000
    1.0000    0.9941
    2.0000    0.9765
    3.0000    0.9476
    4.0000    0.9080
    5.0000    0.8586
```

DELETED SHEET

FIG. 5I

6.0000	0.8004
7.0000	0.7347
8.0000	0.6627
9.0000	0.5860
10.0000	0.5062
11.0000	0.4248
12.0000	0.3434
13.0000	0.2635
14.0000	0.1867
15.0000	0.1141
16.0000	0.0471
17.0000	-0.0135
18.0000	-0.0666
19.0000	-0.1117
20.0000	-0.1485
21.0000	-0.1766
22.0000	-0.1961
23.0000	-0.2073
24.0000	-0.2106
25.0000	-0.2065
26.0000	-0.1959
27.0000	-0.1795
28.0000	-0.1583
29.0000	-0.1335
30.0000	-0.1060
31.0000	-0.0769
32.0000	-0.0474
33.0000	-0.0182
34.0000	0.0095
35.0000	0.0350
36.0000	0.0577
37.0000	0.0769
38.0000	0.0923
39.0000	0.1035
40.0000	0.1106
41.0000	0.1134
42.0000	0.1121
43.0000	0.1071
44.0000	0.0987
45.0000	0.0873
46.0000	0.0736
47.0000	0.0581
48.0000	0.0414
49.0000	0.0242
50.0000	0.0070
51.0000	-0.0096
52.0000	-0.0250
53.0000	-0.0389
54.0000	-0.0507
55.0000	-0.0603
56.0000	-0.0674
57.0000	-0.0719
58.0000	-0.0738
59.0000	-0.0731

DELETED SHEET

FIG. 5J

60.0000	-0.0701
61.0000	-0.0649
62.0000	-0.0578
63.0000	-0.0492
64.0000	-0.0393
65.0000	-0.0287
66.0000	-0.0177
67.0000	-0.0066
68.0000	0.0041
69.0000	0.0141
70.0000	0.0231
71.0000	0.0309
72.0000	0.0372
73.0000	0.0420
74.0000	0.0451
75.0000	0.0465
76.0000	0.0463
77.0000	0.0445
78.0000	0.0414
79.0000	0.0370
80.0000	0.0315
81.0000	0.0253
82.0000	0.0185
83.0000	0.0113
84.0000	0.0042
85.0000	-0.0029
86.0000	-0.0095
87.0000	-0.0155
88.0000	-0.0208
89.0000	-0.0252
90.0000	-0.0287
91.0000	-0.0311
92.0000	-0.0325
93.0000	-0.0328
94.0000	-0.0321

DELETED SHEET

FIG. 5K

```
  113.0000    0.0187
  114.0000    0.0179
  115.0000    0.0168
  116.0000    0.0154
  117.0000    0.0138
  118.0000    0.0121
  119.0000    0.0103
  120.0000    0.0085
  121.0000    0.0067
  122.0000    0.0051
  123.0000    0.0036
  124.0000    0.0024
  125.0000    0.0013
  126.0000    0.0006
  127.0000    0.0001
  128.0000   -0.0000
%================================================================
```

38

```
% STEP 10 ITERATION CONVERGENCE IS MEASURED BY THE
%          CONVERGENCE OF THE LS ERRORS IN
%      figure (1), figure(2)
%================================================================
% plots
figure(1)
plot(err_LS(:,1),err_LS(:,7),'k')
legend('Total LS error relative to iteration=1')
ylabel('Total LS error relative to iteration=1')
xlabel('Iteration number')
title('TOTAL LS ERROR J  VS. ITERATION')
grid on
hold on
%====
figure(2)
plot(err_LS(:,1),err_LS(:,2),'k')
hold on
plot(err_LS(:,1),err_LS(:,3),'k--')
plot(err_LS(:,1),err_LS(:,4),'k')
plot(err_LS(:,1),err_LS(:,5),'b')
plot(err_LS(:,1),err_LS(:,6),'b--')
title('LS ERROR CONTRIBUTORS VS. ITERATION')
legend('passband','stopband','deadband','ISI','ACI')
ylabel('LS error relative to total=1')
xlabel('Iteration number')
grid on
hold on
%================================================================
```

DELETED SHEET

FIG. 5L

```
39
% STEP 11 PARAMETERS ARE SELECTED TO OPTIMIZE:
%      - WAVELET FILTER PERFORMANCE IN figure(3)
%      - WAVELET RIPPLE, ISI, ACI  SNR LOSSES IN figure(4)
%      - WAVELET TIME RESPONSE IN figure(5)
%============================================================
figure(3)
plot(freq*M, hw_db,'k')
axis([0 200 -100 10])
grid on
xlabel('Frequency/Wavelet sample rate')
ylabel('Power Spectrum, dB')
hold on
x2=length(hw_ref);
x3=length(hw_wsr);
plot(freq(1:x2)*M,hw_ref, 'b--')
plot(freq(1:x3)*M,hw_wsr, 'b-.')
legend('Wavelet response', 'pass & stop templates', 'Wavelet sample
rate')
title('WAVELET FREQUENCY RESPONSE')
grid on
axis([0 1.4 -100 0])
hold on
%====
figure(4)
plot(loss_LS(:,1),loss_LS(:,2),'k')
hold on
plot(loss_LS(:,1),loss_LS(:,3),'k--')
plot(loss_LS(:,1),loss_LS(:,4),'b')
plot(loss_LS(:,1),loss_LS(:,5),'b--')
title('SNR LOSS VS. ITERATION')
legend('total','ripple','ISI','ACI')
ylabel('SNR LOSS, dB')
xlabel('Iteration number')
grid on
hold on
%====
figure(5)
xx=(-m:m)';
xx=xx/M;
plot(xx,hn','k')
hold on
xlabel('Time/Wavelet sample rate')
ylabel('Wavelet time response')
hold on
title('WAVELET TIME RESPONSE')
grid on
axis([-8 8 -0.4 1])
%============================================================
```

DELETED SHEET

FIG. 5M

```
40
% STEP 12 CALCULATION OF NEW WAVELET WAVEFORM "hn_new"
%           FOR THE PARAMETERS:
%           - "p"  SCALE (DILATION)
%           - "q"  TRANSLATION
%           - "k"  FREQUENCY
%=============================================================
% Wavelet parameters
p = 2  % scale change or dilation
q = 2  % time translation
k = 3  % frequency translation
%=============================================================
% STEP 12.1 WAVELET SAMPLE INTERVAL "M_new" AND LENGTH "N_new"
%====
%== Wavelet sample interval M_new for:

%     Case 1: Fix M_new = M and dilate sampling
%       hn = hn(n 2^-p - q M)
%       n_new = n 2^-p
%             = n_p for n = n_0 + n_p 2^-p
%
%   Case 2: Fix sampling and dilate M_new = 2^p M
%       hn = hn(n - q M_new)
        M_new = M*(2^p);
%====
N_new = M_new*L+1;  % Wavelet length
%====
nodd= fix( N_new/2 );
nodd = N_new - 2 * nodd ;
if ( nodd == 1)
  m_new = (N_new - 1 ) /2   %  N is odd
else
   m_new = N_new/2 ;   %    N is even
end
%=============================================================
% STEP 12.2 MATRIX "bw_matrix_new" FOR MAPPING WAVELET
%           FREQUENCY DESIGN HARMONICS INTO NEWWAVELET IMPULSE
%           RESPONSE IN TIME
%====
bw_matrix_new = zeros(m_new,n_f);
for i_r=1:m_new       % freq
   ang = 2*pi* rem( (i_r)*(0:n_f-1)/(N_new-1),1); % time
   bw_matrix_new(i_r+1, :) = 2 * cos(ang);
end
bw_matrix_new(1,:) = ones(1,n_f);
%=============================================================
% STEP 12.3 MAP WAVELET FREQUENCY DESIGN HARMONICS "hw_eig"
%           INTO NEW WAVELET IMPULSE RESPONSE IN TIME "hn_new"
%====
%==== hn_0 = hn_new without translations in time & frequency
hw_eig2    = hw_eig;
hw_eig2(1) = 0.5*hw_eig(1);
%====
```

DELETED SHEET

FIG. 5N

```
b_vector = bw_matrix_new * hw_eig2;
if ( nodd == 1)   % N_new is odd
   hn_0(1:m_new) = 0.5*b_vector((m_new+1):-1:2);
   hn_0(m_new+1) = b_vector(1);
   hn_0(m_new+2:N_new) = hn_0(m_new:-1:1);
else              % N_new is even
   hn_0(m_new:-1:1)= 0.5 * b_vector(1:m_new);
   hn_0( m_new+1:1:2*m) = hn_0(m_new:-1:1);
end  % nodd
hmax_0 = max( abs(hn_0) ) ;
%==== normalized hn_0 is new baseband Wavelet with q=k=0
hn_0 = hn_0/ hmax_0;
%==== hn_1 is hn_0 with translation in time q*M_new
for n=1:N_new+q*M_new
   if n <= q*M_new
      hn_1(n) = 0;
   else
      hn_1(n) = hn_0(n-q*M_new);
   end
end
%====
%==== hn_new is hn1 with translation in frequency by k
for n=1:N_new+q*M_new
   hn_new(n) = hn_1(n)*exp( i*(2*pi*k*(n-1)/(M_new*L)) );
end
%================================================================
% STEP 12.4 PLOT WAVELET TIME RESPONSE FOR:
%        - MOTHER WAVELET "hn"
%        - NEW WAVELET "hn_new" WITHOUT FREQUENCY TRANSLATION
%====
figure(6)
xx1 = (L/2)*(1-1/2^p)*M_new ;
xx2 = (L/2)*(1+1/2^p)*M_new ;
for n=1:N_new+q*M_new
   if n<xx1 | n>xx2
      hn1(n) = 0;
   else
      hn1(n) = hn(n-xx1+1);
   end
end
x_n = (1:N_new+q*M_new)/M_new;
x_n = x_n-L/2;
plot(x_n,hn1,'k')
hold on
plot(x_n,hn_1,'k--')
grid on
hold on
legend('MOTHER WAVELET','NEW WAVELET')
xlabel('Time/hn\_new sample rate')
ylabel('Wavelet time response')
hold on
title('TIME RESPONSE FOR MOTHER, NEW WAVELETS')
%================================================================
```

DELETED SHEET

FIG. 50

```
% STEP 12.5 PLOT WAVELET FREQUENCY RESPONSE FOR:
%           - MOTHER WAVELET "hn"
%           - NEW WAVELET "hn_new"
%           vs. frequency/hn      sample rate
%           vs. frequency/hn_new sample rate
%=============================================================
figure(7) % vs. frequency/hn sample rate
ich = 0;
arg_rot = twopi* rem( (0:N-1)*ich /nc , 1 );
[freq, hw_db] = freq_rsp(hn, arg_rot, n_fft);
plot(freq*M, hw_db,'k')
hold on
ich=k;
arg_rot = twopi* rem( (0:N_new-1)*ich /M_new , 1 );
[freq, hw2_db] = freq_rsp(hn_0, arg_rot, n_fft);
plot(freq*M,hw2_db,'k--')
axis([0 8 -100 10])
grid on
legend('MOTHER WAVELET','NEW WAVELET')
xlabel('Time/hn sample rate')
ylabel('Wavelet time response')
hold on
title('POWER SPECTRUM OF MOTHER, NEW WAVELETS')
xlabel('Frequency/hn sample rate')
ylabel('Power Spectrum, dB')
%====
%==== plot frequency response of hn, hn_new
%     vs. frequency/hn_new sample rate
figure(8)
plot(freq*M_new, hw_db,'k')
hold on
plot(freq*M_new,hw2_db,'k--')
axis([0 8 -100 10])
grid on
legend('MOTHER WAVELET','NEW WAVELET')
xlabel('Time/hn sample rate')
ylabel('Wavelet time response')
hold on
title('POWER SPECTRUM OF MOTHER, NEW WAVELETS')
xlabel('Frequency/hn\_new sample rate')
ylabel('Power Spectrum, dB')
%=============================================================
```

DELETED SHEET

FIG. 5P

41

```
% STEP 13 FUNCTIONS USED IN MATLAB PROGRAM
%=============================================================
% STEP 13.1 FUNCTION "pmn" COMPUTES MATRIX FOR J(BAND) IN
%           EQ. 23
%====
function p_matrix= pmn(omega_l,omega_u, N,an)
%=============================================================
%     compute the real, symmetric, and positive definite matrix
%     input:    omega_l: lower edge (radians)
%               omega_u: upper edge (radians)
%               N: filter length,     an(.): 1xm column vector
%     output
%      p_matrix(n,m): a nXm real,symmetry and positive-definite matrix
%=====================================================================
 twopi = 2. * pi;
%     check filter lenght is odd or even
 nodd = fix(N/2);
 nodd = N - 2 * nodd;
 if ( nodd == 1)
    m = ( N-1) /2;   %    filter length 'N' is odd
  else
   m = N/2 ;            %    N is even
  end
if ( nodd == 1)
  for n= 0:m
   for m1= 0:m
      if ( m1 ==n )
          if ( n ~= 0)
p_matrix(n+1,m1+1)=1./pi*((an(n+1)*an(n+1)+0.5)*(omega_u-omega_l)-....
2.* an(n+1) * ( sin( n*omega_u )- sin( n*omega_l ) ) ....
/n + (sin(2.* n*omega_u) - sin(2.*n*omega_l))/( 4.* n) );
         else
p_matrix(n+1,m1+1)=1./pi*(an(n+1)-1.)*(an(n+1)-1.)*(omega_u-omega_l);
          end
       else
          if ( m1 ~= 0 & n ~= 0)
p_matrix(n+1,m1+1)=1./pi*(an(n+1)*an(m1+1)*(omega_u-omega_l)....
-( an(m1+1) *m1*( sin( n*omega_u ) - sin( n*omega_l ) )+  ....
an(n+1)  *n *( sin(m1*omega_u) -  sin(m1*omega_l ) ) )/( m1*n ) + ( ...
(n+m1)* (  sin( (n-m1)*omega_u ) -sin((n-m1)*omega_l)) ...
+(n-m1)*(sin( (n+m1)*omega_u )-sin((n+m1)*omega_l)))/(2.*(n*n -m1*m1)));
           else
              if (n == 0)
p_matrix(n+1,m1+1)=1./pi*(an(n+1)-1.)*(an(m1+1)*(omega_u-omega_l)-....
( sin(m1*omega_u )-sin( m1*omega_l) ) /m1 );
             end
             if (m1 == 0)
p_matrix(n+1,m1+1)=1./pi*(an(m1+1)-1.)*(an(n+1)*(omega_u-omega_l)-.....
( sin(n*omega_u )-sin(n*omega_l) ) /n );
            end
         end
         end
  end % end of m1 loop
 end  % end of n loop
else
%====
```

DELETED SHEET

FIG. 5Q

```
% =====    when N is even  ========
   for n = 0:m-1
     for m1 = 0:m-1
        if ( m1 == n )

p_matrix(n+1,m1+1) = 1./pi * (  ...
( an(n+1)*an(n+1) + 0.5) * ( omega_u - omega_l ) - ...
2. * an(n+1) * ( sin( (n+.5) * omega_u) -  ...
sin( (n+.5) * omega_l) )/( n + 0.5 ) +  ...
( sin( (2*n+1) * omega_u ) -sin( (2*n+1) * omega_l ) ) ...
/( 2. * ( 2.*n + 1) )  )  ;
          else
p_matrix(n+1,m1+1) = 1./pi * (  ...
an(n+1) * an(m1+1) * ( omega_u - omega_l ) - ...
an(m1+1)*(sin((n+.5)*omega_u)-sin((n+.5)*omega_l))/( n + 0.5) - ...
an(n+1)*(sin((m1+.5)*omega_u)-sin((m1+.5)*omega_l))/(m1+0.5)+ ...
(sin( (n-m1)*omega_u) - sin( (n-m1)*omega_l) ) /(2.* (n-m1)) +  ...
(sin(( n+m1+1)*omega_u)-sin(( n+m1+1)*omega_l))/(2.*(n+m1+1)));
          end
       end % end of m1 loop
   end  % end of n loop
end    % end of  if nodd =1
%================================================================
% STEP 13.2 FUNCTION "freq_rsp" COMPUTES FOURIER TRANSFORM OF
%           INPUT "hn" VS.  FREQUENCY/WAVELET SAMPLE RATE
%====
function [freq, hw_db] = freq_rsp(hn, arg_rot, n_freq )
% Fourier transform of input hn
% in normalized freq interval (0., 0.5)
% frequency response
% n_freq # of frequency
twopi = 2. * pi;
df = 0.5/ (n_freq -1) ;
n_filter = length(hn);
m=(n_filter-1)/2;
freq = (0:df:0.5);
for nf = 1: n_freq
  arg=twopi * rem( freq(nf) * ((1:n_filter) -1-m),1);
  hw = sum( hn .*exp( (-arg+arg_rot)*i) );
  hw_mag(nf) = abs( hw);
end
hw_max = max( abs(hw_mag) );
hw_mag = hw_mag /hw_max;
hw_db = 20. * log10( hw_mag+ 1.e-20);
%================================================================
```

FIG. 6 PSD for Wavelet and Square-Root Raised Cosine

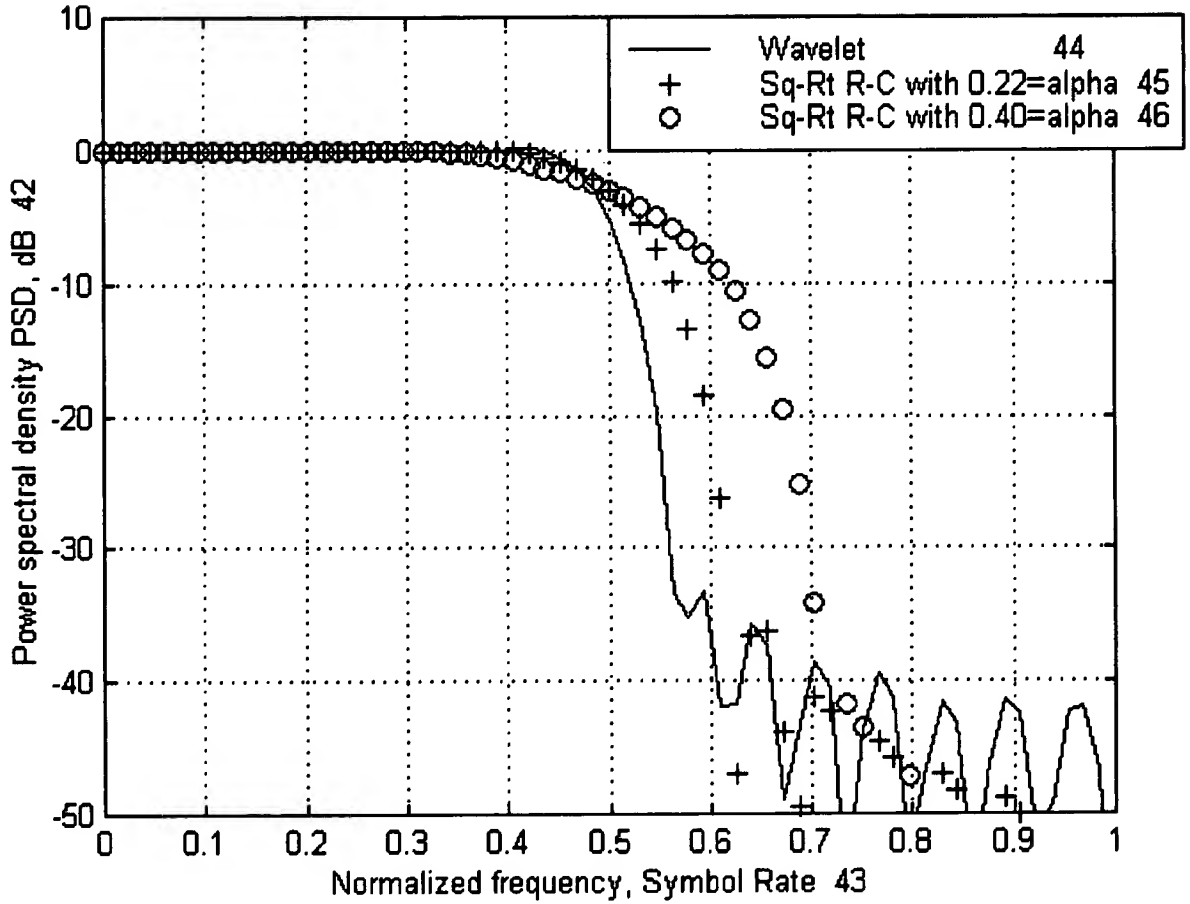

FIG. 7 PSD for New Waveform BEM and GMSK

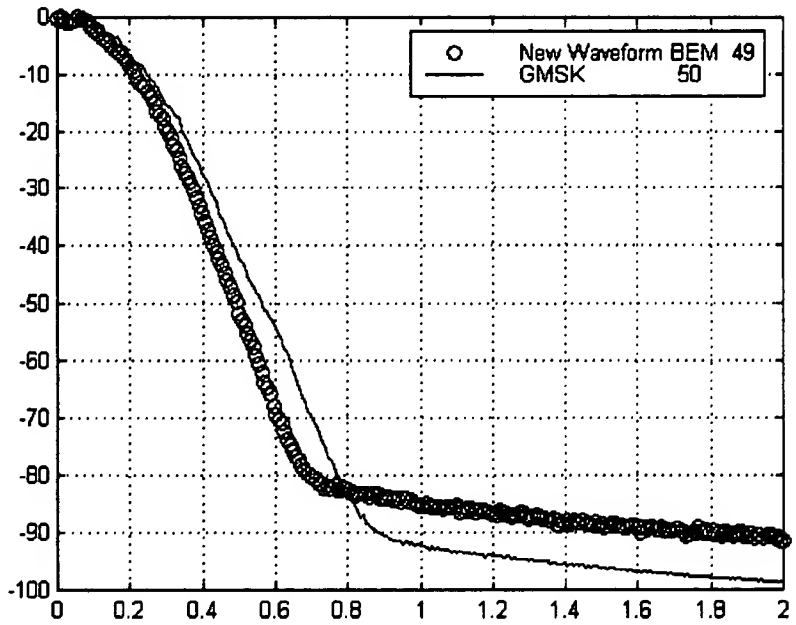

Power spectral density PSD, dB 47

Normalized frequency, bit rate 48

FIG. 8 Radar Ambiguity Functions of New Waveform and Unweighted Chirp Waveform

New Wavelet Ambiguity Function **51**

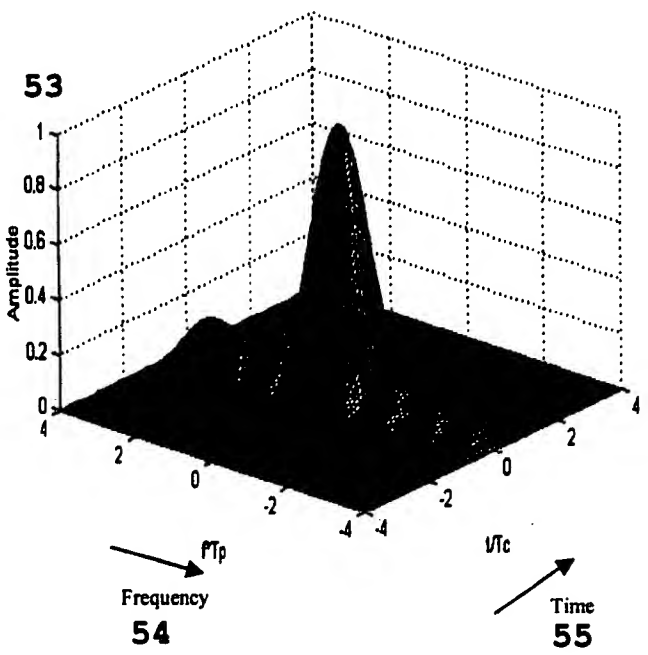

Unweighted Chirp Ambiguity Function **52**

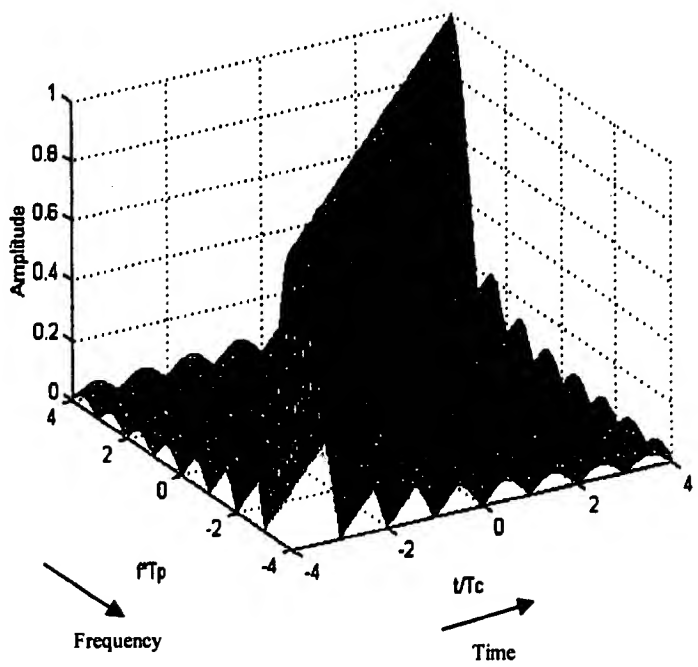

APPLICATION NO. 09/826,118

TITLE OF INVENTION: Wavelet Multi-Resolution Waveforms

INVENTOR: Urbain A. von der Embse

Currently amended CLAIMS

APPLICATION NO. 09/829,118

INVENTION: ~~N~~/w Multi-Resolution Waveforms

INVENTORS: Urbain ~~Alfred~~ A. von der Embse

CLAIMS

WHAT IS CLAIMED IS:

Claim **1**. (~~currently amended~~deleted) ~~A means for the design of new multi-resolution waveforms and filters in the Fourier domain with properties which~~

~~provide extensions of the Wavelet concept to the Fourier domain or equivalently the frequency domain~~

~~provide single waveform designs for all of the waveform s at multiple scales~~

~~provide designs which requires a relatively few design coordinates compared to the FIR time response samples for the waveform~~

~~provide design methodologies which can incorporate application metrics to improve the waveform performance~~

~~provide designs that allow the use of direct design methodologies that circumvent the need to solve a Wavelet iterated filter bank construction to obtain the waveforms thereby providing improved flexibility to meet the application goals~~

Claim **2**.(deleted) ~~2. A means for the design of multi-resolution waveforms and filters in the frequency domain or equivalently the Fourier of the t-f space for waveform and filter applications, with properties which~~

~~provide a means for single design to be used for all of the waveforms at the multiple resolutions or frequency bands~~

~~provide a means for designs that require a relatively few design coordinates compared to the number of digital samples covered by the Wavelet~~

~~provide a means for the designs to include frequency and time application metrics to improve the waveform performance~~

~~provide a means to use direct design methodologies in the frequency-time domain e for all of the waveforms and filters for the multiple frequency bands~~

Claim **3**. (~~currently amended~~deleted)

~~A method for the design of multi-resolution waveforms which allows Fourier domain techniques to be used. Properties can include some or more of the listed properties in (1) and (2)~~

Claim **4**. (deleted)

~~A method for the design of multi-resolution waveforms which can incorporate Fourier domain techniques into design methodologies which can include analytical and iterated filter bank construction design techniques.~~

Claim **5**. (~~currently amended~~deleted)

~~A method for the analysis and design of multi-resolution waveforms using Fourier domain techniques which take advantage of the new invention disclosures on the characterization and design of multi-resolution waveforms in the Fourier domain.~~

Claim **6**. (~~currently amended~~deleted) ~~A new formulation in (5) for multi-resolution waveform as a function of the dc multi-resolution waveform which adds the concept of a frequency index that allows the multi-resolution waveform to be placed arbitrarily throughout the t-f space thereby 1) avoiding the restrictions of the Wavelet iterated filter construction for tiling a t-f space, and 2) allowing the new multi-resoloution waveforms to be used for multi-resolution communications and for bandwidth-on-demand communications application, in place of traditional Wavelets.~~

Claim **7**. (new) An iterative eigenvalue least-squares LS method for designing digital mother Wavelets at baseband for means for the design of new multi-resolution waveforms and filters, said method comprising steps:

power spectral density PSD representative requirements for said mother Wavelet ψ frequency ω response $\psi_{\omega}(\omega)$ in a multi-channel filter bank, specify

a) passband frequency range for waveform transmission,

b) stopband spacing between adjacent filters,

c) bounds on ripple over said passband,

d) stopband filter attenuation,

e) rolloff with frequency outside stopband,

f) quadrature mirror filters QMF require the sum of said PSD's for contiguous filter responses to be flat over deadband which is said stopband,

g) symbol-to-symbol interference ISI,

h) adjacent channel interference ACI,

said LS error metrics to measure said requirements (a)-(h) are derived as functions of said Wavelet $\psi(n)$ assuming

i) T and 1/T are sample interval and sample rate equal to Nyquist sample rate,

j) ψ is real and symmetric about n=0,

k) n= 0, +/-1, . . ., +/-ML/2 digital index over said ψ,

l) M is interval between contiguous said ψ,

m) 1/MT is said ψ symbol rate and channel-to-channel separation,

n) L is length of said ψ in units of said M,

said multiple-resolution properties require said LS metrics to be constructed as functions of said Wavelet Fourier harmonics $\psi_k(k)$ with k=0, +/-1,. . ., +/-(N_k-1) and $N_k \geq L$ is a design parameter,

it is sufficient to use positive n=0,1,. . ., ML/2 and k=0,1,. . .,N_k-1 since said $\psi(n)$ and $\psi_k(k)$ are real and symmetric,

ML/2+1 x N_k matrix bw wherein "x" reads "by" maps $\psi_k(k)$ into $\psi(n)$ to within a scale factor by equations

$$\psi(n) = \sum_k bw(n+1,k+1)\psi_k(k) \text{ for } n\geq 0,\ k\geq 0,$$

$$bw(n+1,k+1) = 1 \text{ for } n=0,$$

$$= 2\cos(2\pi nk/ML) \text{ otherwise,}$$

= row n+1, column k+1 element of bw,

said LS error metrics are converted by said bw mapping into quadratic forms in said h_k equal to $J(band)=h_k' R\, h_k$ wherein said h_k' is the transpose of h_k and said R is a real square symmetric matrix of LS errors in meeting said requirements,

LS ISI,ACI error metrics J(ISI),J(ACI) are derived as non-linear quadratic forms in h and converted by said bw matrix to the non-linear quadratic form in h_k equal to $J(ISI)=\delta E'\delta E$, $J(ACI)=2\delta E'\delta E$ wherein $\delta E = AHh_k$ is a column vector and matrix "A" in the matrix product AH is a function of said h hereby introducing said non-linearity, and said AH differ for ISI and ACI error metrics,

LS cost function J is the weighted sum of said LS error metrics

$$J = \sum w(\text{LS metric})\ J(\text{LS metric})$$

with summation over said LS metrics= passband, stopband, QMF deadband, ISI, ACI with normalized weights

$\sum w(\text{LS metric})=1$,

said weights are free design parameters,

said iterative eigenvalue LS algorithm at each step finds the optimum eigenvalue and eigenvector which minimize said quadratic form J in h_k for a constant said "A",

said eigenvector is the optimum h_k which minimizes said J and said bw equation derives the corresponding optimum h which minimizes said J,

step 1 in said iterative algorithm finds said optimum eigenvalue, eigenvector, h_k, h of J reduced by deleting said non-linear ISI and ACI LS quadratic error metrics,

said h is used to evaluate said "A" matrices for step 2,

step 2 finds said optimum eigenvalue, eigenvector, h_k, h for minimum J using said "A" from step 1,

said h is used to evaluate said "A" for step 3,

steps 3,4, etc. continue until said minimum J converges to a steady value and,

said optimum $\psi_k(k)$ uses said bw to calculate optimum $\psi(n)$ for implementation as said Wavelet FIR digital waveform and filter time response.

Claim **8**. (new) An LS method for designing digital mother Wavelets at baseband for multi-resolution waveforms and filters, said method comprising steps:

said PSD waveform representative requirements and assumptions are recited in (a)-(n) in Claim **7**,

said multiple-resolution properties require said LS metrics to be constructed as functions of said $\psi_k(k)$,

said LS error metrics for said passband, stopband, and QMF deadband requirements are derived as squared vector norm functions of said h and converted by said bw matrix into

$J(band) = \|Bh_k\|^2$ wherein $\|Bh_k\|$ is the vector norm of the column vector Bh_k and said B is the matrix of LS errors in meeting said requirements and wherein said squared vector norm is suitable for LS optimization,

LS ISI,ACI error metrics J(ISI),J(ACI) are derived as squared vector norm functions equal to $J(ISI=\|\delta E\|^2$, $J(ACI)=2\|\delta E\|^2$ using said column vectors $\delta E = AHh_k$ in claim 7,

LS cost function J is said weighted sum of said LS error metrics equal to $J=\sum w(LS\ metric)J(LS\ metric)$ defined in claim 7,

an LS gradient search algorithm finds optimum $h_k(k)$ to minimize J,

step 1 of said LS gradient search algorithm uses a Remez-exchange algorithm to find said optimum $h_k(k)$ for said J reduced to said passband and stopband LS metrics,

step 2 uses the estimated $h_k(k)$ from step 1 to initialize said gradient search,

step 3 selects one of several available gradient search algorithms, gradient search parameters, and stopping rules,

step 4 implements said algorithm, parameters, and stopping rule selected in step 3 to derive said optimum $h_k(k)$ to minimize J and,

said optimum h_k uses said bw to calculate optimum $\psi(n)$ for implementation as said Wavelet FIR digital waveform and filter time response.

Claim 9. (new) Wherein said mother Wavelet generates multi-resolution dilated Wavelets, comprising steps and design: said Wavelet parameters are

a) scaling parameter p dilates sampling by factor 2^p equivalent to sub-sampling by factor 2^p,

b) translation parameter q translates said ψ by qM digital samples,

c) frequency offset k is set by design,

d) symbol repetition interval said M remains constant,

e) Wavelet length said L in units of said M remains constant,

step 1 uses said design harmonics ψ_k to generate said FIR time response $\psi(n_p)$ at baseband with said bw equation

$$\psi(n_p) = \sum_k bw(n_p+1, k+1)\ \psi_k(k)$$

recited in claim **7** with

$$bw = 2\cos(2\pi\ n_p k/ML) \text{ for } n_p>0$$

wherein $n_p=n/2\hat{}p$ is n sub-sampled or equivalently dilated by the factor $2\hat{}p$,

step 2 uses said $\psi(n_p)$ to construct said multi-resolution Wavelet $\psi_{p,q,M,L,k}$ with equation

$$\psi_{p,q,M,L,k} = 2\hat{}(-p/2)\ \psi(n_p-qM)\ \exp(j2\pi\ kn_p/ML)$$

which is said FIR time response for parameters p,q,M,L,k wherein the subset p,M,L are the scale parameters,

design of said multi-resolution Wavelet includes

f) said T for n is increased to T2^p for n_p,

g) said 1/T is reduced to 1/T2^p,

h) said ψ symbol rate 1/MT equal to said channel-to-channel separation is reduced to 1/MT2^p in Hz and,

i) said ψ length (ML+1)T in seconds is stretched to (ML+1)T2^p in seconds.

Claim **10** (new) Wherein said mother Wavelet generates multi-resolution constant sample rate dilated Wavelets, comprising steps and design:

said Wavelet parameters are

a) said p dilates said ψ to increase said length from ML+1 to M_pL+1 where $M_p=M2\hat{}p$ is the dilated interval

between contiguous ψ's,

b) said q translates said ψ by qM_p digital samples,

c) said k is set by design,

d) said $M_p=M2^p$ is dilated M,

e) said L remains constant,

step 1 uses said design harmonics ψ_k to generate said FIR time response $\psi(n_p)$ at baseband with said bw equation

$$\psi(n) = \sum_k bw(n+1,k+1)\ \psi_k(k)$$

recited in claim **7** with

$$bw = 2\cos(2\pi\ nk/M_pL) \text{ for } n>0,$$

step 2 uses said $\psi(n)$ to construct said multi-resolution Wavelet $\Psi_{p,q,M,L,k}$ with equation

$$\Psi_{p,q,M,L,k} = 2^{(-p/2)}\ \psi(n-qM_p)\ \exp(j2\pi\ kn/M_pL)$$

which is said FIR time response for parameters p,q,M,L,k,

design of said multi-resolution Wavelet includes

f) said T remains constant,

g) said 1/T remains constant,

h) said ψ symbol rate 1/MT equal to said channel-to-channel separation is reduced to $1/M_pT=1/MT2^p$ in Hz and,

i) said ψ length (ML+1)T in seconds is stretched to (ML2^p+1)T in seconds.

Claim **11**. (new) Wherein said mother Wavelet generates multi-resolution up-sampled Wavelets, comprising steps and design:

said Wavelet parameters are

a) said p up-samples said digital sampling rate 1/T to 2^p/T,

b) said q translates said ψ by qM digital samples,

c) said k is a design parameter,

d) said M is constant,

e) said L is constant,

step 1 uses said design harmonics h_f, ψ_k to generate said FIR time response $\psi(n_p)$ at baseband with said equation

$$\psi(n_p) = \sum_k bw(n_p+1, k+1)\ \psi_k(k)$$

recited in claim **7** with

$$bw = 2\cos(2\pi\ n_p k/ML) \text{ for } n_p>0$$

wherein n_p is n up-sampled by the factor 2^p and defined by equations

$$n_p = n\ p + n\ 2^p$$

$$n\ p = 0,1,2,\ .\ .\ .,2^p-1$$

wherein n p is the index over the additional samples added to each sample n by said up-sampling,

step 2 uses said $\psi(n_p)$ to construct said multi-resolution Wavelet $\psi_{p,q,M,L,k}$ with equation

$$\psi_{p,q,M,L,k} = 2^{(-p/2)}\ \psi(n_p-qM)\ \exp(j2\pi\ kn_p/ML)$$

which is said FIR time response for parameters p,q,M,L,k, design of said multi-resolution Wavelet includes

f) said T is decreased to T/2^p,

g) said 1/T is increased to 2^p/T,

h) said ψ symbol rate 1/MT equal to said channel-to-channel separation is increased to 2^p/MT in Hz and,

i) said ψ length (ML+1)T in seconds is reduced to (ML +1)T/2^p in seconds.

Claim **12** (new) Wherein said multi-resolution Wavelets have properties comprising:

said scale parameters p,M,L and said design parameter 1/T specify said multi- resolution Wavelets at baseband and said q,k specify time, frequency translations from baseband,

said design harmonics $\psi_k(k)$ of mother Wavelet are said design coordinates for multi-resolution Wavelets,

said design harmonics $\psi_k(k)$ use said bw matrix to generate said multi-resolution Wavelet baseband time response $\psi(n)$ for said dilation, dilation of Wavelet length, and up-sampling as recited in Claims **9-11** and which is translated

in time and frequency to said multi-resolution Wavelet $\Psi_{p,q,M,L,k}$,

said design harmonics $\psi_k(k)$ are few in number compared to said $\psi(n)$,

said ψ is designed to support a bandwidth-time product $B_fT=1+\alpha$ with no zero excess bandwidth $\alpha=0$,

said multi-resolution Wavelets are designed to behave like an accordion in that at different scales said Wavelets are stretched and compressed versions of the mother Wavelet with appropriate time and frequency translation,

said optimization techniques in claims **7,8** assume said $\psi(n)$ symmetric about n=0 and are applicable to other arrangements of $\psi(n)$ with self-evident modifications,

optimization algorithms for finding said optimum set of $\psi_k(k)$ use said linear LS waveform and filter design methods recited in claims **7,8** and also use other methods and,

said linear waveform and filter LS design methods can be modified to design waveforms for applications including bandwidth efficient modulation BEM and synthetic aperture

APPLICATION NO. 09/826,118

TITLE OF INVENTION: Wavelet Multi-Resolution Waveforms

INVENTOR: Urbain A. von der Embse

Clean version of how the CLAIMS will read.

APPLICATION NO. 09/829,118

INVENTION: Multi-Resolution Waveforms

INVENTORS: Urbain A. von der Embse

CLAIMS

WHAT IS CLAIMED IS:

Claim 1. (deleted)

Claim 2. (deleted)

Claim 4. (deleted)

Claim 5. (deleted_

Claim 6. (deleted)

Claim **7**. (new) An iterative eigenvalue least-squares LS method for designing digital mother Wavelets at baseband for multi-resolution waveforms and filters, said method comprising steps:

power spectral density PSD representative requirements for said mother Wavelet ψ frequency ω response $\psi_{\omega}(\omega)$ in a multi-channel filter bank, specify

a) passband frequency range for waveform transmission,

b) stopband spacing between adjacent filters,

c) bounds on ripple over said passband,

d) stopband filter attenuation,

e) rolloff with frequency outside stopband,

f) quadrature mirror filters QMF require the sum of said PSD's for contiguous filter responses to be flat over deadband which is said stopband,

g) symbol-to-symbol interference ISI,

h) adjacent channel interference ACI,

said LS error metrics to measure said requirements (a)-(h) are derived as functions of said Wavelet $\psi(n)$ assuming

i) T and 1/T are sample interval and sample rate equal to Nyquist sample rate,

j) ψ is real and symmetric about n=0,

k) n= 0, +/-1, . . ., +/-ML/2 digital index over said ψ,

l) M is interval between contiguous said ψ,

m) 1/MT is said ψ symbol rate and channel-to-channel separation,

n) L is length of said ψ in units of said M,

said multiple-resolution properties require said LS metrics to be constructed as functions of said Wavelet Fourier harmonics $\psi_k(k)$ with k=0, +/-1,. . ., +/-(N_k-1) and $N_k \geq L$ is a design parameter,

it is sufficient to use positive n=0,1,. . ., ML/2 and k=0,1,. . .,N_k-1 since said $\psi(n)$ and $\psi_k(k)$ are real and symmetric,

ML/2+1 x N_k matrix bw wherein "x" reads "by" maps $\psi_k(k)$ into $\psi(n)$ to within a scale factor by equations

$$\psi(n) = \sum_k bw(n+1,k+1)\psi_k(k) \text{ for } n\geq 0,\ k\geq 0,$$

$$bw(n+1,k+1) = 1 \text{ for } n=0,$$

$$= 2\cos(2\pi\, nk/ML) \text{ otherwise,}$$

= row n+1, column k+1 element of bw,

said LS error metrics are converted by said bw mapping into quadratic forms in said h_k equal to $J(band)=h_k' R\, h_k$ wherein said h_k' is the transpose of h_k and said R is a real square symmetric matrix of LS errors in meeting said requirements,

LS ISI,ACI error metrics J(ISI),J(ACI) are derived as non-linear quadratic forms in h and converted by said bw matrix to the non-linear quadratic form in h_k equal to $J(ISI)=\delta E'\delta E$, $J(ACI)=2\delta E'\delta E$ wherein $\delta E = AHh_k$ is a column vector and matrix "A" in the matrix product AH is a function of said h hereby introducing said non-linearity, and said AH differ for ISI and ACI error metrics,

LS cost function J is the weighted sum of said LS error metrics

$$J = \sum w(\text{LS metric})\, J(\text{LS metric})$$

with summation over said LS metrics= passband, stopband, QMF deadband, ISI, ACI with normalized weights

$$\sum w(\text{LS metric})=1,$$

said weights are free design parameters,

said iterative eigenvalue LS algorithm at each step finds the optimum eigenvalue and eigenvector which minimize said quadratic form J in h_k for a constant said "A",

said eigenvector is the optimum h_k which minimizes said J and said bw equation derives the corresponding optimum h which minimizes said J,

step 1 in said iterative algorithm finds said optimum eigenvalue, eigenvector, h_k, h of J reduced by deleting said non-linear ISI and ACI LS quadratic error metrics,

said h is used to evaluate said "A" matrices for step 2,

step 2 finds said optimum eigenvalue, eigenvector, h_k, h for minimum J using said "A" from step 1,

said h is used to evaluate said "A" for step 3,

steps 3,4, etc. continue until said minimum J converges to a steady value and,

said optimum $\psi_k(k)$ uses said bw to calculate optimum $\psi(n)$ for implementation as said Wavelet FIR digital waveform and filter time response.

Claim **8**. (new) An LS method for designing digital mother Wavelets at baseband for multi-resolution waveforms and filters, said method comprising steps:

said PSD waveform representative requirements and assumptions are recited in (a)-(n) in Claim **7**,

said multiple-resolution properties require said LS metrics to be constructed as functions of said $\psi_k(k)$,

said LS error metrics for said passband, stopband, and QMF deadband requirements are derived as squared vector norm functions of said h and converted by said bw matrix into

$J(band) = \|Bh_k\|^2$ wherein $\|Bh_k\|$ is the vector norm of the column vector Bh_k and said B is the matrix of LS errors in meeting said requirements and wherein said squared vector norm is suitable for LS optimization,

LS ISI,ACI error metrics J(ISI),J(ACI) are derived as squared vector norm functions equal to $J(ISI=\|\delta E\|^2$, $J(ACI)=2\|\delta E\|^2$ using said column vectors $\delta E = AHh_k$ in claim **7**,

LS cost function J is said weighted sum of said LS error metrics equal to $J=\sum w(LS\ metric)J(LS\ metric)$ defined in claim **7**,

an LS gradient search algorithm finds optimum $h_k(k)$ to minimize J,

step 1 of said LS gradient search algorithm uses a Remez-exchange algorithm to find said optimum $h_k(k)$ for said J reduced to said passband and stopband LS metrics,

step 2 uses the estimated $h_k(k)$ from step 1 to initialize said gradient search,

step 3 selects one of several available gradient search algorithms, gradient search parameters, and stopping rules,

step 4 implements said algorithm, parameters, and stopping rule selected in step 3 to derive said optimum $h_k(k)$ to minimize J and,

said optimum h_k uses said bw to calculate optimum $\psi(n)$ for implementation as said Wavelet FIR digital waveform and filter time response.

Claim **9**. (new) Wherein said mother Wavelet generates multi-resolution dilated Wavelets, comprising steps and design:

said Wavelet parameters are

a) scaling parameter p dilates sampling by factor 2^p equivalent to sub-sampling by factor 2^p,

b) translation parameter q translates said ψ by qM digital samples,

c) frequency offset k is set by design,

d) symbol repetition interval said M remains constant,

e) Wavelet length said L in units of said M remains constant,

step 1 uses said design harmonics ψ_k to generate said FIR time response $\psi(n_p)$ at baseband with said bw equation

$$\psi(n_p) = \sum_k bw(n_p+1, k+1)\ \psi_k(k)$$

recited in claim **7** with

$$bw = 2\cos(2\pi\ n_p k/ML) \text{ for } n_p>0$$

wherein $n_p=n/2\text{^}p$ is n sub-sampled or equivalently dilated by the factor 2^p,

step 2 uses said $\psi(n_p)$ to construct said multi-resolution Wavelet $\psi_{p,q,M,L,k}$ with equation

$$\psi_{p,q,M,L,k} = 2\text{^}(-p/2)\ \psi(n_p-qM)\ \exp(j2\pi\ kn_p/ML)$$

which is said FIR time response for parameters p,q,M,L,k wherein the subset p,M,L are the scale parameters,

design of said multi-resolution Wavelet includes

f) said T for n is increased to T2^p for n_p,

g) said 1/T is reduced to 1/T2^p,

h) said ψ symbol rate 1/MT equal to said channel-to-channel separation is reduced to 1/MT2^p in Hz and,

i) said ψ length (ML+1)T in seconds is stretched to (ML+1)T2^p in seconds.

Claim **10** (new) Wherein said mother Wavelet generates multi-resolution constant sample rate dilated Wavelets, comprising steps and design:

said Wavelet parameters are

a) said p dilates said ψ to increase said length from ML+1 to M_pL+1 where $M_p=M2\text{^}p$ is the dilated interval between contiguous ψ's,

b) said q translates said ψ by qM_p digital samples,

c) said k is set by design,

d) said M_p=M2^p is dilated M,

e) said L remains constant,

step 1 uses said design harmonics ψ_k to generate said FIR time response $\psi(n_p)$ at baseband with said bw equation

$$\psi(n) = \sum_k bw(n+1,k+1)\ \psi_k(k)$$

recited in claim **7** with

$$bw = 2\cos(2\pi\ nk/M_pL) \text{ for } n>0,$$

step 2 uses said $\psi(n)$ to construct said multi-resolution Wavelet $\psi_{p,q,M,L,k}$ with equation

$$\psi_{p,q,M,L,k} = 2\text{^}(-p/2)\ \psi(n-qM_p)\ \exp(j2\pi\ kn/M_pL)$$

which is said FIR time response for parameters p,q,M,L,k,

design of said multi-resolution Wavelet includes

f) said T remains constant,

g) said 1/T remains constant,

h) said ψ symbol rate 1/MT equal to said channel-to-channel separation is reduced to $1/M_pT=1/MT2\text{^}p$ in Hz and,

i) said ψ length (ML+1)T in seconds is stretched to (ML2^p+1)T in seconds.

Claim **11**. (new) Wherein said mother Wavelet generates multi-resolution up-sampled Wavelets, comprising steps and design:

said Wavelet parameters are

a) said p up-samples said digital sampling rate 1/T to 2^p/T,

b) said q translates said ψ by qM digital samples,

c) said k is a design parameter,

d) said M is constant,

e) said L is constant,

step 1 uses said design harmonics h_ℓ,ψ_k to generate said FIR time response $\psi(n_p)$ at baseband with said equation

$$\psi(n_p) = \sum_k bw(n_p+1,k+1)\ \psi_k(k)$$

recited in claim **7** with

$$bw = 2\cos(2\pi\, n_p k/ML) \text{ for } n_p>0$$

wherein n_p is n up-sampled by the factor 2^p and defined by equations

$$n_p = n\_p + n\ 2^p$$

$$n\_p = 0,1,2,\ldots,2^p-1$$

wherein n_p is the index over the additional samples added to each sample n by said up-sampling,

step 2 uses said $\psi(n_p)$ to construct said multi-resolution Wavelet $\psi_{p,q,M,L,k}$ with equation

$$\psi_{p,q,M,L,k} = 2^{(-p/2)}\ \psi(n_p-qM)\ \exp(j2\pi\ kn_p/ML)$$

which is said FIR time response for parameters p,q,M,L,k,

design of said multi-resolution Wavelet includes

f) said T is decreased to T/2^p,

g) said 1/T is increased to 2^p/T,

h) said ψ symbol rate 1/MT equal to said channel-to-channel separation is increased to 2^p/MT in Hz and,

i) said ψ length (ML+1)T in seconds is reduced to (ML +1)T/2^p in seconds.

Claim **12** (new) Wherein said multi-resolution Wavelets have properties comprising:

said scale parameters p,M,L and said design parameter 1/T specify said multi- resolution Wavelets at baseband and said q,k specify time, frequency translations from baseband,

said design harmonics $\psi_k(k)$ of mother Wavelet are said design coordinates for multi-resolution Wavelets,

said design harmonics $\psi_k(k)$ use said bw matrix to generate said multi-resolution Wavelet baseband time response $\psi(n)$ for said dilation, dilation of Wavelet length, and up-sampling as recited in Claims **9-11** and which is translated

in time and frequency to said multi-resolution Wavelet $\psi_{p,q,M,L,k}$,

said design harmonics $\psi_k(k)$ are few in number compared to said $\psi(n)$,

said ψ is designed to support a bandwidth-time product $B_fT=1+\alpha$ with no zero excess bandwidth $\alpha=0$,

said multi-resolution Wavelets are designed to behave like an accordion in that at different scales said Wavelets are stretched and compressed versions of the mother Wavelet with appropriate time and frequency translation,

said optimization techniques in claims **7,8** assume said $\psi(n)$ symmetric about n=0 and are applicable to other arrangements of $\psi(n)$ with self-evident modifications,

optimization algorithms for finding said optimum set of $\psi_k(k)$ use said linear LS waveform and filter design methods recited in claims **7,8** and also use other methods and,

said linear waveform and filter LS design methods can be modified to design waveforms for applications including bandwidth efficient modulation BEM and synthetic aperture